

Journal of Print and Media Technology Research

Scientific contents

A model of sustainable production:
ecological and economic benefits
of high-gloss UV-coating in offset printing
without a relevant loss in gloss quality

Kirsten Radermacher

195

Improving run-time stability with aerosol jet printing
using a solvent add-back bubbler

Arjun Wadhwa, Denis Cormier, Scott Williams

207

A method to compensate fluorescence induced
white point differences in proof-processes by printing
liquid fluorescent brightening agents using inkjet

Daniel Bohn, Michael Dattner, Stefan Febmer, Peter Urban

215

Does the use of black ink still comprise
the “darkest” issue of CMYK printing?

Yuri Kuznetsov and Maria Ermoshina

231

Professional communication

Evaluation of in-line viscosity measurement sensors
in gravure printing

*Henrik Knauber, Peter Schöffler, Thomas Sprinzing,
Armin Weichmann*

241

ISSN 2414-6250



9 772414 625001

Editor-in-Chief

Gorazd Golob (Ljubljana)

Published by **iarigai**

The International Association of Research
Organizations for the Information, Media
and Graphic Arts Industries

www.iarigai.org

Journal of Print and Media Technology Research

A peer-reviewed quarterly

PUBLISHED BY

The International Association of Research Organizations
for the Information, Media and Graphic Arts Industries

Magdalenenstrasse 2, D-64288 Darmstadt, Germany
<http://www.iarigai.org> E-mail: journal@iarigai.org

EDITORIAL BOARD

EDITOR-IN-CHIEF

Gorazd Golob (Ljubljana, Slovenia)

EDITORS

Timothy C. Claypole (Swansea, UK)
Edgar Dörsam (Darmstadt, Germany)
Nils Enlund (Helsinki, Finland)
Mladen Lovreček (Zagreb, Croatia)
Renke Wilken (Munich, Germany)
Scott Williams (Rochester, USA)

ASSOCIATE EDITOR

Markéta Držková (Pardubice, Czech Republic)

SCIENTIFIC ADVISORY BOARD

Darko Agić (Zagreb, Croatia)
Anne Blayo (Grenoble, France)
Wolfgang Faigle (Stuttgart, Germany)
Elena Fedorovskaya (Rochester, USA)
Patrick Gane (Helsinki, Finland)
Diana Gregor Svetec (Ljubljana, Slovenia)
Jon Yngve Hardeberg (Gjøvik, Norway)
Ulrike Herzau Gerhardt (Leipzig, Germany)
Gunter Hübner (Stuttgart, Germany)
Marie Kaplanová (Pardubice, Czech Republic)
John Kettle (Espoo, Finland)
Helmut Kipphan (Schwetzingen, Germany)
Björn Kruse (Linköping, Sweden)
Yuri Kuznetsov (St. Petersburg, Russian Federation)
Magnus Lestelius (Karlstad, Sweden)
Patrice Mangin (Trois Rivières, Canada)
Thomas Mejtoft (Umeå, Sweden)
Erzsébet Novotny (Budapest, Hungary)
Anastasios Politis (Athens, Greece)
Anu Seisto (Espoo, Finland)
Johan Stenberg (Stockholm, Sweden)
Philipp Urban (Darmstadt, Germany)

A mission statement

To meet the need for a high quality scientific publishing in its research fields of interest, the International Association of Research Organizations for the Information, Media and Graphic Arts Industries (iarigai) publishes the peer reviewed quarterly Journal of Print and Media Technology Research.

The Journal is fostering multidisciplinary research and scholarly discussion on scientific and technical issues in the field of graphic arts and media communication, thereby advancing scientific research, knowledge creation and industry development. Its aim is to be the leading international scientific periodical in the field, offering publishing opportunities and serving as a forum for knowledge exchange between all those scientist and researchers interested in contributing to or benefiting from research in the related fields.

By regularly publishing peer-reviewed high quality research articles, position papers, survey and case studies, the Journal will consistently promote original research, networking, international collaboration and the exchange of ideas and know how. Editors will also consider for publication review articles, topical and professional communications, as well as opinions and reflections of interest to the readers. The Journal will also provide multidisciplinary discussion on research issues within the field and on the effects of new scientific and technical development on society, industry and the individual. Thus, it will serve the entire research community, as well as the global graphic arts and media industry.

The Journal will cover fundamental and applied aspects of at least, but not limited to the following fields of research:

Printing technology and related processes

- ◇ Conventional and special printing
- ◇ Packaging
- ◇ Printed fuel cells and other printed functionality
- ◇ Printing on biomaterials
- ◇ Textile and fabric printing
- ◇ Materials science
- ◇ Process control

Premedia technology and processes

- ◇ Color management and color reproduction
- ◇ Image and reproduction quality
- ◇ Image carriers (physical and virtual)
- ◇ Workflow management
- ◇ Content management

Emerging media and future trends

- ◇ Media industry developments
- ◇ Developing media communication value system
- ◇ Online and mobile media development
- ◇ Cross-media publishing

Social impacts

- ◇ Environmental issues and sustainability
- ◇ Consumer perception and media use
- ◇ Social trends and their impact on media

Submissions to the Journal

Submission details and guidelines for authors can be found on the inside back cover of this issue, as well as downloaded from <http://www.iarigai.org/publications/journal>.

Subscriptions

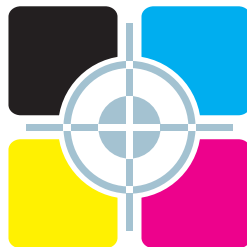
<http://www.iarigai.org/publications/journal/order>
or send your request to office@iarigai.org.

✉ Contact the Editorial office: journal@iarigai.org

Journal of Print and Media Technology Research

3-2016

September 2016



The information published in this journal is obtained from sources believed to be reliable and the sole responsibility on the contents of the published papers lies with their authors. The publishers can accept no legal liability for the contents of the papers, nor for any information contained therein, nor for conclusions drawn by any party from it.

Journal of Print and Media Technology Research is listed in:

Index Copernicus International

PiraBase (by Smithers Pira)

Paperbase (by Innventia and Centre Technique du Papier)

NSD – Norwegian Register for
Scientific Journals, Series and Publishers

Contents

A letter from the Editor <i>Gorazd Golob</i>	193
---	-----

Scientific contributions

A model of sustainable production: ecological and economic benefits of high-gloss UV-coating in offset printing without a relevant loss in gloss quality <i>Kirsten Radermacher</i>	195
Improving run-time stability with aerosol jet printing using a solvent add-back bubbler <i>Arjun Wadhwa, Denis Cormier, Scott Williams</i>	207
A method to compensate fluorescence induced white point difference in proof-processes by printing liquid fluorescent brightening agents using inkjet <i>Daniel Bohn, Michael Dattner, Stefan Fehmer, Peter Urban</i>	215
Does the use of black ink still comprise the “darkest” issue of CMYK printing? <i>Yuri Kuznetsov and Maria Ermoshina</i>	231

Professional communication

Evaluation of in-line viscosity measurement sensors in gravure printing <i>Henrik Knauber, Peter Schöffler, Thomas Sprinzing, Armin Weichmann</i>	241
--	-----

Topicalities

Edited by Markéta Držková

News & more	253
Bookshelf	255
Events	261



A letter from the Editor

Gorazd Golob
Editor-in-Chief

E-mail: gorazd.golob@jpmtr.org
journal@iarigai.org

We are back again with a regular issue of the Journal.

The second issue of 2016 was released as the Special edition: Audience, design, technology and business factors in new media innovation, edited by the guest editors David M. Frohlich & John Mills. On this occasion I would like to thank them for their efforts and excellent work done. They have attracted a number of authors and reviewers who researched in the field of media innovation and strengthened the position of the Journal in this segment.

The present issue is again very multidisciplinary, which is becoming the standard and most recognizable feature of the publication. There are four scientific contributions and one professional paper. The first scientific paper from the field of ecological and economic advantages of UV varnishing is of specific interest, because of the fresh approach that goes beyond the purely technical aspects of the processing of printed matter. It shows us the potential for improvement in the printing process from different point of view, taking into consideration rationalization of the energy and material consumption while reaching the same visual effect for the end user. The second contribution is dealing with aerosol printing technique, lesser known to many experts of printing, where the possibility of significant improvement in process stability and equalizing the print quality even in long term operation is shown. New approach in colour proofing with the use of optical brightening agents in an experimental inkjet printing, with a goal to equalize the quality of color reproduction printed on special proof papers with low content of optical brighteners in comparison to commercial papers with different, usually greater amount of optical brightening agents, is presented in the next research paper. Presentation of the models and methods for compensation of chromatic ink colors with black ink by using various techniques represents the fourth article. This content is complemented by the last article where the possibility of using less-known acoustic wave sensor for the measurement and regulation of ink viscosity in gravure printing system is presented, with the evidence of its suitability for use in practice.

Two of the published papers are based on the contributions of last year's International Research Conference of *iarigai* in Helsinki, but one paper is even from this year's Conference, held in August in Toronto. The authors of the latter, A. Wadhva, D. Cormier and S. Williams, and reviewers involved, deserve special recognition for their effort, quick response and efficiency during reviewing and editorial process. It is important to emphasize that papers accepted for publication are significantly upgraded and extended, comparing to the Conference contributions and already published extended abstracts from the same authors, on the same or similar content.

Associated Editor Markéta Držková (marketa.drzkova@jpmtr.org) again prepared Topicalities including news from the field, overview of published books, outstanding doctoral dissertations in recent time, and events, congresses and workshops of interest to readers of this Journal. Her comment on the content of Color Encyclopedia of Science and Technology drew my attention. Colour printing area is covered only partially, also reflecting the wider (non)visibility and (non)recogni-

tion of scientific and research fields covered by JPMTR, where publication of the research results in the field of retrieving, processing, reproduction (including printing and displaying) and colour perception is relatively well represented.

Again, I would like to invite ambitious authors and reviewers who intend to contribute and participate in the creation of the Journal and developing our research field. According to the quality and high level of presentations and publications of contributions at the Conferences organized by the members of *iarigai*, a lot of interesting posts are expected. This is supported also by the wealth of related research topics elaborated in dissertations; each one presented in JPMTR is freely accessible online or when requested from the author, and of course there are a great number of those which were not reported in the Journal (as the space is limited) but still may be of interest for many readers, and their authors contribute to the development in the field. With quality of published papers we gain the recognition from our colleagues and justify the existence of our interdisciplinary but often unnoticed research area.

Ljubljana, September 2016

JPMTR 084 | 1609
DOI 10.14622/JPMTR-1609
UDC 655.1 | 338.3-035.67-022.316

Original scientific paper
Received: 2016-06-04
Accepted: 2016-09-07

A model of sustainable production: ecological and economic benefits of high-gloss UV-coating in offset printing without a relevant loss in gloss quality

Kirsten Radermacher

Erbschloeer Strasse 22,
D-42369 Wuppertal, Germany

E-mail: k.radermacher@outlook.com

Abstract

This paper presents a guideline for enterprises to realize sustainable production in compliance to economic interests. A special perspective on the product quality that is perceptually noticeable, or required for customer satisfaction, enables to reach economic benefits not conflicting in respect with the principles of sustainability. Therefore, the model of sustainable production was exemplarily demonstrated by the glossiness of cardboard packaging. The investigation was mainly concentrated on the gloss measurement and perception aiming to define a threshold of perceptual gloss that gives information about the product quality required. Gloss has been a part of research work for decades. However, there are no researchers known who were able to quantify a threshold that inform about noticeable gloss differences. Furthermore, the measurement technology of gloss is much more complex than expected. The specular gloss is still the main important feature, and is broadly the essential measure in practical application. However, further gloss types are implemented in so-called goniophotometric instruments. In this paper, the currently available knowledge in gloss perception and measurement is used to generate a measure of perceptible gloss differences. Influencing factors affecting the environmental performance of high-gloss cardboard packages are presented, and suitable methods for measurement are employed. For high-gloss coated cardboard packaging, the volume of the coating roller and the intensity of the UV-curing unit reveal potential for sustainable production under consideration of the threshold of 2.0 Gloss Units that is recommended from a visual test performed. Considering the assumption made for the product example, $0.99 \pm 0.65 \text{ g} \cdot \text{m}^{-2}$ of UV-coating and $6.6 \pm 3.8 \text{ kWh}$ of energy could be saved. The integration of these scenarios in life cycle assessment (LCA) on coatings will help to assume whether these savings are crucial in the whole product life cycle. This paper gives first impressions.

Keywords: gloss measurement, gloss perception, ecological assessment, cardboard packaging, quality assessment

1. Introduction

Sustainability is one of the most important aims in society. In this context, enterprises are forced to establish sustainable strategies, also in the printing and packaging industry. A general presumption is widely spread in enterprises that sustainable strategies mainly conflict with economic objectives. However, an immediate interplay between sustainable initiatives and business competitiveness could not be found (Clausen, Klein and Konrad, 2003).

The model of sustainable production presents potential for optimisation in the manufacturing process in order to generate ecological and economic benefits. It is strongly related to a threshold of product quality due to fulfil customer satisfaction and to reach the required level of livelihood security. As an example, the coating of cardboard packages was investigated concerning gloss quality, and the consumption of materials and energy. Therefore, experiments were performed

employing gloss measurement, visual testing methods, measurement of the coating's weight, and power profiling of the printing machine. In this research study, gloss is the main challenging method of measurement. It is fundamental for this study to quantify the gloss quality and to identify a threshold of gloss perception. All of the following conclusions within the study depend on this gloss level. Gloss has been part of research work for decades but until now several research questions have not been solved.

Applying the proposed model of sustainable production in the packaging industry, ecological and economic potential of the coating process are determined without a loss of gloss quality. Based on this representative example, this study illustrates how sustainable strategies could be organized in enterprises reducing ecological and economic demands without an implication of economic objectives.

2. Literature review

Gloss is one of the main criteria of product quality for carton packages in the printing and packaging industry. An optical feature, such as gloss, can positively affect consumers’ decisions at the point-of-sale (Loefgren, 2005; ProCarton, 2006; Seeger, 2009). Thus, printing enterprises should assess and control gloss in the manufacturing process of cardboard packaging. The monitoring reveals potential for optimisation in quality, and additionally, in ecological and economic aspects, e.g. the use of resources and energy.

Important advances in gloss measurement and perception have been made since the 1930s. Initially expected to be a single objectively measurable attribute of surfaces, gloss was found to be more complex (Chadwick and Kentridge, 2015).

The most simple gloss type is called ‘specular gloss’, and describes the ratio of the portion of light in the reflectance angle to the portion of light in the incidence angle (DIN, 2014). In compliance to this norm, an angle of 20, 60 or 85 degrees is optionally employed depending on the gloss level associated: ‘high-gloss’, ‘medium’ and ‘low-gloss’. In industrial applications, enterprises mostly consider specular gloss in the gloss measurement, although it was found that gloss is a multi-dimensional feature, as shown in Hunter (1937) and Hunter and Harold (1987). They stated that further gloss types have to be involved in gloss measurement. Goniophotometric instruments normally generate measurements of light reflectance in the specular angle and, as well, in areas nearby. These gloss data are sufficient to cover the gloss types proposed by Hunter and Harold (1987), as can be seen in Figure 1.

Along with the multi-dimensionality, it is not apparent whether physical measures correlate with the perceptual judgement of gloss. Wendt (2009) emphasized that gloss is not only a purely physical attribute but also covers psychological perception and interpretation. The ‘perceptual gloss’ describes complex interactions between illumination, object, its surface reflectance, and observer (Chadwick and Kentridge, 2015), and remains gloss measurement being demanding.

Prior research has noted that observers are not able to differentiate strictly the effect of the gloss types, and hence, the test persons mainly interpreted the glossiness of samples jointly (Ged et al., 2010; Harrison and Poulter, 1951). However, a multi-dimensional model including gloss types proposed by Hunter does not exist (Wendt, 2009). The magnitude of each gloss type contributing to the gloss perception has not been identified. Chadwick and Kentridge (2015) concluded from their literature review on the perception of gloss that further work is required to create a suitable model. The variability is high in previous research work on perceptual judgement from object to object and from observer to observer. They stated that the full extent of relevant data have to be generated to reach inter-observer agreements in visual judgements and thus to develop a model.

Research work that deals with an in-depth discussion of perceptible gloss differences is not known. Authors mentioned an unspecific differential threshold of 3 GU (Gloss Unit) up to 12 GU, e.g. Helbig and Bosse (1993) and Kettler (2005). Ignell, Kleist and Rigdahl (2010) mentioned perceptible gloss differences for textured

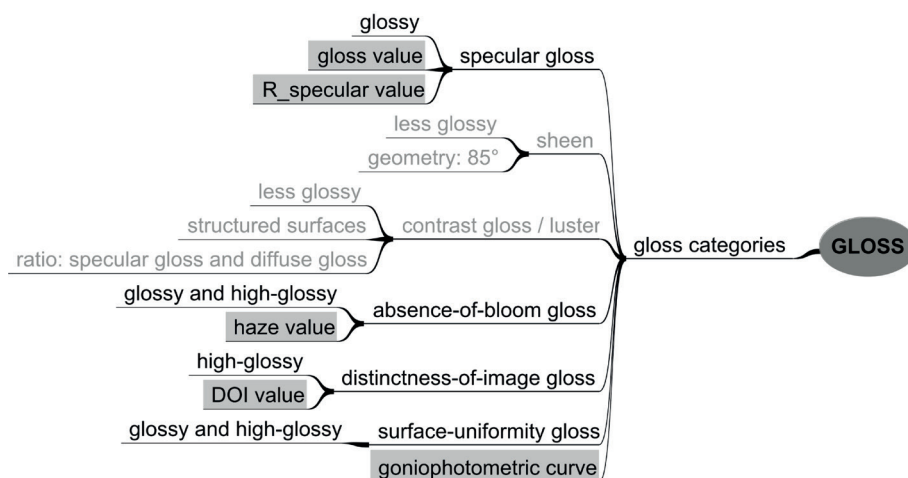


Figure 1: Connection between six gloss types mentioned by Hunter and Harold (1987) and the gloss parameters: gloss (= specular gloss), Rspec (= specular peak), haze (= absence-of-bloom gloss), and DOI (= distinctness-of-image gloss) of the goniophotometric instrument Rbopoint IQ (Rbopoint Instruments Ltd., UK) (cf. Radermacher, Dieckmann and Jung, 2015; Radermacher, 2016)

polymeric specimens of 1 GU to 5 GU, and a lower value of 0.1 GU, measured at 60°. The paper aims to develop sustainable strategies in enterprises in compliance to the product quality required. Therefore, several single aims are addressed in this study: (a) generating gloss measurements with high extent of information,

3. Methods

This study consists of different analyses. Figure 2 presents how these analyses are connected to each other. A pool of influencing factors that may have ecological and economic potential are analysed in gloss measurements of test samples. The statistical relevant data are assessed under consideration of a threshold of perceptual gloss that is extracted from a visual test. Specific factors out of the pool are chosen that do not affect the gloss quality and moreover, have ecological and economic potential in cases of material and energy consumption to implement sustainable production.

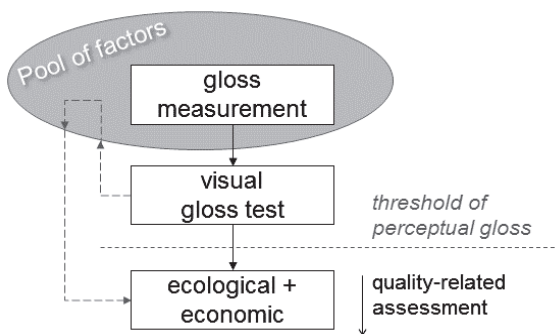


Figure 2: Methods for creating the model of sustainable production including the gloss quality of high-gloss coated cardboard packaging

3.1 Gloss measurement

Seven sets of gloss data (cf. Table 1) were calculated by taking into consideration varying factors in UV-coating that are able to affect resource and energy consumption in the coating process. Each data set was generated out of 150 measurements to achieve higher confidence in the gloss results.

Important factors with ecological and economic potential are associated with the anilox roller of the coating unit, and conditions in the drying and curing unit: (a) screening type, (b) gravure (screening volume, and frequency), (c) power of UV-curing, and (d) existence of IR-drying. The experiment is designed to quantify the effect of each of these influencing factors by varying production conditions in the coating process, as demonstrated in Table 1. For all of these conditions, test samples were created in the printing laboratory. Under consideration of climate-controlled conditions, the test samples were offline UV-coated with trans-

(b) developing a measure of perceptible gloss differences, (c) identifying factors that are able to change, or not to change the glossiness of UV-coated samples, (d) choosing factors that offer ecological and economic potential, and (e) quantifying the potential for optimisation.

parent varnish on the SM52-4+L-Anicolor-UV offset printing machine with a print run of 8 000 sheets per hour (sph) (Heidelberger Druckmaschinen AG, Heidelberg, Germany). The substrate is a white, double coated duplex board with a grammage of 250 g·m⁻² (Multicolor Mirabell, MM Karton, Neuss, Germany).

In Radermacher, Dieckmann and Jung (2015), the effect of the underlying colour on gloss measurements of high-gloss UV-coating was statistically significant for the gloss types: specular gloss at 20° for high-gloss samples according to DIN (2014) ‘G20’ and the absence-of-bloom gloss ‘haze’. The colour-related gloss could also be concluded from results in Karlović, Novaković and Novotny (2010). Thus, in favour of robust results in the comparison of gloss data in this study, the colour of the test samples must not vary. Therefore, the patches of the test samples were previously 1 colour printed (black). A preliminary coating test of four different types of UV-varnishes facilitated the choice of coating that reaches the highest gloss quality. The UV varnish is 100 % polymer-based for a radical polymerisation process.

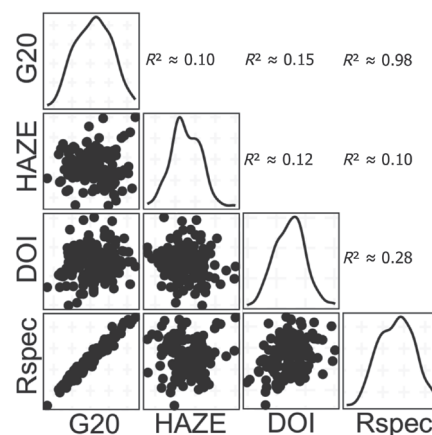


Figure 3: Scatter plot of the gloss parameters, specular gloss at 20° (G20), specular peak (Rspec), absence-of-bloom gloss (haze), and distinctness-of-image gloss (DOI) of data set $i = 2$, and the belonging Pearson's correlation coefficients, see Table 1 (cf. Radermacher, 2016)

The gloss measurements were performed by a gonio-photometric instrument ‘Rhopoint IQ’ (Rhopoint Instruments Ltd., UK). As shown in the statistical correlation analysis of the output variables in Figure 3,

Table 1: Experimental data sets of test samples UV-coated in a sheet-fed offset printing process (SM52-4+L Anicolor UV; print run of 8 000 spb; background colour: black patches)

DATA		CONDITIONS			
ID i	n	type	gravure [cm ³ · m ⁻²] / [lines · cm ⁻¹]	UV-dryer [%]	IR-dryer
1	150	strd	13.0 / 100	100	on
2 *)	150	bnd	13.7 / 100	100	on
3	150	bnd	19.0 / 80	100	on
4	150	bnd	25.5 / 60	100	on
5	150	bnd	13.7 / 100	80	on
6	150	bnd	13.7 / 100	60	on
7	150	bnd	13.7 / 100	100	off
		(a)	(b)	(c)	(d)

Abbreviations: 'strd' = standard roller with conventional cell screening; 'bnd' = roller with three different volumes and hexagonal screening;
 *) In order to fulfil the requirements of statistical analysis, as summarized in Sachs (2004), e.g. independent testing situations for the investigation of different research questions, the random sampling of this data set was repeated.

the parameters G20, haze and distinctness-of-image gloss 'DOP' are not related, and are mutually supportive to define gloss. Contrarily, the Pearson's correlation coefficient of the specular peak 'Rspec' and G20 is extremely high ($r = 0.98 \pm 0.01$ and $t(148) = 62.5$, $p < 0.001$). However, Rspec may have informative potential if G20 does not represent differences between data sets that are visually perceptible. Thus, the gloss measuring was focused on parameters like specular gloss G20, the specular peak Rspec, the absence-of-bloom gloss haze and the distinctness-of-image gloss DOI. The gloss types were estimated separately to overcome the lack of a multi-dimensional model. For each parameter, the mean value \bar{x} , the expected value μ with a 95 % confidence interval, and the mean difference $\Delta\mu_{i,j}$ of data set i to j were statistically calculated by the general two-sample t-testing method, described in Faraway (2006). The open-source software R was utilized for statistical computation.

3.2 Visual judgement

The statistical analysis can solely illuminate statistically significant results. In order to infer the practical relevance, a visual test of transparently high-gloss laminated paper-white samples by 20 test persons was carried out. The test cabine was prepared in agreement to ASTM 4449 (ASTM, 2008), Obein, Knoblauch and Vienot (2004) and Leloup et al. (2011). The testing procedure was constructed aiming to imitate precisely the measuring geometry of gloss instruments. In particular, an illumination and reflectance angle of 20° and the proposed distance between sample and test person for each of the gloss types were strictly kept.

The samples were judged binocular in order to enhance the ability of test persons to identify gloss differences (Obein, Knoblauch and Vienot, 2004). The visual test was separated into three parts: a test of visual capability in compliance to DIN 8596 (DIN, 2009), a test of gloss knowledge and the main visual test by pairwise comparison including a consistency test. The successful answering in the first two tests qualify the test persons to participate in the key test of visual judgement.

3.3 Ecological and economic assessment

Depending on the conclusions from the analyses described in section 3.1 and 3.2, ecological and economic potentials were quantified in this study, especially for (a) the weight of coating and (b) the power profile of the printing machine.

(a) The weight of the dry coating layer was measured gravimetrically applying the scale Mettler AE 200 (Mettler-Toledo GmbH, Giessen, Germany) with a measuring uncertainty of ± 0.1 mg. Sixty samples in dimensions of 50 mm \times 70 mm, were randomly extracted from the mass of samples, and were measured in three procedures. The data set of 180 measurements for each instance were assessed in statistical comparison of $\Delta\mu_{i,j}$ and scaled up to one square metre. The determination of the thickness by scanning the surface mechanically with the Dektak 150 surface profiler failed in a previous test procedure because the high roughness of the coated prints prevents the calibration and levelling of the system. Optical systems will complicate measurements, as well, because of transparent properties of the coating. Thus, the gravimetric measurement seems to be the most suitable method for quantifying the weight of the UV-coating.

(b) A power profile of the printing machine was documented in two test productions using the power quality analyser LEM 3Q (LEM HEME, Skelmersdale, UK). The instrument records 1440 intervals as the maximum in reference to the production time. The energy demand of the coating process was calculated for the

reference-scenario ‘coating of 5000 cardboard packages (size: 155 mm × 90 mm × 45 mm)’ considering the production conditions described above. The real power values of each of the printing status are averaged and related to the production time assumed for the reference-scenario.

4. Results

In this chapter, the results extracted from several analyses that are introduced in chapter 3, are summarized, connected to each other and discussed in order to answer the overall research questions.

4.1 Statistical confirmation of gloss differences

The glossiness of test prints of Table 1 are statistically computed and shown in Table 2. The screening type of the anilox roller of the coating unit ($\Delta\mu_{1,2}$) and the additional IR-drying unit ($\Delta\mu_{2,7}$) influence the gloss of the test prints more effectively than the gravure of the anilox roller ($\Delta\mu_{2,3}$) and the power of UV-curing ($\Delta\mu_{2,6}$) as specified in this test procedure. The values of distinctness-of-image gloss (μ_{DOI}) seems not to be affected notably by any of the coating conditions inves-

tigated. In three out of four factors, the results of the t-tests are not even statistically significant. As known from section 3.1, the specular peak Rspec is just to confirm G20 differences. Thus, the analysis in the following is focussed on the values of specular gloss (μ_{G20}) and absence-of-bloom gloss (μ_{haze}).

The hexagonal raster (‘bnd’) of the ceramic anilox roller (Zecher GmbH, Paderborn, Germany) is expected to transport the varnish out of the chambered doctor blade system reaching a highly smooth surface of the coating in contrast to a ceramic anilox roller with conventional cell raster (‘strd’). This statement is proved by μ_{G20} and μ_{haze} : $\mu_{G20,2}$ is 1.7 ± 0.5 GU higher than $\mu_{G20,1}$, and $\mu_{haze,2}$ is 1.0 ± 0.3 HU (Haze Unit) lower than $\mu_{haze,1}$ (cf. Table 2a).

Table 2: Effect of the influencing factors (a) screening type, (b) gravure (screening volume, and frequency), (c) power of UV-curing, and (d) additional IR-drying on the gloss values μ_{G20} , μ_{haze} , μ_{DOI} , and μ_{Rspec}

DATA		GLOSS VALUES			
<i>i</i>	<i>n</i>	μ_{G20} [GU]	μ_{haze} [GU]	μ_{DOI} [GU]	μ_{Rspec} [GU]
(a) screening type:					
1	150	37.9 ± 0.4	29.4 ± 0.2	4.5 ± 0.2	5.5 ± 0.1
2	150	39.6 ± 0.4	28.3 ± 0.2	4.9 ± 0.2	5.7 ± 0.1
$\Delta\mu_{1,2}$		1.7 ± 0.5	1.0 ± 0.3	0.4 ± 0.3	0.3 ± 0.1
(b) gravure (screening volume, and frequency):					
2	150	41.9 ± 0.4	27.7 ± 0.2	5.1 ± 0.2	6.1 ± 0.1
3	150	42.7 ± 0.3	27.8 ± 0.2	5.3 ± 0.3	6.3 ± 0.1
4	150	37.6 ± 0.3	32.4 ± 0.2	4.6 ± 0.2	5.4 ± 0.1
$\Delta\mu_{2,3}$		0.9 ± 0.5	0.1 ± 0.3 *)	0.1 ± 0.3 *)	0.1 ± 0.1
(c) power of UV-curing:					
2	150	39.6 ± 0.4	28.3 ± 0.2	4.9 ± 0.2	5.7 ± 0.1
5	150	39.1 ± 0.4	29.2 ± 0.2	4.8 ± 0.2	5.7 ± 0.1
6	150	39.0 ± 0.4	28.8 ± 0.2	4.8 ± 0.2	5.6 ± 0.1
$\Delta\mu_{2,6}$		0.6 ± 0.5	0.5 ± 0.3	0.1 ± 0.4 *)	0.1 ± 0.1
(d) additional IR-drying:					
2	150	40.2 ± 0.3	28.4 ± 0.2	4.9 ± 0.2	5.8 ± 0.1
7	150	38.4 ± 0.5	30.0 ± 0.3	4.8 ± 0.2	5.6 ± 0.1
$\Delta\mu_{2,7}$		1.8 ± 0.6	1.5 ± 0.4	0.1 ± 0.2 *)	0.2 ± 0.1

*) No statistically significant results in the two-sample t-testing

The increase of volume from $13.7 \text{ cm}^3 \cdot \text{m}^{-2}$ and a frequency of $100 \text{ lines} \cdot \text{cm}^{-1}$ ('B1') to $19.0 \text{ cm}^3 \cdot \text{m}^{-2}$ and $80 \text{ lines} \cdot \text{cm}^{-1}$ ('B2') rises the gloss value G20 slightly by $0.9 \pm 0.5 \text{ GU}$. The effect on haze is statistically not significant (cf. Table 2b). A volume of $25.5 \text{ cm}^3 \cdot \text{m}^{-2}$ and a frequency of $60 \text{ lines} \cdot \text{cm}^{-1}$ ('B3') leads to a strong reduction of the glossiness of the samples.

The status of curing in the UV-coating process varies with the print run, and also with the intensity of the UV-lamps of the curing unit. Thus, it is suspected that the reduction of the UV-power in the curing unit has an impact on the coating surface. However, the reduction from 100 % to 60 % is actually small. A little decrease of $\Delta\mu_{\text{G20},2,6}$ by $0.6 \pm 0.5 \text{ GU}$ and a small increase of $\Delta\mu_{\text{haze},2,6}$ by $0.5 \pm 0.3 \text{ HU}$ are recognized (cf. Table 2c).

An IR-drying unit (rated output: 23.1 kW at 400 V) is additionally installed in the printing machine. Generally, IR-dryers are needed for hardening inks and coatings that contain physically drying ingredients. The UV-varnish used in this test production is a 100 %-polymeric material. However, as confirmed by further tests in the laboratory, the IR-drying process supports the curing process of coatings, and the creation of mostly smooth surfaces. The gloss values grow by $\Delta\mu_{\text{G20},7,2} = 1.8 \pm 0.6 \text{ GU}$ and decline by $\Delta\mu_{\text{haze},7,2} = 1.5 \pm 0.4 \text{ HU}$ (cf. Table 2d).

4.2 Visual judgement of gloss differences

The statistical results in Table 2 were verified including conclusions from the visual judgement. This visual judgement aims to describe gloss differences in a comparative perceptual test by qualitative means. Twenty test persons (8 female, 12 male) were admitted to participate in the main test. The objects passed the eye test of DIN 8596 (DIN, 2009) and the pre-test demonstrating that they had understood the testing procedure.

Each test pair was judged, in a proceeding of sample i to sample j and vice versa. The consistency of judgement was then calculated in percent out of six test pairs. The overall consistency c is high for all of the three gloss types: $c_{\text{G20}} = 0.75$, $c_{\text{haze}} = 0.80$ and $c_{\text{DOI}} = 0.85$. Thus, the answering of the test persons is assumed to be self-consistent.

For specular gloss G20, a positive trend was derived from the pairwise comparison: The higher the mean difference $\Delta\mu_{\text{G20}}$, the higher the rate of correct answers of the test persons (cf. Figure 4). However, the determination coefficient R^2 of 0.2 is low. The trend was not even noticeable for haze and DOI. Test persons disclosed their difficulties to differentiate these gloss types from G20, despite a declaration of the gloss types at the beginning of the visual test.

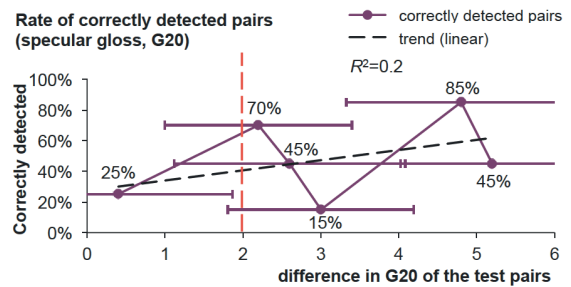


Figure 4: Rates of correctly detected test pairs of high-gloss transparently laminated samples – a result of the visual judgement of 20 test persons (cf. Radermacher, 2016)

For this reason, a measure of the practical relevance was focussed on specular gloss. The threshold for the measured gloss differences was set to 2.0 GU because 70 % of the test persons were still able to detect the gloss difference of the test pairs at a gloss level of 2.2 GU correctly.

Considering a threshold of gloss perception of 2.0 GU, the volume of the anilox roller and the power of the UV-curing unit do not affect the glossiness of cardboard packages perceptibly, and hence offers potential for sustainable production. The effect is quantified in section 4.3 and 4.4.

4.3 Ecological and economic effect of the anilox roller

A change of the anilox roller from 'B2' to 'B1' have no notable influence on the glossiness of the specimens. The gloss difference between $\mu_{\text{G20},\text{B1}} = 41.9 \pm 0.4 \text{ GU}$ and $\mu_{\text{G20},\text{B2}} = 42.7 \pm 0.3 \text{ GU}$ is lower than the threshold of 2.0 GU; instead, the reduction of the volume may show ecological and economic potential.

The dry coating layer was gravimetrically measured, and comparatively analysed regarding to the weight of uncoated test samples. The statistical results are shown in Table 3.

The data confirm that the volume directly correlate with the amount of varnish actually transferred to the substrate. This means that the parameters of the anilox roller (volume, and frequency) can directly improve ecological objectives, e.g. the material consumption of the varnish.

Figure 5 illustrates the variation of the coating amount and the effect on the glossiness of the specimens. The quantity of varnish expressed as a specific weight tends to increase slightly with higher volume of the coating roller. The gravimetric measurements for the coated test prints are presented in 'B1' $\mu_{\text{g},\text{B1}} = 6.5 \pm 0.6 \text{ g} \cdot \text{m}^{-2}$ and in 'B2' $\mu_{\text{g},\text{B2}} = 7.5 \pm 0.5 \text{ g} \cdot \text{m}^{-2}$. As a conclusion, the reduction of material consumption in the manufacturing process can be quantified as $0.99 \pm 0.65 \text{ g} \cdot \text{m}^{-2}$.

Table 3: Mean \bar{x} , deviation σ and expected value μ with a confidence interval of 95 % of gravimetric measurements of uncoated and coated test samples with a size of 50 mm × 70 mm scaled up to 1 m²

	<i>n</i>	\bar{x} [g · m ⁻²]	σ [g · m ⁻²]	μ [g · m ⁻²]
Uncoated paper, 250 g · m ⁻²	180	250.44	2.77	250.44 ± 0.41
Coated paper, B1	180	256.98	3.30	256.98 ± 0.48
Coated paper, B2	180	257.97	3.26	257.97 ± 0.48
Coated paper, B3	180	259.23	3.00	259.23 ± 0.44

Ecological and economic potential coating and gloss level

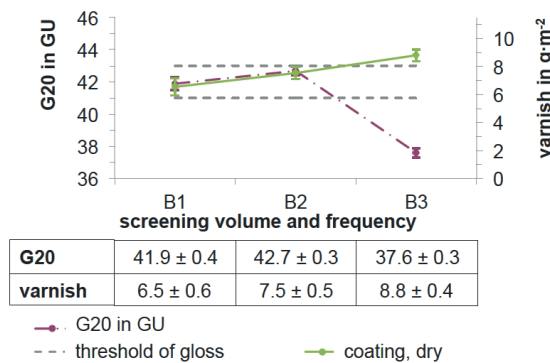


Figure 5: Ecological-economic analysis of UV-coated prints: Variation of gravure (screening volume, and frequency) (B1, B2, and B3) considering a threshold of 2.0 GU

Ecological and economic potential UV-curing and gloss level

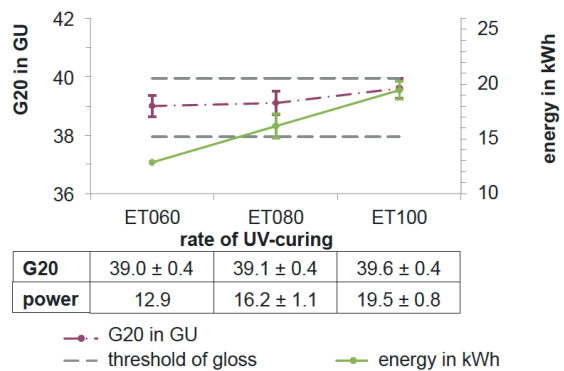


Figure 6: Ecological-economic analysis of UV-coated prints: Variation of the energy in the UV-curing process (100 % curing, dimming to 80 % and 60 %) considering a threshold of 2.0 GU

4.4 Ecological and economic effect of the UV-curing power

The power profile of the printing machine clarifies the real power in watt for different status of the printing machine. As illustrated in Table 4, an energy demand of

19.5 ± 0.8 kWh (with 100 % curing) was calculated. In the case of 80 % power of the curing unit, the energy consumption declines to 16.1 ± 1.1 kWh. The power profile of the printing machine indicates that the dimming of the UV-curing lamps effectively reduces the energy consumption.

Table 4: Power consumption values of the printing machine ‘SM52-4+L Anicolor UV’ at coating 5 000 cardboard packages (plus 100 pcs. of coated paper waste) to different production status (reference-scenario)

Status	Duration [min]	Real power [kW]
Starting	5	14.25 ± 1.4
General preparation of the machine	5	8.86 ± 1.1
Pumping up varnish *)	8	11.48 ± 1.2
Driving down of coating unit	2	18.35 ± 1.5
Preparing UV dryer	1	21.95 ± 2.9
Driving of minimum limit of varnish	5	29.87 ± 1.7
Print run (100 % curing)	38	31.07 ± 2.2
Driving up coating unit	2	32.48 ± 4.3
Pumping down varnish	3	17.70 ± 0.4
Cleaning of coating unit *)	5	18.21 ± 0.5

*) Cleaning and setting of the coating unit is allocated to the daily average production in two-shift operation with an average print run of 10 000 sph (~ 3%)

The ecological and economic potential of the UV-curing power in the coating process is presented in Figure 6.

The effect on the gloss quality and the energy in kWh are visualized comparatively. The steady decrease of the power of UV-curing lamps from 100 % to 60 % does

5. Discussion and conclusion

This study presents a special perspective on sustainable production. The model enables to discuss ecological benefits including a threshold of quality differences. The consumption of materials and energy that will not affect the product quality could be seen as a kind of wastage, see also Pommer et al. (2003). For the example of gloss quality, addressed in this study, two factors were found out to give ecological and economic benefits: The intensity of UV-curing and the amount of UV-varnish. This conclusion was based on results of goniophotometric gloss measurements and visual testing. A threshold of 2.0 GU was defined to be visually noticeable. Additional analyses were utilized to quantify the ecological and economic advantages.

In the gravimetric measurement of the coating, it was confirmed that an increase of the volume of the anilox roller raises in fact the coating layer thickness of the test prints. Generally, the measuring method has a high deviation. However, it was stated that mechanical and optical systems for profiling coating surfaces, which are available in the laboratory, would not be applicable to this request. A reduction of about $0.99 \pm 0.65 \text{ g} \cdot \text{m}^{-2}$ was concluded to have ecological and economic potential not affecting the gloss quality of the specimens.

The power profile of the printing machine was recorded to construct the energy demand of the coating process in a modular way. This proceeding enables to develop different scenarios based on specific assumption in the coating process. This power values illuminates that the IR-drying unit has an essential effect on the glossiness of the test samples although the UV-varnish does not contain physically drying ingredients but exclusively 100 % polymers. It could be concluded that the built-up of heat at the coatings of the samples positively influences the UV-curing process and reaches better pre-conditions to create smooth coating surfaces. The intensity of the UV-curing was not found to be relevant regarding to the level of gloss quality. The dimming from 100 % to 60 % does not cause perceptible gloss differences, but can reduce the energy demand by about $6.6 \pm 3.8 \text{ kWh}$. This comparative analysis of ecological and economic aspects is concentrated on the energy demand. It was not stated in this study whether the potential of the migration of monomers and photo-initiators will be negatively implicated in this case. For this study, the equipment

not influence the glossiness of the prints negatively considering the threshold of perceptible gloss differences determined in section 4.2. Assuming a linear correlation between dimming rate and energy demand, the reduction of the curing intensity to 60 % leads to a potential for energy reduction of $6.6 \pm 3.8 \text{ kWh}$.

was not available to include this information. It is recommended to examine if the energy reduction does not influence the quality of the curing and increase the risk for human health. Research work has been conducted to develop effective measures for the curing degree of UV-coatings and UV-inks. Until now, these methods for determination of the curing have not been established in printing companies, and hence, the degree of curing cannot be controlled during printing. That is why the dimming of the UV-dryer is not a usual behaviour in practical application to be sure that the coating is completely polymerized. However, in general, this is representative to demonstrate the model of sustainable production, and to identify different influencing factors with high effect on the glossiness.

The analysis of these factors is of major importance for the model of sustainable production. This kind of effect analysis is the basis of the model, and hence, requires high accuracy in the testing procedures, as standard conditions in the laboratory (e.g. climate) and constant testing set-up (e.g. machine, material), for all of the test variations to create reliable results. These pre-conditions were considered in this study so that systematic errors in the conclusions could mainly be eliminated. The gloss measurement was focused on the gloss types, specular gloss 'G20', absence-of-bloom gloss 'haze' and distinctness-of-image gloss 'DOI'. The study presents that these gloss types are not correlated and can be included in a multi-dimensional model. Additionally, the specular peak 'Rspec' was included although this gloss type is strongly related to specular gloss. The manufacturer of the gloss instrument recommends to use this measure for the specification of perceptual gloss that is not detected by the specular gloss type. These four gloss types were calculated separately in compliance to Billmeyer and O'Donnell (1987) because a standard model was not obtained to describe gloss perception in a multi-dimensional way. Goniophotometric gloss values were generated using statistical methods. The mean differences were statistically confirmed with a confidence of 95 %, as a general requirement in statistical computation (Sachs, 2004; Sachs and Hedderich, 2009). Although Rspec was expected to give informative results to G20, this gloss type was not found to be relevant in this study. The distinctness-of-image gloss DOI did not generate consistent information, too; DOI seems not to be sensitive in any of the adjustments in

the coating process investigated in this study. A statistical relevance was not realized in the main of the data sets. Thus, it may be concluded that distinctness-of-image gloss is a measure of different application methods, and does not differentiate modifications of production conditions in one of the techniques, as coating in a printing machine. Nevertheless, specular gloss and haze are two gloss types that create important information about the coating in this study.

In order to estimate the practical relevance of the gloss differences, a visual test was conducted. The visual judgement did not present robust results. A positive trend of gloss differences measured and judged was only visible for specular gloss demonstrating a high deviation. This seems to confirm the statement of Chadwick and Kentridge (2015) that further work on relevant data is required to generate inter-observer agreements in visual judgement. However, the threshold of perceptible gloss differences was defined reasonably and quantify suggestions of Helbig and Bosse (1993), Kettler (2005) and Ignell, Kleist and Rigdahl (2010) more precisely.

This paper presents how principles of sustainable production could effectively be used in the printing and packaging industry. In accordance to the proposed model, decision-making is primarily based on a comparative level of perceptual product quality. In a wider context, the ecological benefits could be discussed not from a comparative but from an absolute perspective. This means, the level of quality that is actually required could be included in the model of sustainable production. This kind of quality level considers a threshold that is needed to fulfil customer satisfaction. In the case of carton packages, this threshold could be defined by research work on consumers' behaviour.

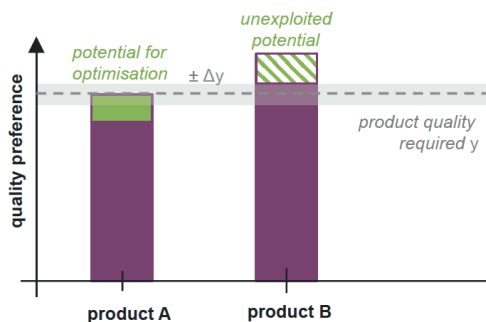


Figure 7: Potential of sustainable production in product comparison under consideration of the product quality required: product A has potential for optimisation; product B creates unexploited potential and hence shows potential for reduction

As shown in the scheme in Figure 7, the absolute value for product quality $y \pm \Delta y$ may give rich information about the potential for process optimisation in product A, and the stage of wastage in product B.

This model of sustainable production reaches a high level of practical applicability, and is additionally flexible to be adapted to several industries. Ecological and economic objectives are essential in producing industries. However, this model does not conflict with the principles of sustainability: Ecological and economic aspects are forbidden to be balanced in the sustainable discussion. Instead, the model considers a minimum limit of product quality required to secure the livelihood of enterprises.

The example of coated cardboard packages presents absolute values of resource consumption. This potential is related to assumptions made in the test specimens and in the set-up of the coating process. There is no information about the overall potential in the product life-cycle and its emissions to the environment from the perspective of the final product. The life-cycle assessment (LCA) is a method that estimates the environmental impact from the material extraction to the end-of-life phase. The LCA method has been part of research work for decades. The inclusion of the stages of production was found to be essential for strategic decision-making of enterprises; whereby, LCAs are known to be particularly complex.

For the specific product in this study, Radermacher (2016) reports LCA results for this kind of coating under consideration of the different production conditions in this study. This publication reports that the volume of the anilox roller affects the ecological benefit more remarkably than the dimming rate of the UV-curing unit does. Depending on the specific impact category, the reduction of the varnish improves the overall impact by $15.0 \pm 12.9\%$ to $24.4 \pm 14.8\%$. For the energy consumption in the coating process, the reduction is just by $0.4 \pm 0.1\%$ to $6.1 \pm 2.6\%$ of the whole product life cycle.

These results give first impressions about the magnitude of the environmental impact that the coating might have. Additionally, it points out one problem of the LCA methodology: the uncertainty of data. The deviation in the impact factors assessed is caused, for example, by the mass of information included, the scope of data, its adaption and the assumptions in the calculation. This might imply that LCA is not appropriate although it is the most informative method including potential impacts based on scientific research and going further than the 'less is better' argument. Because of the extensive perspective on the whole product life-cycle, this approach detects displacements of burdens to other stages of the life-cycle (Fava, 2002) and could prevent mistakes in decision-making. Especially the last-mentioned fact is important for enterprises in the context of sustainable production and should be forced in future strategic development. However, further research work on the LCA is required to include this kind of environmental assessment more consistently in businesses.

Acknowledgements

This work presents certain of the main outcomes of the author's Ph.D. thesis (Radermacher, 2016). I would like to thank my supervisors Prof. Dr. Ulrich Jung and Prof. Dr. Joachim M. Marzinkowski of the University of Wuppertal for their invaluable support.

The experimental work was also supported by German companies of the printing and paper industry. They provided paperboard and UV-varnish for the test production in the printing laboratory of the University. In particular, I like to thank gratefully 'MM Karton GmbH' (Neuss, Germany) and 'Heidelberger Druckmaschinen AG' (Heidelberg, Germany). Thanks to the students participating in gloss measuring and visual tests for the study. Hanno Gottschalk, Professor of Applied Mathematics at the University of Wuppertal, contributed to the study by briefing on statistical methods and computation with R. Thank you for your precious input.

References

- ASTM, 2008. *ASTM D4449 – 08 Standard Test Method for Visual Evaluation of Gloss Differences Between Surfaces of Similar Appearance*. West Conshohocken, PA, USA: ASTM.
- Billmeyer Jr., F.W. and O'Donnell, F.X.D., 1987. Visual gloss scaling and multidimensional scaling analysis of painted specimens. *Color Research & Application*, 12(6), pp. 315–326.
- Chadwick, A.C. and Kentridge, R.W., 2015. The perception of gloss: A review. *Vision Research*, 109, Part B (April 2015), pp. 221–235.
- Clausen, J., Keil, M. and Konrad, W., 2003. *The relationship between competitiveness, environmental performance and management of small and medium sized European manufacturing firms*, Technical Report IÖW 168/03. [pdf] Berlin: Institut für ökologische Wirtschaftsforschung. Available at: <https://www.ioew.de/uploads/tx_ukioewdb/IOEW_SR_168_The_relationship_between_competitiveness_environmental_performance_and_management_of_small_and_medium_sized_European_manufacturing_firms.pdf> [Accessed 20 July 2016].
- DIN Deutsches Institut für Normung e.V., 2014. *DIN EN ISO 2813:2014. Paints and varnishes – Determination of gloss value at 20°, 60° and 85°*. Berlin: DIN.
- DIN Deutsches Institut für Normung e.V., 2009. *DIN EN ISO 8596:2009. Ophthalmic optics – Visual acuity testing – Standard optotype and its presentation*. Berlin: DIN.
- Faraway, J.J., 2006. *Extending the Linear Model with R: Generalized Linear, Mixed Effects and Nonparametric Regression Models*. Boca Raton: Chapman & Hall/CRC.
- Fava, J.A., 2002. Life cycle initiative: A joint UNEP/SETAC partnership to advance the life cycle economy. *International Journal of Life Cycle Assessment*, 7(4), pp. 196–198.
- Ged, G., Obein, G., Silvestri, Z., Le Rohellec, J. and Viénot, F., 2010. Recognizing real materials from their glossy appearance. *Journal of Vision*, 10(9), pp. 1–17.
- Harrison, V.G.W. and Poulter, S.R.C., 1951. Gloss measurement of papers – the effect of luminance factor. *British Journal of Applied Physics*, 2(4), pp. 92–97.
- Helbig, T. and Bosse, R., 1993. *Druckqualität: Grundlagen der Qualitätsbewertung im Offsetdruck*. Frankfurt/Main: Polygraph Verlag.
- Hunter, R.S. and Harold, R.W., 1987. *The Measurement of Appearance, 2nd edition*. New York: John Wiley & Sons Inc.
- Hunter, R.S., 1937. Methods of determining gloss. *Journal of Research of the National Bureau of Standards*, 18(1), pp.19–39.
- Ignell, S., Kleist, U. and Rigdahl, M., 2010. Evaluating contrast gloss of textured polymeric surfaces. *Polymer Engineering & Science*, 50(11), pp. 2114–2121.
- Karlović, I., Novaković, D. and Novotny, E., 2010. The influence of surface topography of UV coated and printed cardboard on the print gloss. *Journal of Graphic Engineering and Design*, 1(1), pp. 23–31.
- Kettler, V., HW-Industries GmbH & Co. KG, 2005. *Verfahren zur Herstellung von Laminat-Paneele*. DE10217919B4.
- Leloup, F.B., Pointer, M.R., Dutré, P. and Hanselaer, P., 2011. Luminance-based specular gloss characterization. *Journal of the Optical Society of America*, 28(6), pp. 1322–1330.
- Loefgren, M., 2005. Winning at the first and second moments of truth: an exploratory study. *Managing Service Quality: An International Journal*, 15(1), pp. 102–115.

Obein, G., Knoblauch, K. and Vienot, F., 2004. Difference scaling of gloss: nonlinearity, binocularity, and constancy. *Journal of Vision*, 4(9), pp. 711–720.

Pommer, K., Bech, P., Wenzel, H., Caspersen, N. and Olsen, S.I., 2003. *Handbook on Environmental Assessment of Products*. [pdf] Danish Environmental Protection Agency. Available at: <<http://lca-center.dk/wp-content/uploads/2015/08/Handbook-on-environmental-assessment-of-products.pdf>> [Accessed 19 April 2016].

ProCarton Association of European Cartonboard and Carton Manufacturers, 2006. Shopper am POS: Verkaufsfoerdernd verpacken: sinnvoll und sinnlich. [pdf] Bensheim: ProCarton. Available at: <<http://www.inspiration-verpackung.de/assets/A-PDF-Downloads-Bihler/ShopperBroschreVerkaufsfoerdernd-verpacken100522.pdf>> [Accessed 22 March 2016].

Radermacher, K., 2016. *Ökologisch-ökonomische Entscheidungen in Unternehmen: Auswirkungen auf die Produktqualität am Beispiel der Druck- und Verpackungsindustrie*. Muenchen: oekom.

Radermacher, K., Dieckmann, D. and Jung, U., 2015. Dependency of colored background on gloss measurement of high-glossy UV coatings. *International Journal of Printing, Packaging & Allied Sciences*, II, pp. 12–21.

Sachs, L. and Hedderich, J., 2009. *Angewandte Statistik: Methodensammlung mit R, 13. edn*. Heidelberg: Springer.

Sachs, L., 2004. *Angewandte Statistik: Anwendung statistischer Methoden, 11. edn*. Heidelberg: Springer.

Seeger, H., 2009. *Praxisbuch Packaging: Wie Verpackungsdesign Produkte verkauft*. Muenchen: mi-Wirtschaftsbuch, FinanzBuch Verlag GmbH.

Wendt, G., 2009. *Psychophysikalische Untersuchungen zur Glanzwahrnehmung*. Ph.D. dissertation. Christian-Alberts-Universität. [pdf] Available at: <http://macau.uni-kiel.de/servlets/MCRFileNodeServlet/dissertation_derivate_00003093/diss_wendt_2010.pdf?hosts=local> [Accessed 20 July 2016].



JPMTR 085 | 1610
DOI 10.14622/JPMTR-1610
UDC 655.1 | 62-1/-9

Research paper
Received: 2016-06-05
Accepted: 2016-09-10

Improving run-time stability with aerosol jet printing using a solvent add-back bubbler

Arjun Wadhwa¹, Denis Cormier², Scott Williams³

¹ Quest Integrated, LLC,
19823 58th Pl. South, Suite 200, Kent, WA 98032 (USA)

E-mail: a.wadhwa@qi2.com

² Industrial and System Engineering,
Rochester Institute of Technology,
81 Lomb Memorial Drive, Rochester, NY 14623 (USA)

E-mail: drceic@rit.edu

³ School of Chemistry and Materials Science,
Rochester Institute of Technology,
85 Lomb Memorial Drive, Rochester, NY 14623 (USA)

E-mail: sawppr@rit.edu

Abstract

Aerosol jet printing is a non-contact process capable of printing on conformal and flexible surfaces. Aqueous or solvent nano-inks are pneumatically atomized under nitrogen. The atomizing gas flow through the atomization cup leads to evaporation and removal of volatile solvent(s). As the ink solid loading fraction increases with the loss of solvent during atomization, the rheological changes eventually lead to instabilities in print output. A potential solution to this problem is to moisten the incoming atomizing gas with a solvent add-back system. In this study, neat co-solvent solutions of ethanol and ethylene glycol at 85 : 15 and 30 : 70 mixing ratios were atomized using nitrogen flow rates ranging from 600 to 1000 cm³·min⁻¹ (ccm, cubic centimeters per minute). It was observed that ethanol, being the more volatile solvent, was depleted from the neat solution at a much higher rate than ethylene glycol. When nitrogen gas was passed through a bubbler prior to atomization, an excessive amount of ethanol was returned to the neat solution. The solvent loss rate from an ethanol rich neat solution (80%) was higher compared to an ethylene glycol rich neat solution. Perfecting the solvent add-back rate to an ink will enable longer print runs in a manufacturing environment.

Keywords: aerosol jet printing, direct write, ink stability, solvent evaporation rate

1. Introduction and background

Direct-write (DW) printing refers to a class of additive manufacturing processes in which inks or pastes are digitally deposited in any desired geometric pattern onto a substrate of interest. Substrate examples could include molded plastic parts, 3D printed parts, composite panels, etc. Direct-write printing is rapidly gaining importance in several industries. For example, significant weight reductions are possible when electrical traces are printed onto or even within a non-planar component surface instead of using externally routed wires and connectors (Kessler et al., 2009). Printed antennas that conform to non-planar surfaces provide tremendous flexibility in location, number, and size of antennas (Deffenbaugh et al., 2013). A broad spectrum of electronic components such as ring oscillators (Ha et al., 2013), thin film transistors (Jones et al.,

2010), and hydrogen sensors (Liu et al., 2012) can be printed directly on a wide-variety of substrates, regardless of whether or not the substrate is planar.

Whereas conventional lithography processes have much higher feature resolutions than current DW printing technologies, DW processes are able to deposit a much wider array of materials. Practically speaking, any nano-material that can be synthesized in ink form can be DW printed. For example, solid oxide fuel cells employing yttria-stabilized zirconia (YSZ) electrolyte layers and YSZ-nickel oxide composite anodes have been aerosol jet printed (Sukeshini et al., 2012). Specifically, aerosol jet printed poly(3-hexylthiophene) (P3HT) polymer semiconductor inks for use in printed transistors was reported by Kim et al. (2013). Aerosol

jet printing was also used to deposit biologically active inks (Grunwald et al., 2010).

When used in printed electronics applications, DW processes are also attractive from an environmental perspective. Rather than plating copper, conductive inks (e.g. copper, silver, gold, etc.) can be selectively printed thereby minimizing material use and hazardous waste disposal.

For any relatively new manufacturing technology, the transition from a research and development environment to a production environment is largely dictated by factors such as cost, throughput, and process stability and repeatability. This paper specifically focuses on run-time printing stability on a production scale aerosol jet printing platform when using co-solvent blended ink systems that have, in many cases, vastly different boiling points or evaporation rates.

1.1 Aerosol jet printing

1.1.1 Process fundamentals

Aerosol Jet (AJ) printing is a DW printing technique for depositing a pre-set pattern or layout (Hon, Li and Hutchings, 2008). It is capable of producing fine pitch structures below $50\ \mu\text{m}$ using nano-ink suspensions with particle sizes up to a recommended maximum of approximately $700\ \text{nm}$ and with an ink viscosity range from 0.7 to $2500\ \text{mPa}\cdot\text{s}$ (Goth, Putzo and Franke, 2011). The AJ process steps are illustrated in Figure 1, and typical process parameters are given in Table 1. A fluid can be atomized in the reservoir either pneumati-

cally with nitrogen gas or ultrasonically. The maximum wet droplet diameter is typically on the order of 2 to $5\ \mu\text{m}$ (Mahmud et al., 2010).

Although AJ printing has been used for numerous interesting applications produced in very small quantities, the process as a manufacturing option has not been widely studied. Hoerber et al. (2011) studied the effect of process parameters on printed line width and thickness. They observed that the line width increased with increases in atomization and sheath flow rates. Also, line width and height increased when the number of print passes was increased. Conversely, line width decreased when the translation speed increased.

Sukeshini et al. (2010) studied the effect of varying the nozzle stand-off distance and virtual impactor exhaust flow rate values. It was observed that for the YSZ ink used in the study, the amount of material deposited increased to a maximum; and then, decreased as virtual impactor exhaust flow rate was increased. Several studies determined a process parameter window that influences the line quality, electrical properties and adhesion of AJ printed silver lines (Verheecke et al., 2012; Mahajan, Frisbie and Francis, 2013).

1.1.2 Current aerosol jet challenges

For AJ printing to be a viable production tool, run-time stability will depend on a consistent ink composition. Many inks are colloidal dispersions in a solvent (single solvent or co-solvent). Surfactants are optionally included to lower the ink surface tension, and dispersants are often used to prevent particle coagulation.

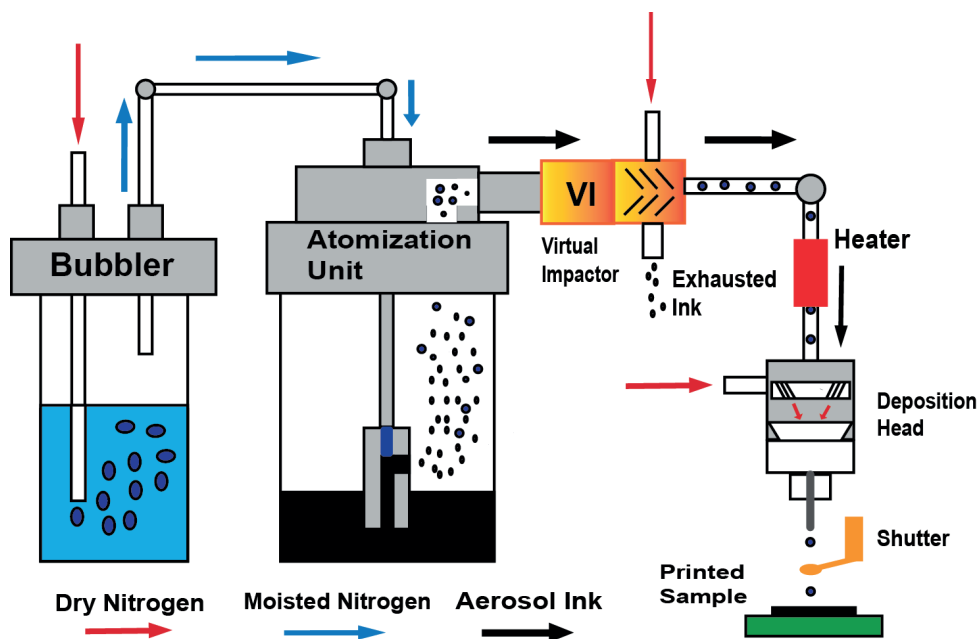


Figure 1: Schematic representation of the aerosol jet printing process

Table 1: Aerosol jet printing process parameters

Process Parameter	Units	Recommended Range
Atomization Flow Rate	$\text{m}^3 \cdot \text{s}^{-1}$	8.33×10^{-6} to 20.0×10^{-6}
Virtual Impactor Flow Rate	$\text{m}^3 \cdot \text{s}^{-1}$	6.67×10^{-6} to 18.3×10^{-6}
Sheath Gas Flow Rate	$\text{m}^3 \cdot \text{s}^{-1}$	0.50×10^{-6} to 1.67×10^{-6}
Tube Heater Temperature	$^{\circ}\text{C}$	20 to 90
Platen Temperature	$^{\circ}\text{C}$	20 to 90
Nozzle Diameter	μm	100, 150, 200, 250, 300
Nozzle Stand-Off Distance	mm	3 to 10

During atomization, nitrogen gas flow over the ink surface causes preferential loss of high volatile components through evaporation. Preferential component loss will create changes in the physical ink properties. The high vapor pressure (low boiling point) solvent removal rate would depend on the dry atomizing gas flow rate (nitrogen gas flow rate) over the solvent, and the component fractional vapor pressure as illustrated in Equation 1.

$$Q_v = Q_{N_2} \cdot \frac{P_v}{P_T \cdot P_v} \quad [1]$$

where Q_v is the flow rate of solvent vapors ($\text{m}^3 \cdot \text{s}^{-1}$), Q_{N_2} is the flow rate of atomizing gas ($\text{m}^3 \cdot \text{s}^{-1}$), P_T is the total pressure (kPa), and P_v is the vapor pressure (kPa) of volatile solvent component.

With a 69 kPa (10 psi) atomization cup pressure, Figure 2 illustrates the simulated loss of ethanol (P_v) from the atomizing cup via evaporation at different nitrogen flow rates and temperatures using Equation 1. Antoine's equation was used to calculate the partial pressure due to ethanol as a function of temperature. To illustrate, a common solvent blend used in aerosol jet printing are

ethanol and ethylene glycol mixtures. In comparison, ethanol has a low normal boiling point (78.4°C) and higher normal vapor pressure (5.95 kPa) than ethylene glycol (197.1°C and 0.0075 kPa, respectively). Ethylene glycol loss during atomization, therefore, is approximately 0.1% that of ethanol. Consequently, in co-solvent inks containing both low and high vapor pressure constituents, one can effectively focus on the high vapor pressure solvent component when trying to control ink stability. As shown in Figure 2, the expected rate of solvent transfer with the atomization gas, and therefore solvent loss in the atomization cup, increases significantly with both carrier gas flow rate and temperature.

We propose to control solvent loss by feeding the atomizing gas through a bubbler system prior to the atomizing cup as seen in Figure 1. The idea was that moist atomizing gas will “add back” solvent into the atomizing cup. We are not aware of any research using such an add-back method. The aim of this paper, therefore, was to study the impact of this solvent add-back approach by monitoring the solvent blend composition during atomization over time while holding the atomization cup temperature constant at 23°C .

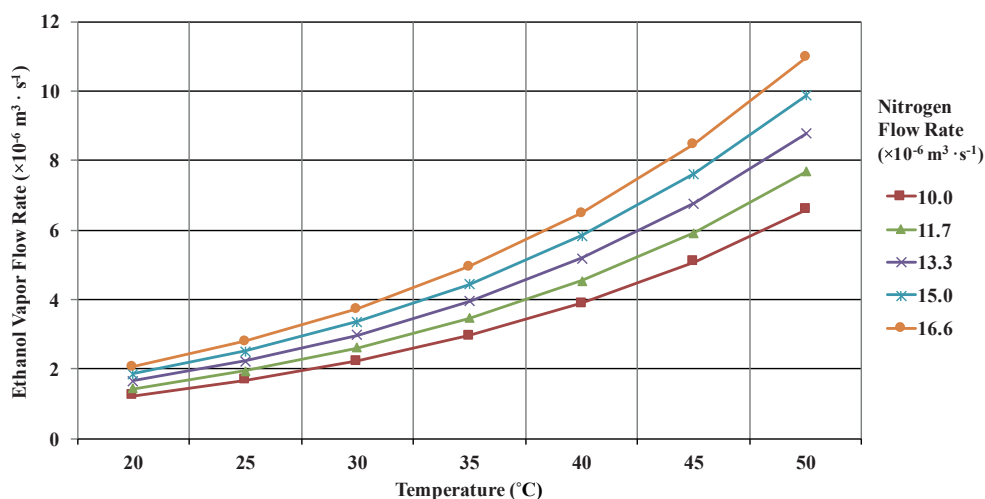


Figure 2: Simulated ethanol loss from the atomization cup as a function of different nitrogen flow rates and atomization cup temperatures

2. Materials and methods

All experiments were conducted using an Optomec Aerosol Jet system equipped with two pneumatic atomizers. A bubbler add-back system, as seen in Figure 1, contains ethanol, the more volatile solvent component (vide infra). Nitrogen gas was bubbled through the solvent, thereby transferring solvent vapor. The saturation state, of the more volatile component, in the atomization cup will depend on flow rate and cup temperature. In this study, atomization cup temperature was kept constant at approximately 23 °C.

In order to study AJ ink stability as a function of process parameter values, two types of neat co-solvent solutions of ethylene glycol (higher boiling point, lower vapor pressure) and ethanol (lower boiling point, higher vapor pressure) were prepared. No pigment components were added in this study. The co-solvent blend is used in a number of commercial nano-inks, and was therefore a representative co-solvent system of practical significance. The less volatile ink blend consisted of 30% mass fraction of ethanol and 70% mass fraction of ethylene glycol. The more volatile ink blend consisted of 85% mass fraction of ethanol and 15% mass fraction of ethylene glycol. These two inks were AJ printed over an extended

period of time (210 minutes or 3.5 hours) at different atomization flow rates ranging from $10.0 \times 10^{-6} \text{ m}^3 \cdot \text{s}^{-1}$ to $16.6 \times 10^{-6} \text{ m}^3 \cdot \text{s}^{-1}$. Experiments were conducted without the solvent add-back system, and then again, with the solvent add-back system. Samples of the neat solutions were extracted from the atomization cup at 30 minute time intervals in order to determine the stability of the neat solution as measured by the relative proportions of the two co-solvents.

The relative ethanol and ethylene glycol proportions, in a given sample, were determined by measuring the refractive indices on an Abbe Refractometer. Using the rule of mixtures, the percentage of ethanol in any sample can be determined using Equation 2 in order to quantitatively determine the rate at which the more volatile ethanol solvent was being lost during atomization.

$$\text{Mass fraction of Ethanol} = \frac{RI_{EG} - RI_S}{RI_{EG} - RI_{Eth}} \times 100 (\%) \quad [2]$$

where RI_{EG} is the refractive index of ethylene glycol (measured value = 1.43854), RI_S is the refractive index of the extracted ink sample, and RI_{Eth} is the refractive index of ethanol (measured value = 1.36163).

3. Results and discussion

3.1 Ink stability without solvent add-back

Figures 3 and 4 show results of experiments for the low volatility and high volatility inks, respectively, run without the solvent add-back system.

Figures 3 and 4 clearly demonstrate a substantial ethanol loss in a relatively short amount of time (3½ hours) when atomization was done with dry nitrogen gas. For the 30% ethanol ink, nearly half of the ethanol was lost in just three hours of printing. The high vapor pressure solvents (e.g. ethanol) allow aerosol ink droplets to rapidly dry on the substrate. As high vapor pressure co-solvent is depleted in the ink, the drying speed and surface energy of the ink changes – sometimes dramatically. As the drying time of printed lines increases due to loss of high vapor pressure co-solvents in the atomizing cup, the printed lines have time to both (1) spread out and form wider traces; or, (2) retract into discontinuous beads resulting from a surface tension increase. These printed fluid and drying dynamics are common for many print processes using liquid inks. For example, an ink containing 85% ethanol would have a starting surface tension of about $23 \text{ mN} \cdot \text{m}^{-1}$ (data not shown). Upon complete ethanol loss in co-solvent ink, the surface tension would match that associated with ethylene glycol ($47.7 \text{ mN} \cdot \text{m}^{-1}$) resulting in a dynamic increase in contact angle with the substrate. Practically

speaking, this means that the quality of the printed lines, as indicated by line width, thickness, and overspray, will change as the high vapor pressure solvent is depleted. Figures 3 and 4 point towards a strong need for an alternative approach to atomization with high vapor pressure co-solvent blends. The aforementioned solvent add-back system was a relatively simple low-cost approach.

3.2 Ink stability with solvent add-back

In order to quantitatively assess the solvent add-back system effectiveness on ink stability, a second set of experiments were run using the solvent add-back system (see Figure 1). The bubbler contained the more volatile ethanol since the rate of evaporation of ethylene glycol at room temperature is substantially lower than that of ethanol. Figures 5 and 6 show results of experiments for the 30% and 85% ethanol inks at $10.0 \times 10^{-6} \text{ m}^3 \cdot \text{s}^{-1}$ (low flow) and $16.6 \times 10^{-6} \text{ m}^3 \cdot \text{s}^{-1}$ (high flow) nitrogen atomization flow rates, respectively. The dry nitrogen (no solvent add-back) results are also plotted for comparison.

Figure 5 shows ethanol concentration for the low ethanol (30% mass fraction) solution. The ideal outcome would be a horizontal line indicating that the ethanol concentration remains constant over the 3½ hours of

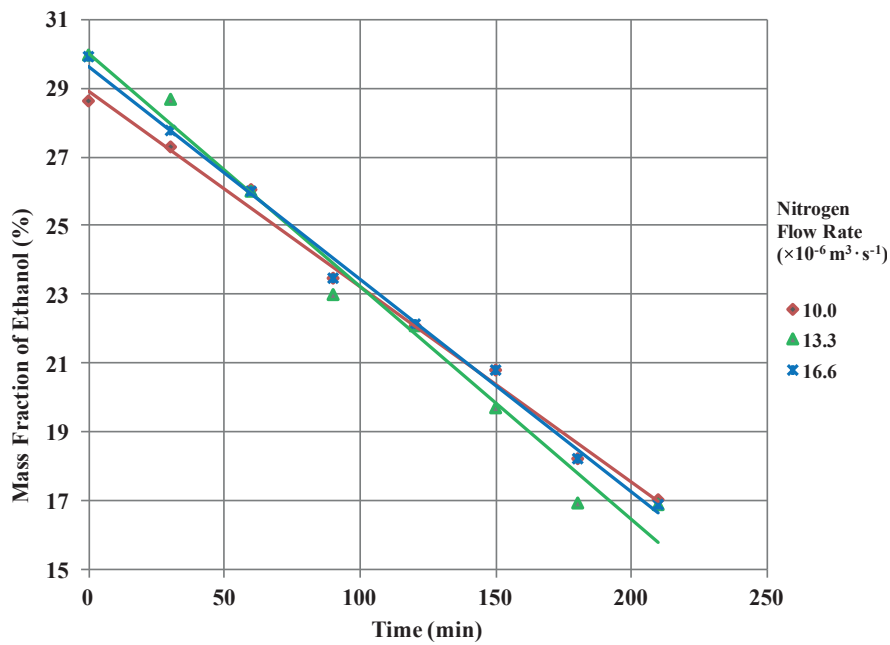


Figure 3: Mass fraction of ethanol versus time plot for atomization of a 30 % ethanol 70 % ethylene glycol co-solvent mixture without the bubbler add-back system

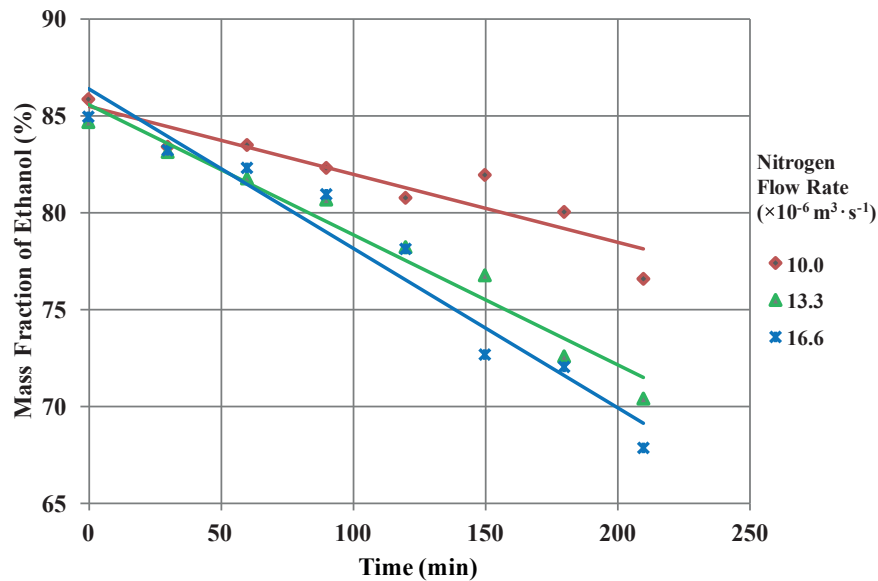


Figure 4: Mass fraction of ethanol versus time plot for atomization of an 85 % ethanol 15 % ethylene glycol co-solvent mixture without bubbler add-back

atomization. As opposed to the trends observed without an add-back system, Figure 5 illustrates that the ethanol concentration actually increased with each flow condition using a bubbler. Clearly, the rate of ethanol addition to the atomization cup was greater than ethanol loss from the cup. Possibilities to be explored

further are differences in the ethanol evaporation rates, in the two cups, due to differential flow rate anomalies; or, ethanol partial pressure depression created by the mixed solvent system used in the atomization cup. Figure 6 illustrates a similar trend for the high (85%) ethanol ink solution. As expected, the ethanol loss rate

with dry nitrogen was greatest at high atomization flow rates ($16.6\text{ m}^3\cdot\text{s}^{-1}$ or 1000 cubic centimeters per minute). When the solvent add-back bubbler technique was used, the ethanol concentration was nearly consistent with run-time.

Since it appears that a simple solvent add-back technique was able to compensate for the loss of low boiling point solvent during atomization is promising. Figure 5, however, points to the need for further development work to overcome excessive solvent add-back.

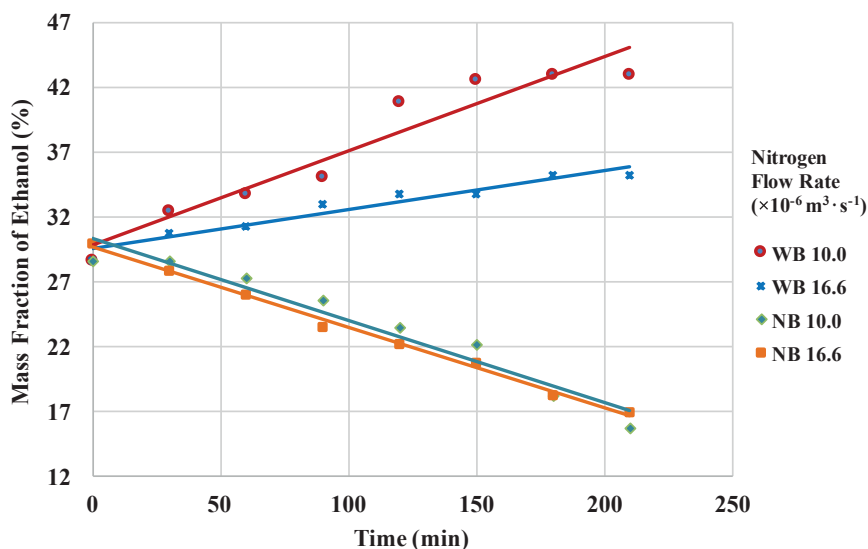


Figure 5: Mass fraction of ethanol versus time plot for atomization of 30 % ethanol 70 % ethylene glycol co-solvent mixture with (with bubbler; WB) and without (no bubbler; NB) the solvent add-back

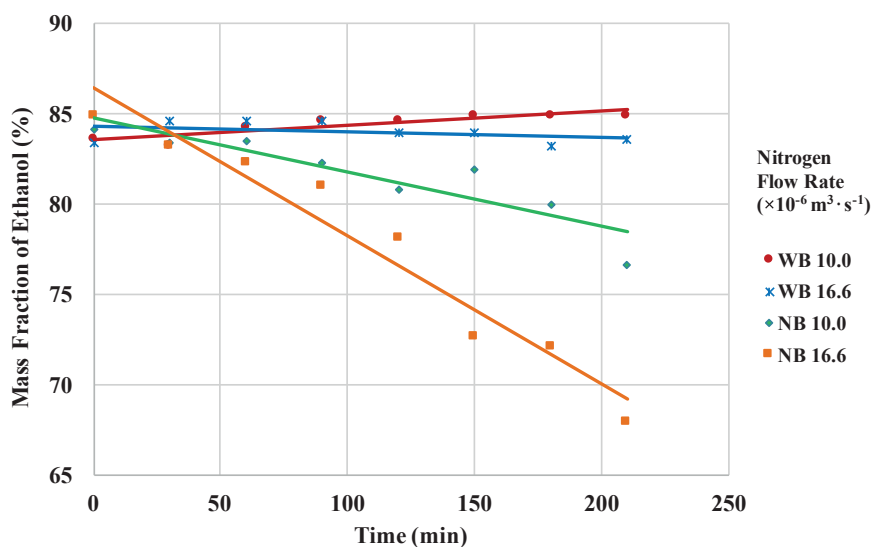


Figure 6: Mass fraction of ethanol versus time plot for atomization of 85 % ethanol 15 % ethylene glycol co-solvent mixture with (WB) and without (NB) the solvent add-back

4. Conclusions

Many ink formulations, used in AJ printing, use blends of low and high boiling point co-solvents. In some applications, slow drying inks that flow out and

form a continuous coating are desired; whereas, other applications call for fast drying inks used to print narrow lines and/or features with high aspect ratios.

Depending upon the application, the low boiling point solvent composition may range from just a few percent up to nearly 100 %. This paper has demonstrated that AJ printing with dry nitrogen gas leads to rapid loss of low boiling point, high evaporation rate, solvent(s). As the ink concentrates, the nanoparticle loading fraction increases, and the wetting and spreading ink behaviour may dramatically change. Ultimately, inks with high concentrations of low boiling point solvents may become unprintable due to a rapid shift to the higher boiling point solvent concentration. A potential solution to this problem is to add solvent back into the atomizing cup through the use of a bubbler.

The solvent add-back method uses a bubbler to moisten the nitrogen gas before it enters the atomizing cup.

This study has shown that the bubbler solvent add-back approach has the potential to overcome excessive co-solvent concentration change with low boiling point (high vapor pressure) rich solvent components. It is, however, also possible to overcompensate solvent addition when the concentration of low boiling point solvent is relatively low.

In studying Figure 5, one can envision that a blend of dry and moist nitrogen gas, in the correct ratios, will lead to continuous printing with a constant ethanol concentration. In ongoing future work, we will present new results demonstrating the effects of mixing these two mass flow conditions – dry and vapor-rich carrier gas flows. Two mass flow controllers may be needed to independently control the ratios of dry and wet nitrogen in order to maintain equilibrium.

Acknowledgments

The Authors would like to thank the contribution of Optomec Inc. for donation of the Aerosol Jet Printing Platform. This work was also supported by a grant from the National Science Foundation (USA) (NSF-PFI 12-511).

References

- Deffenbaugh, P., Church, K., Goldfarb, J. and Chen, X., 2013. Fully 3D printed 2.4 GHz Bluetooth/Wi-Fi antenna. In: *IMAPS, 46th International Symposium on Microelectronics*. 30 September – 3 October 2013. Orlando, FL: International Microelectronics Assembly and Packaging Society.
- Goth, C., Putzo, S. and Franke, J., 2011. Aerosol Jet printing on rapid prototyping materials for fine pitch electronic applications. In: *IEEE Electronic Components and Technology Conference (ECTC)*. 31 May – 3 June 2011. Lake Buena Vista, FL: IEEE Components, Packaging and Manufacturing Technology Society.
- Grunwald, I., Groth, E., Wirth, I., Schumacher, J., Maiwald, M., Zoellmer, V. and Busse, M., 2010. Surface biofunctionalization and production of miniaturized sensor structures using aerosol printing technologies. *Biofabrication*, 2(1), p. 014106.
- Ha, M., Seo, J.W., Prabhumirashi, P.L., Zhang, W., Geier, M.L., Renn, M.J., Kim, C.H., Hersam, M.C. and Frisbie, C.D., 2013. Aerosol jet printed, low voltage, electrolyte gated carbon nanotube ring oscillators with sub-5 μ s stage delays. *Nano letters*, 13(3), pp. 954–960.
- Hon, K.K.B., Li, L. and Hutchings, I.M., 2008. Direct writing technology – Advances and developments. *CIRP Annals – Manufacturing Technology*, 57(2), pp. 601–620.
- Hoerber, J., Goth, C., Franke, J. and Hedges, M., 2011. Electrical functionalization of thermoplastic materials by Aerosol Jet Printing. In: *13th IEEE Electronics Packaging Technology Conference (EPTC)*. 7–9 December 2011. Singapore: IEEE. pp. 813–818.
- Jones, C.S., Lu, X., Renn, M., Stroder, M. and Shih, W.-S., 2010. Aerosol-jet-printed, high-speed, flexible thin-film transistor made using single-walled carbon nanotube solution. *Microelectronic Engineering*, 87(3), pp. 434–437.
- Kessler, S.S., Dunn, C.T., Borgen, M., Raghavan, A., Duce, J. and Banks, D.L., 2009. A cable-free digital sensor-bus for structural health monitoring of large area composite structures. In: *Annual Conference of the Prognostics and Health Management Society*. 28–30 September 2009. San Diego, CA: PHM Society.
- Kim, S.H., Hong, K., Lee, K.H. and Frisbie, C.D., 2013. Performance and stability of aerosol-jet-printed electrolyte-gated transistors based on poly(3-hexylthiophene). *ACS applied materials & interfaces*, 5(14), pp. 6580–6585.
- Liu, R., Ding, H., Lin, J., Shen, F., Cui, Z. and Zhang, T., 2012. Fabrication of platinum-decorated single-walled carbon nanotube based hydrogen sensors by aerosol jet printing. *Nanotechnology*, 23(50), p. 505301.
- Mahajan, A., Frisbie, C.D. and Francis, L.F., 2013. Optimization of aerosol jet printing for high-resolution, high-aspect ratio silver lines. *ACS Applied Materials & Interfaces*, 5(11), pp. 4856–4864.

- Mahmud, Z., Hoey, J.M., Lutfurakhmanov, A., Daus, J., Swenson, O.F., Schulz, D.L. and Akhatov, I.S., 2010. Experimental characterization of aerosol flow through a micro-capillary. In: *ASME 2010 8th International Conference on Nanochannels, Microchannels, and Minichannels collocated with 3rd Joint US-European Fluids Engineering Summer Meeting*. 1–5 August 2010, Montreal, Quebec: ASME. pp. 949–958.
- Sukeshini, A.M., Jenkins, T., Gardner, P., Miller, R.M. and Reitz, T.L., 2010. Investigation of aerosol jet deposition parameters for printing SOFC layers. In: *ASME 2010 8th International Conference on Fuel Cell Science, Engineering and Technology*. 14–16 June 2010, Brooklyn, New York: ASME. pp. 325–332.
- Sukeshini, M., Meisenkothen, F., Gardner, P. and Reitz, T.L., 2012. Aerosol Jet printing of functionally graded SOFC anode interlayer and microstructural investigation by low voltage scanning electron microscopy. *Journal of Power Sources*, 224, pp. 295–303.
- Verheecke, W., Van Dyck, M., Vogeler, F., Voet, A. and Valkenaers, H., 2012. Optimizing aerosol jet printing of silver interconnects on polyimide for embedded electronics applications. In: T. Otto, ed., *8th International DAAAM Baltic Conference "Industrial Engineering"*. 19–21 April, Tallinn, Estonia: Tallinn University of Technology. pp. 373–379.

JPMTR 086 | 1605
 DOI 10.14622/JPMTR-1605
 UDC 655.1 = 774.8 (535.37)

Research paper
 Received: 2016-02-27
 Accepted: 2016-05-24

A method to compensate fluorescence induced white point differences in proof-processes by printing liquid fluorescent brightening agents using inkjet

Daniel Bohn¹, Michael Dattner², Stefan Fehmer³, Peter Urban¹

¹ University of Wuppertal,
 Faculty for Electrical Engineering,
 Information Technology and Media Technology,
 42119 Wuppertal, Germany

E-mails: Dbohn@uni-wuppertal.de
 Michael.dattner@bst-international.com
 S.Fehmer@laudert.de
 Purban@uni-wuppertal.de

² BST eltromat Int. GmbH,
 Heidsieker Heide 53, 33739 Bielefeld, Germany

³ Laudert GmbH & Co. KG,
 Von-Braun-Straße 8, 48691 Vreden, Germany

Abstract

One of the key goals in producing paper and cardboard in the print industry is to achieve a high whiteness degree. This is usually realized by fluorophores called OBAs (Optical Brightening Agents) or FBAs (Fluorescent Brightening Agents). The heavy use of FBAs in production substrates, while proof substrates contain a varying amount of FBAs, results into serious difficulties in any color management process, especially in terms of a white point correction. In this study, an alternative procedure is presented to achieve an illumination independent colorimetric correlation and a visual match between most proof- and production substrates. This is achieved by printing defined amounts of liquid FBA using inkjet with variable area coverage.

Keywords: OBA, color management, FBA compensation, OBA compensation, carrier

1. Introduction

One of the key goals in producing paper and cardboard in the print industry is to achieve a high whiteness degree. A high whiteness level not only imparts the impression of cleanliness and worth, but also leads to a large printable contrast of the substrate and the print (Blum et al., 2002, p. 3). Therefore, paper producers make great efforts to increase the level of whiteness of papers. Already, in the production of raw materials, be that pulp, mechanical pulp or pigment, great efforts are done to obtain raw materials with a very high whiteness level. In the actual paper production, additives and auxiliary materials are avoided which could jeopardize the whiteness of the substrate (Blum et al., 2002, p. 3).

Despite all that, fiber based substrates usually show an increase of absorption in the blue region of the electromagnetic spectrum between 380 nm and 450 nm. The main reason for this spectral behavior is the absorption of typical fiber based substrate components such as lignin.

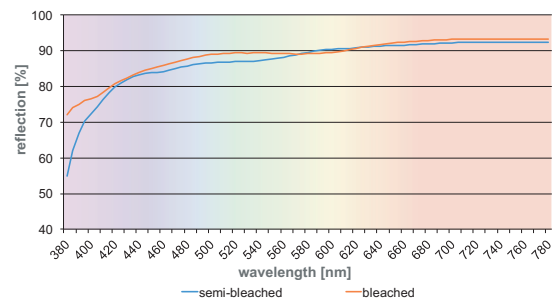


Figure 1: Reflectance of bleached and semi-bleached pulp

Figure 1 shows the spectral response of a bleached and a semi-bleached pulp. The spectral response of pulp is lower in the short wavelength range than in the long wavelength region. Therefore, paper looks yellowish. By bleaching the pulp, the yellow tint is reduced to some extent but not fully eliminated (Bieber et al., 1989, p. 18). To overcome this yellowish tint, several addi-

tives (fillers) are available and used by the paper industry to improve the whiteness level, such as titan dioxide (TiO_2) or calcium carbonate (CaCO_3) (Nelson, 2007, p. xix). Bieber demonstrates that papers loaded with expensive fillers like TiO_2 show an overall decrease of absorption for each wavelength but they still cannot fully compensate for the yellowish tint (Bieber et al., 1989, p. 19).

1.1 Fluorescent Brightening Agents in general

A very cheap, and therefore, commonly used additives to overcome the yellowish tint are so called Fluorescent Brightening Agents (FBAs) – fluorophore substances that show fluorescence effects (Ai, 2015, p. 3). They are excited in the invisible UV range as well as partially in the blue region (250 nm to 425 nm) of the electromagnetic spectrum and emit mainly “blue light” in the visible spectral range between 410 nm and 550 nm.

More generally, fluorescence is the result of a three-stage process that occurs in certain molecules called fluorophores or fluorescent dyes. A fluorescent probe is a fluorophore designed to respond to a specific stimulus. The process responsible for the fluorescence of fluorescent probes and other fluorophores is illustrated by a Jablonski diagram and can be divided into three stages (Ai, 2015, p. 3):

Stage 1:

A photon is supplied by an external source such as an incandescent lamp and is absorbed by a fluorophore, creating an excited electronic singlet state (S_1').

Stage 2:

The excited state exists for a finite time (typically 1–10 nanoseconds). During this time, the fluorophore undergoes conformational changes and is also subject to a multitude of possible interactions with its molecular environment. These processes have two important consequences. First, the energy of S_1' is partially dissipated, yielding a relaxed singlet excited state (S_1) from which fluorescence emission originates. Second, not all the molecules initially excited by absorption (Stage 1) return to the ground state (S_0) by fluorescence emission. The fluorescence quantum yield is the ratio of the number of fluorescence photons emitted (Stage 3) to the number of photons absorbed (Stage 1).

Stage 3:

A photon of energy is emitted, returning the fluorophore to its ground state S_0 . Due to energy dissipation during the excited state lifetime, the energy of this photon is lower, and therefore of longer wavelength, than the excitation photon.

1.1.1 Fluorescent Brightening Agent types

Widely used FBAs are 1,3,5-triazinyl-derivates of 4,4'-diaminostilbene with the ability to carry additional

sulfonic acid groups (Blum, Linhart and Frenzel, 2002, p. 2). Next to such “classical” FBAs, newer types such as derivates of 4,4'-distyrylbiphenyl are known (Blum et al., 2002, p. 3). Figure 2 shows a general chemical formation of a diaminostilbene molecule.

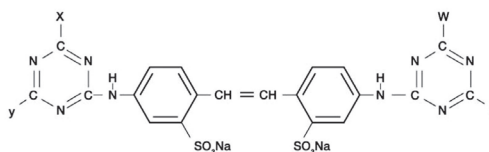


Figure 2: A typical chemical structure of diaminostilbene (Brandt, 2008, p. 7)

Mainly three types of optical brighteners or FBAs are used by the paper industry, all based on the mentioned diaminostilbene molecule shown in Figure 2. The main difference originates from the number of solubilizing sulfonic acid groups (Blum, Linhart and Frenzel, 2002, p. 3; Holik, 2006):

- The diaminostilbene-disulfonated FBA has two sulfonic groups; the two other substituents could be hydrophilic groups. This FBA has a very good affinity to cellulose, but limited solubility and is mostly used in the wet-end.
- The most commonly used FBA is the tetrasulfonated type. The tetrasulfonated FBA is a versatile substance because of its medium affinity and good solubility. It can be used in most stages of paper-making: wet-end, size-press and coating.
- The hexasulfonated FBAs are especially used in coatings where high brightness is required.

1.1.2 Fluorescent Brightening Agent concentration

The intensity of the fluorescent emission of FBAs highly depends on the FBAs concentration in the substrate coating and/or the pulp (Bieber et al., 1989, pp. 22–23). Generally, a higher FBA concentration results in a more intense emission. Figure 3 shows four laboratory substrates that only differ in their FBA concentration.

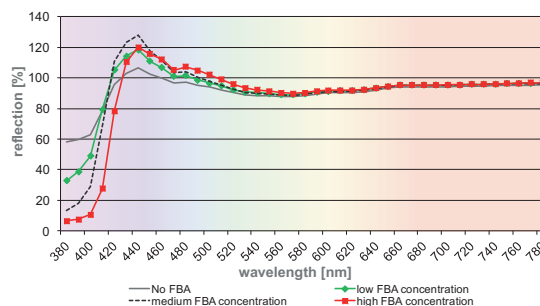


Figure 3: Influence of the FBA concentration on the emission, under M1 measurement condition

However, the FBA concentration cannot be increased infinitely. At a certain point, a so called “greening effect” can be observed (Bieber et al., 1989, p. 40). This effect results because FBAs need sufficiently enough OH binding groups to develop a stable blue emission (Blum, Linhart and Frenzel, 2002, p. 2). As a result, the emission between 460 nm and 550 nm is still increasing, while the main emission (peak emission) at 450 nm stagnates or even drops (‘medium FBA concentration’ vs. ‘high FBA concentration’ in Figure 3). Hence, the original blue emission shows a greenish tint. Please note that the substrates offer a limited amount of OH binding groups (cf. chapter 1.1.4).

1.1.3 Available ultraviolet radiation

Dattner, Bohn and Urban (2011) showed that the relative spectral power distribution (RSPD) in the UV range indicates the intensity of the FBA emission in the blue-range of the electromagnetic spectrum. That means that a high intensity of UV radiation within the RSPD leads to an intensive emission and vice versa.

Figure 4 shows the spectral response of a brightened substrate for several UV radiation levels.

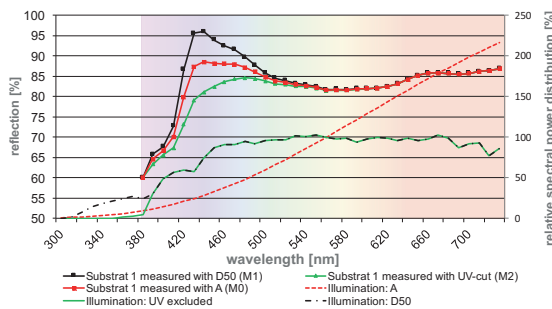


Figure 4: Influence of available UV radiation on the FBA emission concerning measurement condition M1, M2 and M0

The differences and the individual influences of the illuminant ‘UV excluded’ (M2; no radiation in the UV range), the illumination ‘A’ (M0; low radiation in the UV range) and the illumination ‘D50’ (M1; high radiation in the UV range) are shown in Figure 4 (Please note: The measurement conditions M0, M1 & M2 are explained in chapter 1.2). It is shown that a higher amount of UV radiation leads to a stronger emission in the visible blue spectrum. Especially this FBA property leads to serious issues in proofing process and will be discussed in detail.

1.1.4 Carrier and substrate composition

In order to enable fluorescence of FBAs, so called carrier substances are needed. Carrier enables a monomolecular distribution of FBAs in one layer (Blum, Linhart and Frenzel, 2002, p. 2). Typically, carriers are added to the coating and/or the paper pulp. Possible carriers are water

soluble polymers (e.g. polyvinyl alcohol $[(C_2H_4O)_x]$), carboxymethyl cellulose (a cellulose derivative with carboxymethyl groups $[CH_2CO_2H]$), anionic or non-anionic degraded starch, and casein (Blum, Linhart and Frenzel, 2002, p. 3). Several other substances as carriers are possible (Blechsmidt, 2013, p. 447).

Many substrates, especially uncoated substrates, show a high concentration of cellulose fibers which also act as carriers (Blechsmidt, 2013, p. 447). Other substrates (especially proof substrates) contain only a small number of carrier molecules or none at all, as shown also in the results of this study.

1.1.5 Competitive absorbing substances

While the intensity of the emission highly depends on the amount of UV radiation available in the extinction range of any FBA, the FBA absorption can be reduced by other competitive absorbing substances in the paper composition that also show a strong absorption in this range. Figure 5 shows the spectral response of several slightly brightened (Substrates 1 & 2) and unbrightened substrates (Substrates 3 & 4) including the UV range.

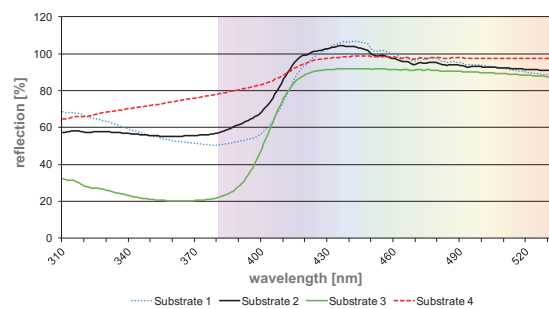


Figure 5: Spectral response of four substrates in the UV and blue range, under M1 measurement condition

When comparing the four substrates in Figure 5, only ‘substrate 4’ shows a decent absorption in the UV range. It can be assumed that loading this substrate with FBAs would lead to a high FBA emission efficiency. Compared to this, the assumed FBA emission efficiency would be lower for substrates 1, 2 & 3 because of their higher absorption in the UV range due to other competitive absorbing substances in the substrates.

1.1.6 Spectral response of Fluorescent Brightening Agents

Fluorophores are available with various excitation and emission characteristics. All types of FBAs used in the paper industry (cf. chapter 1.1.1) show a very comparable emission characteristic (shape of the spectral response curve) (cf. Figure 6). Please note that differences in the emission intensity occur because of different amounts of FBAs in each substrate.

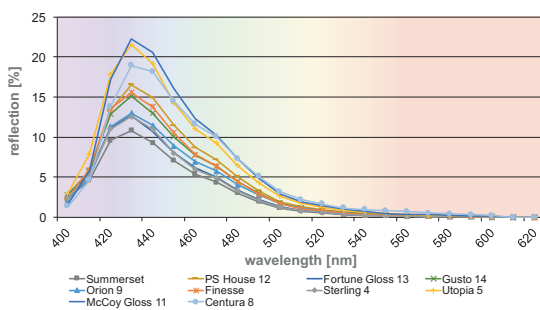


Figure 6: FBA emission of several proof- and production substrates, measured under M1 measurement conditions

Figure 6 shows the FBA emission of a representative collection of production substrates. Note: Only the FBA emission is shown. This is done by measuring each substrate once with the M2 condition and once with the M1 condition and calculating the difference of both measurements for each wavelength (cf. Equation 1).

$$\widehat{\beta}_{\text{emission}}(\lambda) = \beta_{\text{M1}}(\lambda) - \beta_{\text{M2}}(\lambda) \quad [1]$$

where $\widehat{\beta}_{\text{emission}}(\lambda)$ is the wavelength depending emission of a brightened substrate, $\beta_{\text{M1}}(\lambda)$ is the measurement of a substrate using M1 condition, and $\beta_{\text{M2}}(\lambda)$ is the measurement of a substrate using M2 condition.

1.2 Influence of Fluorescent Brightening Agents on the proofing process

ISO 3664:2009 (International Organization for Standardization, 2009a) in combination with ISO 13655:2009 (International Organization for Standardization, 2009b) defines the measurement/illumination conditions M0, M1, M2, and M3. The measurement condition M1 is based upon the known D50 relative spectral power distribution defined by ISO 13655:2009, but it is extended to the spectrum of the illuminant's UV range in its definition. This means a “real” illumination must have a comparable amount of UV radiation as defined in ISO 13655:2009 within defined tolerances (International Organization for Standardization, 2009a). The M1 condition is also obligatory for new light boxes. Practically, using ISO 3664:2009 conforming measurement equip-

ment and light boxes induces an increase of excitation of the FBAs. Hence, FBA induced effects are increased.

The standardized measurement condition M0 is based on standard illuminant A (low UV radiation), M2 is based on any standard illuminant without UV component and M3 is based on any illuminant with polarization filters.

The consequence of the heavy use of FBAs in production substrates is the now obligatory consideration of the UV amount. Therefore, it becomes possible that a brightened substrate (e.g. an offset production paper) is measured with a spectral photometer as it is perceived by the operator in a light booth if both are relying on the M1 condition (and therefore a comparable high UV intensity).

Today, most proof substrates are not or only slightly brightened, while many production substrates show a very high FBA concentration. This difference leads to serious issues in proofing processes, especially with regard to ISO 3664:2009. Figure 7 shows two measurement situations (M2 & M1) that result in different ΔE_{00} values for unequally brightened substrates. The expected visual color difference $\Delta E_{\text{percepted}}$ in the case of a light booth using the M1 condition, is also presented to show the correlation to measurements with the M1 condition and the difference to the M2 condition (ΔE_{00} and $\Delta E_{\text{percepted}}$ are theoretically equal if both devices, the measurement device as well as the light booth, offer the same UV amount). Please note that a conventional white point correction is already performed for the following proof substrates. Therefore, the identified ΔE_{00} values are only caused by the fluorescence effect.

Table 1 shows that a measurement of the production substrate ‘Heaven42’ from the company Scheufelen GmbH + Co. KG, and the proof substrate ‘Epson SPP 205’ from the company EPSON Deutschland GmbH result in a $\Delta E_{00} = 1.99$, if measurement condition M2 is used. In contrast, measurement condition M1 results in a high $\Delta E_{00} = 8.02$ because of large differences in the FBA concentration of both substrates. Consequentially a $\Delta E_{\text{percepted}} = 8.02$ can be expected.

Table 1: Resulting color differences ΔE_{00} caused by highly deviating FBA concentrations

Substrate	Measurement condition M2	Measurement condition M1	Light booth
Proof substrate: Epson SPP 205 (unbrightened)	$L^* = 94.6$ $a^* = -0.1$ $b^* = -1.9$	$L^* = 94.6$ $a^* = -0.4$ $b^* = -2.9$	
Production substrate: Heaven 42 (highly brightened)	$L^* = 93.1$ $a^* = 0.0$ $b^* = -3.9$	$L^* = 93.7$ $a^* = 2.3$ $b^* = -12.9$	
Color difference	$\Delta E_{00} = 1.99$	$\Delta E_{00} = 8.02$	$\Delta E_{\text{percepted}} = 8.02$

Table 2: Resulting color differences ΔE_{00} caused by medium high deviating FBA concentrations

Substrate	Measurement condition M2	Measurement condition M1	Light booth
Proof substrate: Trust Premium Glossy (slightly brightened)	$L^* = 95.1$ $a^* = 0.2$ $b^* = -5.3$	$L^* = 95.6$ $a^* = 1.2$ $b^* = -5.3$	
Production substrate: Heaven 42 (highly brightened)	$L^* = 93.1$ $a^* = 0.0$ $b^* = -3.9$	$L^* = 93.7$ $a^* = 2.3$ $b^* = -12.9$	
Color difference	$\Delta E_{00} = 1.69$	$\Delta E_{00} = 5.59$	$\Delta E_{\text{percepted}} = 5.59$

Even if a proof substrate is brightened, it is not assured to gain a sufficient match, especially for highly brightened production substrates (cf. Table 2).

Table 2 shows that measurements of the production substrate ‘Heaven42’ and the proof substrate ‘Trust Premium Glossy’ from the company Schoeller Technocell GmbH & Co. KG lead to a $\Delta E_{00} = 1.69$, if measurement condition M2 is used. In contrast, measurement condition M1 results in a medium high $\Delta E_{00} = 5.59$ because of still large differences in the FBA concentration of both substrates. Consequentially a $\Delta E_{\text{percepted}} = 5.59$ can be expected.

Table 1 and 2 show that it is quite possible to identify color differences between a brightened production paper and a corresponding unbrightened proof substrate using the M2 condition. These differences do not correspond to the differences that are perceived in a light booth using the M1 condition. Furthermore, if both substrates are observed under a non ISO 3665:2009 conforming illumination, FBA induced differences on the perception become hardly predictable.

So far, only the direct effect of the substrate is shown. Usually, printing substrates are printed with various colors and various ink systems. Each color, color combination and area coverage combination leads to an individual influence on the FBAs absorption and emission (Dattner, Bohn and Urban, 2011).

Figure 7 gives an overview about color shift induced by FBAs at different locations in the CIELAB color space for the production substrate ‘Heaven42’. Please note: The L^* value is only very slightly affected by FBAs and is therefore not plotted in this graph.

It is shown that almost all color coordinates are more or less affected by the substrate’s FBA. This results in a gamut grow in the blue region of the CIELAB color space while a slight gamut decrease in the green and yellow region can be identified. It can be concluded that not only the substrate is affected and critical in the proofing process, but also colors printed on it.

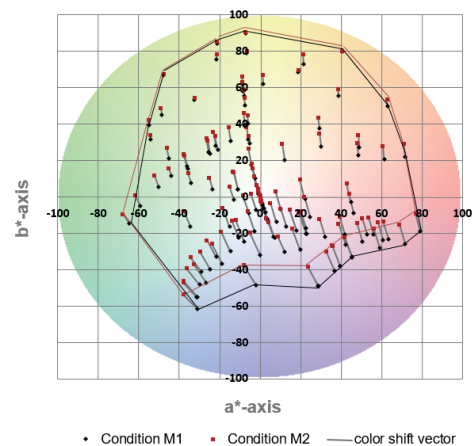


Figure 7: Influence of FBAs on color coordinates of colors and the resulting color gamut

1.3 State of the scientific knowledge

It is documented and explored that the effect of different FBAs in various printing substrates leads to individual, illumination dependent effects with unprinted and fully printed surfaces (Erhard, Alber and Götze, 2003; Löffler and Green, 2008; Zwinkels, 2008). The optical behavior of halftone samples on brightened substrates is also empirically determined (Kraushaar and Gefner, 2006; Fiebrandt, 2007; Pertler and Bertholdt, 2007), but not physically founded. In the past few years, several physically founded models have been developed and described (Dattner, Bohn and Urban, 2011).

While these models show a good prediction performance, they cannot solve the initial issue, that a brightened paper will often show a higher reflection in the blue region of the spectrum for the measurement condition M1 than a corresponding unbrightened proof substrate.

The ISO standard 3664:2000, which specifies viewing and measurement conditions for images on reflective media, has been revised in 2009 and is therefore replaced by ISO 3664:2009. While ISO 3664:2000 defines a UV metamerism index (MI_{UV}) to be smaller or

equal than 4, ISO 3664:2009 now requires $MI_{UV} < 1.5$ and recommends $MI_{UV} < 1.0$. That relates to a tolerance of the UV amount, compared to D50 being 100 %, from 60 % to 130 %. This results in a much closer correlation between the actual used illumination and the CIE daylight illuminant D50. In case of a perfect match of the UV content in the spectra, MI_{UV} becomes 0 (Kraushaar, 2012). Therefore, if the measurement device as well as the used illumination of a light booth both comply to ISO 3664:2009, the influence of FBAs are taken into account within the defined tolerances.

The Graphic Technology Research Association (fogra, 2014) recently released fogra51/fogra52 in the context of ISO 3664:2009. This is the “codename” or the label for the characterization data reflecting ISO 12647-2:2013 based printing on matt and glossy

coated offset papers (International Organization for Standardization, 2013). Using FBA rich proofing substrates, in particular to simulate FBA rich production substrates, was subject in a fogra analysis reflecting the upcoming permanence criteria of ISO 12647-7 by achieving a proof to print match (Kraushaar, 2014). Fogra51 (PSO Coated V3) defines an M1 target of $L^* = 95.0$, $a^* = 1.5$ and $b^* = -6.0$ to take FBA induced effects into account. In contrast, fogra52 (PSO Uncoated V3) defines an M1 target of $L^* = 93.5$, $a^* = 2.5$ and $b^* = -10$ (Kraushaar, 2013). In this context, new proof substrates have been developed and certified, that include some amount of FBA. The Felix Schöller Group (2016) offers fogra51 and fogra52 certified proof substrates having white points as shown in Table 3. The shown CIELAB values are provided by the Felix Schöller Group (2016).

Table 3: Properties of typical brightened proof substrates conforming to fogra51 & fogra52 under M1 condition

Substrate	Certification	Appearance	Grammage (g/m ²)	Color coordinate (M1)		
				L*	a*	b*
TRUST premium	Fogra 51	Glossy	250	95.6	1.2	-5.3
TRUST premium	Fogra 51	Semi-glossy	250	96.8	0.9	-5.1
TRUST economy	Fogra 52	Matte	150	96.9	2.3	-10.2
TRUST commercial	Fogra 52	Semi-glossy	195	96.0	1.5	-10.3

2. Methods

The final goal of this study is to simulate illumination independent any brightened production substrate with any unbrightened or slightly brightened proof substrate by printing an FBA ink layer with a variable area coverage using inkjet.

2.1 Equipment

2.1.1 Inkjet printers

In this study, two commercially available printers are used. For the actual print of the FBA ink compositions, a Canon ix6550 (DIN A3+) is used, while additional color test patches are printed in a second step using an Epson Stylus Pro 4900 proof printer.

2.1.2 Measurement devices

For the analysis of substrates and printed FBA layers a TEC5 UV-VIS laboratory spectral photometer in combination with a 45°/0° geometry and a xenon permanent light source is used. The spectral resolution is 1 nm and the spectral range is 310 nm to 990 nm. By using filters, several illumination types can be simulated, including M0, M1 and M2 in accordance to ISO 13655:2009 (International Organization for Standardization, 2009b).

The realized UV amount of the M1 measurement condition is 115% compared to nominal value, i.e. within tolerances according to ISO 3665:2009 (International Organization for Standardization, 2009a). For the analysis of printed color test charts on the FBA layers, an EFI ES-2000 is used. This device is capable to perform 45°/0° measurements with the measurement conditions M0, M1 & M2. The spectral range is limited to the visible range of the electromagnetic spectrum (380 nm to 730 nm) and offers a spectral resolution of 10 nm.

2.1.3 Measurement conditions

All measurements are done with a black backing in accordance to ISO 13655:2009, using a 45°/0° measurement geometry (International Organization for Standardization, 2009b). Colorimetric values are calculated for a 2° observer and the illuminant type D50.

2.2 Substrates

As pointed out, the goal of this study is to use any proof substrate to simulate any production substrate. Because interactions especially between different FBAs and the substrate are expected, four different proof substrates are examined.

2.4 Test chart

The test chart, developed for this study, has a wedge with test patches with area coverages ranging from 0 % up to 100 %. Because the black channel of the printer is used for the FBAink, the test chart is build up out of different area coverages of black. Therefore, a 100 % black area coverage equals a 100 % FBA ink layer area coverage (cf. Figure 9).

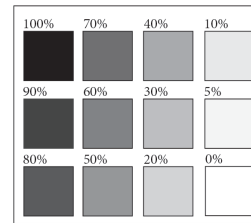


Figure 9: Test chart for FBA-ink area coverage variable investigations

3. Results

3.1 Area coverage controlled Fluorescent Brightening Agent emission

The intensity of the fluorescence is directly controlled by the area coverage of the printed FBA upon a unbrightened or slightly brightened proof substrate. To illustrate the principle, Figure 10 shows the influence of a printed FBA layer upon a proof substrate (Epson SPP 205) with area coverages starting with 0 % up to 100 % (Figure 10 top: Illumination condition M0; Figure 10 middle: Illumination condition M1; Figure 10 bottom: UV black light).

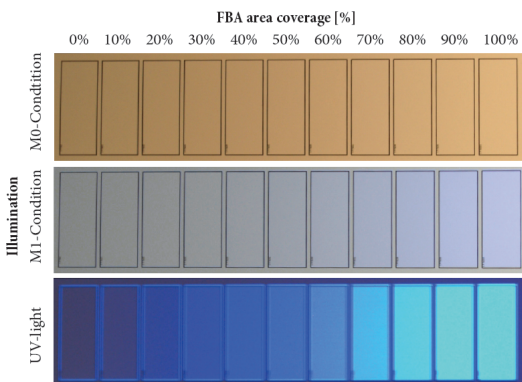


Figure 10: Illustration of the FBA induced emission effect for several area coverages and illuminations in a light booth

It can be demonstrated that an increasing FBA area coverage leads to a more intense emission in the blue region of the electromagnetic spectrum. This effect is slightly visible under M0 (low UV amount), but clearly visible if viewed using M1 (high UV amount). To outline the effect, an additional image with pure UV light is presented (cf. Figure 10).

Figure 11 shows the spectral response of these test patches, if measured using the M1 condition.

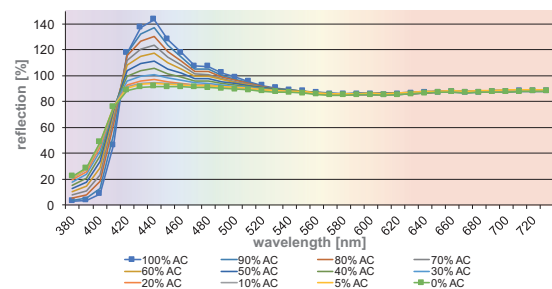


Figure 11: Spectral response of a variable area coverage (AC) of FBA ink for the proof substrate 'Epson SPP 205' with different FBA ink layer coverages, measured under M1 measurement condition

As expected, an increase of the FBA area coverage leads to a more intense emission between 420 nm and 550 nm, while the spectral response between 550 nm

Table 6: Color coordinates of investigated proof substrates with and without FBA ink (0 % or 100 % area coverage, respectively)

Substrate	FBA concentration	FBA area coverage (%)	Condition M1			Δb^*
			L^*	a^*	b^*	
Epson SPP 205	no FBA ink	0	94.57	-0.39	-2.84	13.18
	5 %	100	95.44	2.95	-16.03	
EFI 3170	no FBA ink	0	95.92	2.64	-6.72	6.61
	5 %	100	96.60	4.37	-13.33	
EFI Best Xpress	no FBA ink	0	96.21	0.24	-2.69	11.87
	5 %	100	96.71	3.42	-14.56	
EFI 9120XF	no FBA ink	0	96.54	0.84	-4.72	8.33
	5 %	100	97.34	2.13	-13.06	

and 780 nm remains unaffected. It can also be shown, that a higher FBA area coverage leads to a stronger absorption between 380 nm and 420 nm. Thereby, an 100 % FBA area coverage shows the strongest absorption while a 0 % FBA area coverage (pure, unbrightened substrate) shows an absorption minimum.

3.2 Fluorescence emission of ink compositions without carrier

3.2.1 Influence of Fluorescent Brightening Agent area coverage

Figure 12 shows the color coordinates in an a^*b^* diagram of all four proof substrates (cf. chapter 2.2) with FBA area coverages ranging from 0 % up to 100 % for the measurement condition M1 and an ink with a 5 % FBA concentration (Ink 3, cf. chapter 2.3). The area coverage of 0 % for each substrate is marked with a red dot. A 100 % area coverage is marked with a green dot. Additionally, Table 6 gives detailed information about the color coordinates of each substrate/ink combination (0 % & 100 % area coverage are shown). Please note that the L^* value is not considered in the following because it is only slightly affected by different intensity of FBA emissions (cf. Table 6). In the case of the substrates ‘Epson SPP 205’, ‘EFI 3170’ and ‘EFI Best Xpress’, a comparable behavior can be observed: With an increase of the FBA area coverage, a strongly increasing negative b^* value can be found, while the a^* value only increases slightly. Thereby, the a^*b^* shift is almost linear in all four cases (cf. Figure 12). Differences can be found for the maximum realizable FBA emission, represented by the Δb^* value (cf. Table 6). While the ‘Epson SPP 205’ shows with $\Delta b^* = 13.18$ the strongest FBA induced shift, the ‘EFI Best Xpress’ shows with $\Delta b^* = 11.87$ only a slightly lower realizable emission. Interestingly, the ‘EFI 3170’ substrate shows with $\Delta b^* = 6.61$ a much lower maximum emission. Only the substrate ‘EFI 9120XF’ shows, regarding the a^*b^* shift, a significant divergent behavior. While the b^* value is developing as expected, the a^* value only increases slightly. Hence, the FBA induced emission becomes slightly greenish (cf. chapter 1.1.2).

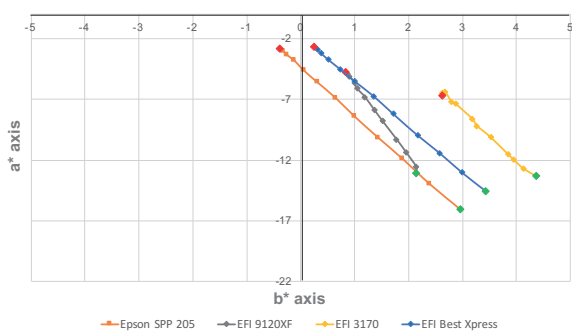


Figure 12: Influence of a variable area coverage of FBA ink (5 % FBA) for four proof substrates, under M1 measurement condition

Figure 13 shows exemplarily for two substrates (‘EFI 3170’ & ‘EFI Best Xpress’) the corresponding spectral responses for 0 % FBA area coverage, 50 % FBA area coverage and 100 % FBA area coverage, each. It can be observed, that only the emission intensity increases while the emission shape remains the same for both substrates. Also, the wavelength range between 550 nm and 780 nm remains unaffected.

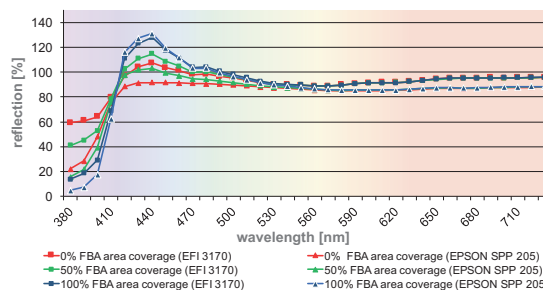


Figure 13: Spectral response of two substrates with 0 %, 50 % & 100 % FBA ink area coverage each, under M1 measurement condition

3.2.2 Influence of Fluorescent Brightening Agent area coverage in combination with concentration

Figure 14 (top-left) shows the interdependence of the FBA area coverage and the FBA concentration for the proof substrate ‘Epson SPP 205’. It can be seen that an FBA concentration of 5 % results in a value of $b^* = -16.07$ ($\Delta b^* = 13.22$) for a FBA area coverage of 100 %. With an increasing FBA concentration a maximum b^* value of 17.81 can be achieved for a 20 % FBA concentration. Up to this concentration, the already known linearity between a^* and b^* holds true (cf. chapter 3.1). For a 40 % concentration, a different behavior can be identified. Already for lower FBA area coverages it can be observed that the b^* value is still increasing while there is (compared to lower concentrations) a significant drift in the a^* value. An FBA area coverage of 90 % leads to a maximum b^* value of 16.10 but the a^* value starts to drop. For an FBA area coverage of 100 % the b^* value starts to decrease while the a^* value drops even more. As a consequence, the bluish emission becomes greenish. This effect is known as ‘greening’ or ‘greying’ (cf. chapter 1.1.2). Fluorophores need to be fixed in a monomolecular planar layer to a substrate to develop a stable emission (cf. chapter 1.1). It can be stated that the ‘Epson SPP 205’ substrate does not offer sufficient OH groups for this FBA concentration.

Figure 14 (top-right) shows the interdependence of the FBA area coverage and the FBA concentration for the proof substrate ‘EFI Best Xpress’. This substrate shows a comparable behavior like the ‘Epson SPP 205’ proof substrate. This substrate shows for 20 % FBA concentration and 100 % FBA area coverage the most intense emission ($\Delta b^* = 18.27$). This substrate also shows for

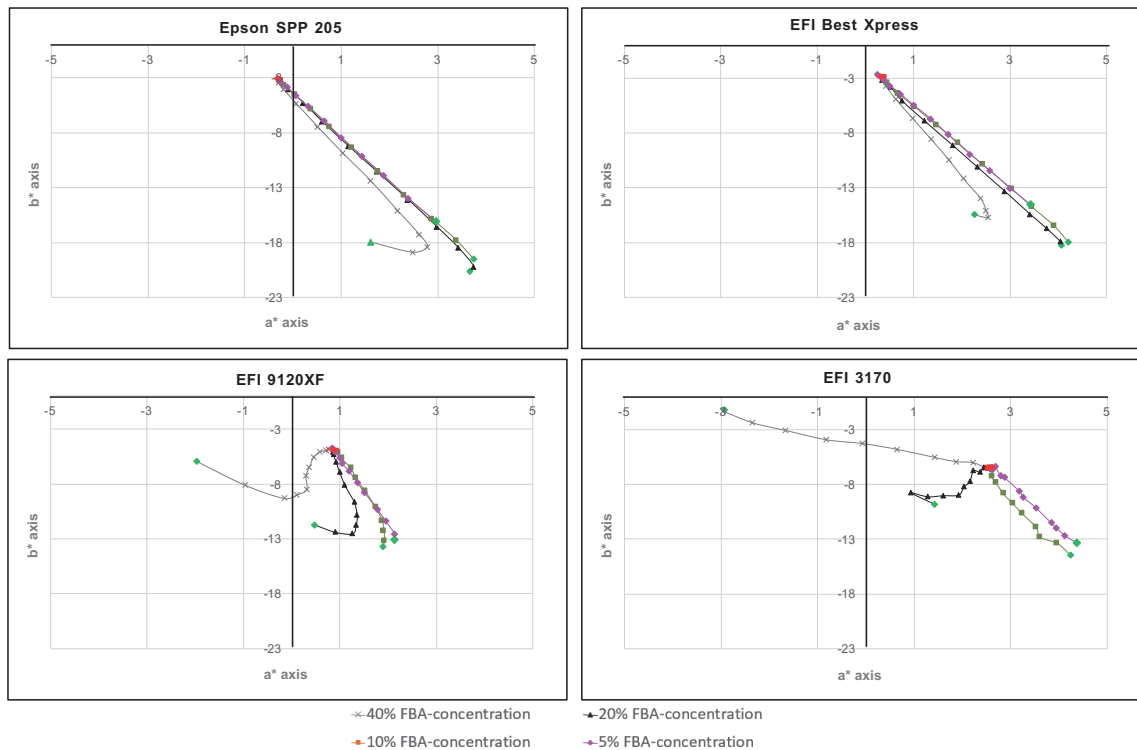


Figure 14: The a^*b^* color coordinates depending on the FBA area coverage and concentration for four proof substrates (top-left ‘Epson SPP 205’; top-right ‘EFI Best Xpress’; bottom-left ‘EFI 9120XF’; bottom-right ‘EFI 3170’), under M1 measurement condition

40 % a comparable, uncharacteristic behavior like the ‘Epson SPP 205’. Again, it can be assumed that this is a greening effect because the substrate does not offer sufficient OH binding groups.

Figure 14 (bottom-left) shows the interdependence of the FBA area coverage and the FBA concentration for the proof substrate ‘EFI 9120XF’. In contrast to the previous discussed substrates, this substrate shows only a decent increase in its b^* value ($\Delta b^* = 8.92$) for a 100 % FBA area coverage and an FBA concentration of 10 %. If the FBA concentration is increased to 20 %, the previously observed a^*b^* drift also occurs but in this case already for 20 % FBA concentration. Even for a 10 % FBA concentration this effect can be observed. If the FBA concentration is increased to 40 %, the FBA area coverage depending color drift becomes even more complex. While a strong a^* drift can be observed already for low concentrations (compared to the corresponding FBA concentration of the ‘Epson SPP 205’ substrate), the b^* value increases up to an FBA coverage of 60 % for a FBA concentration of 20 %. Then it stops to increase and starts to drop again, while the a^* value drops even more (up to $\Delta a^* = 2.9$ for a 40 % FBA concentration). It can be stated that the greening effect is responsible. This already becomes relevant for a 10 % FBA concentration. Even for a 5 % FBA concentration a greening effect can be identified. As a result, it can be assumed that this substrate offers less

OH groups than the proof substrates ‘Epson SPP 205’ and ‘EFI Best Xpress’.

Finally, Figure 14 (bottom-right) shows the interdependence of the FBA area coverage and the FBA concentration for the proof substrate ‘EFI 3170’. This substrate shows a stable FBA emission only for an FBA area coverage of 100 % with an FBA concentration of 5 % ($b^* = -13.31$; $\Delta b^* = 6.65$). If the FBA concentration is increased to 10 %, a greening effect can be identified. This substrate shows a much stronger a^*b^* shift for higher FBA concentrations compared to the other three substrates. If the FBA concentration is increased to 40 %, the b^* value is not increasing for any FBA area coverage. In opposite, already a 5 % FBA area coverage leads to a decrease in the b^* value. If the area coverage is increased to 100 %, the b^* value shifts from -6.56 to -1.18 , while the a^* value shifts from 2.63 to -2.93 ($\Delta a^* = 5.56$). In this case, it can be assumed that this substrate does not offer any OH binding groups at all to enable a stable emission.

It can be concluded, that a 5 % FBA ink composition shows already high FBA emission intensities with only a slightly greening effect for the proof substrate ‘EFI 3170’. Unfortunately, depending on the substrate, the realizable FBA emission intensity is limited. Therefore, in the next chapter this concentration is used to analyse the impact of a carrier on the emission intensity.

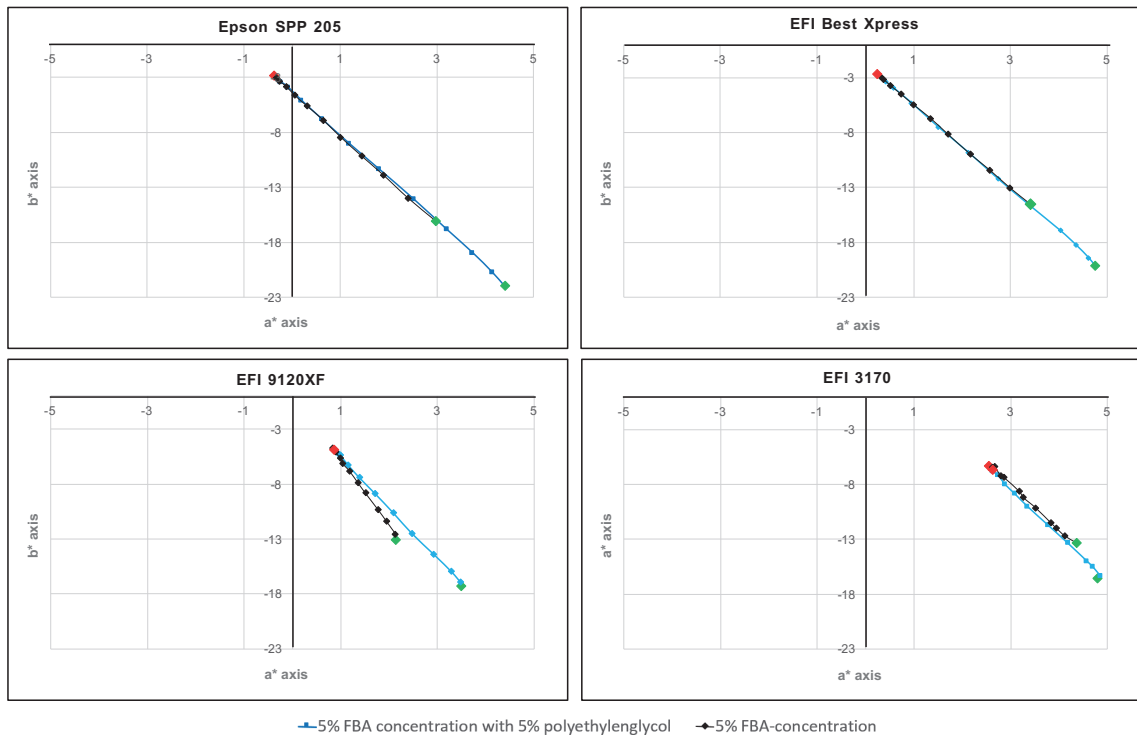


Figure 15: The a^*b^* color coordinates for several FBA area coverages and a 5 % FBA concentration with and without 5 % polyethylene glycol of four proof substrates (top-left ‘Epson SPP 205’; top-right ‘EFI Best Xpress’; bottom-left ‘EFI 9120XF’; bottom-right ‘EFI 3170’), under M1 measurement condition

3.3 Fluorescence emission of ink compositions with carrier

As pointed out in the chapter 1, carrier substances are known to prevent the so called “greening effect”. Furthermore, these carriers are also known in principle to improve the FBA efficiency. For this study, polyethylene glycol is used exemplarily as a carrier with a concentration of 5 % in combination with Ink 3 (5 % FBA). Polyethylene glycol ($C_{2n}H_{4n+2}O_{n+1}$) is suitable because this substance fulfills the requirements: it is water soluble, colorless and compatible with the used FBA.

Figure 15 (top-left) shows the 5 % FBA ink without carrier and the 5 % FBA ink performance with 5 % polyethylene glycol as a carrier compared to each other for the proof substrate ‘Epson SPP 205’. It is found that the addition of 5 % polyethylene glycol leads to a significant improvement in the FBAs emission, and therefore the efficiency compared to 5 % FBA without carrier (without carrier: $b^* = -16.07$; with carrier: $b^* = -21.98$). No greening effect is observed.

Figure 15 (top-right) shows the 5 % FBA ink without carrier and the 5 % FBA ink performance with 5 % polyethylene glycol as a carrier compared to each other for the proof substrate ‘EFI Best Xpress’. Again, it is found that the addition of 5 % polyethylene glycol leads to a significant improvement in the FBAs emission

compared to 5 % FBA without carrier (without carrier: $b^* = -14.55$; with carrier: $b^* = -20.12$). As well, no greening effect is observed.

Figure 15 (bottom-left) shows the 5 % FBA ink without carrier and the 5 % FBA ink performance with 5 % polyethylene glycol as a carrier compared to each other for the proof substrate ‘EFI 9120XF’. In this case, the addition of 5 % polyethylene glycol leads to a strong increase of the FBAs emission compared to 5 % FBA without carrier (without carrier: $b^* = -13.07$; with carrier: $b^* = -17.29$), although still remaining lower than on ‘Epson SPP 205’ and ‘EFI Best Xpress’ substrates. Furthermore, while the use of 5 % FBA concentration without carrier leads to a slight greening effect, the addition of polyethylene glycol fully prevents this effect.

Finally, Figure 15 (bottom-right) shows the performance of 5 % FBA ink without carrier and the 5 % FBA ink with 5 % polyethylene glycol as a carrier compared to each other for the proof substrate ‘EFI 3170’. The addition of 5 % polyethylene glycol has similar effects as in the case of ‘Epson SPP 205’ and ‘EFI Best Xpress’ substrates, only in smaller scale (without carrier: $b^* = -13.31$; with carrier: $b^* = -16.53$). Again, no greening effect is observed.

Figure 16 (left) shows the influence of the 5 % FBA ink without carrier with several area coverages for all

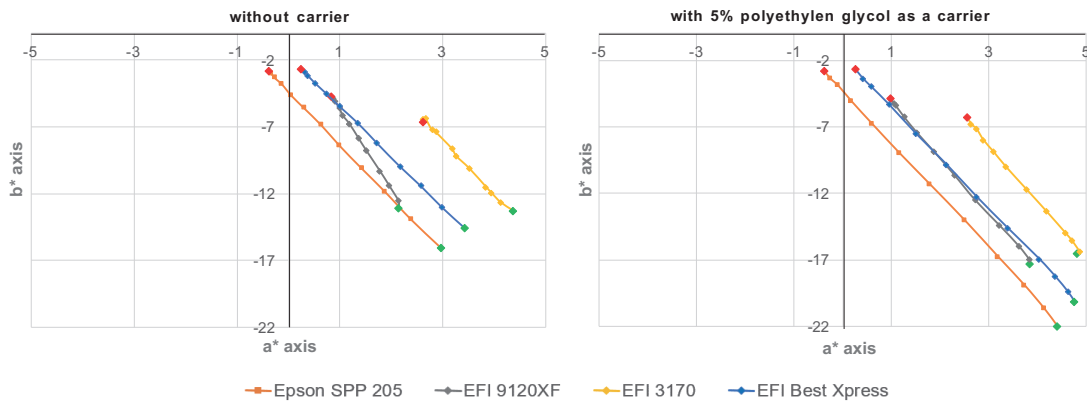


Figure 16: Visualization of the influence of polyethylene glycol as a carrier; left: without carrier; right: with 5 % polyethylene glycol as a carrier, for four proof substrates, under M1 measurement condition

examined proof substrates, as already presented in the chapter 3.1. In contrast, Figure 16 (right) shows the influence of the same ink if 5 % polyethylene glycol is added to the ink composition. Again, the previously presented negative increase of the b^* value can be seen. Additionally, Figure 16 (right) shows that the linearity observed previously for the substrates ‘Epson SPP 205’, ‘EFI 3170’ & ‘EFI Best Xpress’ can also be achieved for the substrate ‘EFI 9120XF’ by adding 5 % polyethylene glycol to the ink and prevent this way any greening.

Summarized, it is shown that the addition of 5 % polyethylene glycol as a carrier not only prohibits any greening but also leads to a significant increase of the FBAs emission, and therefore the efficiency. This is important for the final goal of this study because this way any proof substrate can be used to simulate theoretically every production substrate without the risk of greening. Furthermore, the realizable intense blue emission offers the possibility to use lower FBA area coverages to simulate even massively brightened production substrates for all proof substrates in this study.

3.4 White point simulation of production substrates

The actual white point simulation is presented and exemplarily done for the highly brightened production substrate ‘Heaven42’ and the proof substrate ‘EFI 3170’, in two separate steps.

3.4.1 Spectral fit of the wavelength range from 550 nm to 780 nm

The wavelength range of 550 nm to 780 nm is relevant to modify the overall spectral response of the proof substrates to the production substrates spectral response by printing small amounts of cyan, magenta, yellow and black. This range results from the fact that any FBAs influence is limited to the range of 380 nm to 550 nm. To achieve a good match, we propose to print a test chart with defined small amounts

of CMYK upon the corresponding proof substrate before any FBA addition is performed. Each patch can be measured using either measurement condition M2, M1 or M0. The spectral difference ΔE_s between each test patch printed on the proof ($\widehat{\beta}(\lambda)$) and the production ($\beta(\lambda)$) substrate is calculated using the ‘Spectral Metric’ (LSS, Least square sum) following Equation 2 (Dattner, 2010, p. 38).

$$E_s := \sum_{\lambda} \left(\beta(\lambda) - \widehat{\beta}(\lambda) \right)^2 \quad [2]$$

Table 7 shows the actual LSS values of each CMYK combination for the proof substrate ‘EFI 3170’ and the production substrate ‘Heaven42’ in case of given CMYK combinations, calculated from the Equation 2.

Table 7: Overview of used CMYK combinations to minimize the LSS value

Cyan	Magenta	Yellow	Black	ΔE_s (LSS)
(%)				
0	0	0	0	421.25
0	0	0	1	806.62
0	0	0	2	1104.82
0	0	0	3	623.94
1	0	0	0	974.30
2	0	0	0	346.18
0	1	0	0	757.25
0	2	0	0	873.68
0	0	1	0	260.82
0	0	2	0	380.84
1	1	0	0	570.63
1	0	1	0	240.82
0	1	1	0	412.21

A yellow area coverage of 1 % in combination with a cyan area coverage of 1 % leads to a minimum. This white point modification results in a $\Delta E_{00} = 6.15$

between both substrates for the measurement condition M1 compared to a $\Delta E_{00} = 8.25$ if no white point adjustment is performed.

Figure 17 shows the corresponding spectral responds of the production substrate ‘Heaven42’, the proof substrate ‘EFI 3170’ (without adjustment) and the proof substrate ‘EFI 3170’ with white point adjustment (1% Cyan; 1% Yellow), limited to the relevant wavelength range of 550 nm to 780 nm.

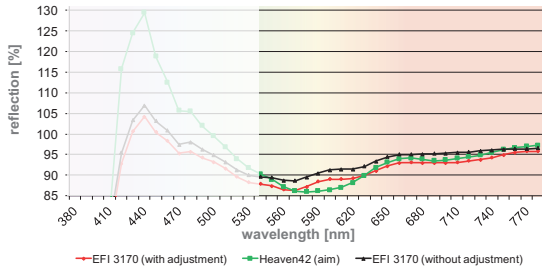


Figure 17: Spectral fit of the wavelength range 550 nm to 780 nm of the production substrate ‘Heaven42’ and ‘EFI 3170’ with & without adjustment, under M1 measurement condition

3.4.2 Spectral fit of the wavelength range from 380 nm to 550 nm

To compensate and adjust the remaining difference between both substrates ($\Delta E_{00} = 6.15$), different amount of liquid FBA is printed onto the adjusted proof substrate using inkjet printing. In a first step, the actual FBA emission of the production substrate needs to be determined. This is done spectrally by performing two measurements (M1 & M2) and applying Equation 1. Figure 18 shows the resulting spectral difference of both measurements.

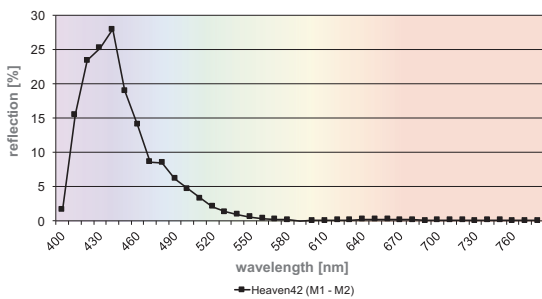


Figure 18: FBA induced spectral response of the production substrate ‘Heaven42’ using measurement conditions M1 & M2

By a further use of Equation 2 (limited to 380 nm to 550 nm) with $(\beta(\lambda))$ of the production substrate measured with the M1 condition and $\beta(\lambda)$ of the same production substrate measured with the M2 condition, the corresponding LSS value can be determined. This LSS value performs as an indicator for the FBA induced emission intensity. In this case, an LSS value of 1364.04 is determined for the production substrate ‘Heaven42’.

To determine the required FBA area coverage, a test chart with 5% FBA ink, including 5% polyethylene glycol as a carrier, is printed with area coverages of 0%, 5%, 10%, 20%, ..., 100% onto the adjusted proof substrate (cf. chapter 2.4). Each printed patch needs to be measured and calculated as it is done for the production substrate. Figure 19 shows the resulting LSS values for each FBA ink area coverage printed onto the ‘EFI 3170’ proof substrate with $(\beta(\lambda))$ for the already modified proof substrate and $\beta(\lambda)$ for the same but in its FBA concentration modified proof substrate.

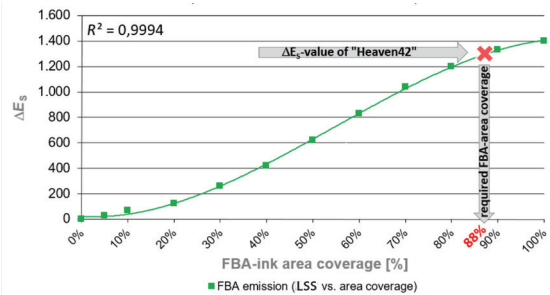


Figure 19: Determination of the required FBA ink area coverage

Figure 19 shows the correlation between the FBA area coverage and the resulting FBA emission intensity. The production papers LSS value is inserted accordingly, which leads to an interpolated FBA area coverage of 88% to obtain a maximum correlation between the proof substrate and the production substrate. This third-degree polynomial interpolation ($R^2 = 0.9994$) is based on all measured FBA area coverages.

The final achieved color difference between the modified ‘EFI 3170’ proof substrate and the production substrate ‘Heaven42’ is $\Delta E_{00} = 0.89$. To outline this result, Figure 20 shows the spectral response of the unmodified proof substrate, the modified proof substrate and the production substrate ‘Heaven42’.

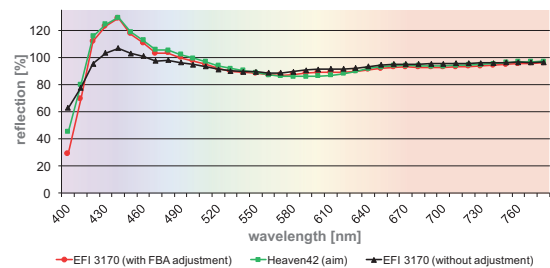


Figure 20: Spectral visualization of the performance of the enhanced white point simulation on the production substrate ‘Heaven42’ and proof substrate ‘EFI 3170’ (without and with adjustment, at 88% FBA ink coverage), under M1 measurement condition

Figure 20 clearly illustrates the excellent correlation between the proof substrate and the production substrate, if a spectral white point and an FBA emission adjustment is performed.

4. Discussion

This study shows that liquid hexasulpho-based FBAs can be printed successfully in an area coverage variable inkjet process. While some of the investigated proof substrates show a greening depending on the FBA concentration, this effect is avoidable by adding a carrier to the FBA ink formulation, improving the overall FBA emission efficiency in addition. Furthermore, it is shown that the emission intensity cannot be extended infinitely by increasing the FBA concentration. Because all FBA adjusted proof substrates show a strong FBA emission intensity already for a 5% FBA concentration (with 5% polyethylene glycol), there is no need to use higher concentrations.

As a result, it is shown that all examined proof substrates can be used to simulate any brightened production substrate regardless the illumination condition. This holds true, if the overall spectral response for each wavelength of a given proof substrate is equal or higher compared to the production substrate to be simulated. This condition is fulfilled for all investigated proof substrates in this study.

Exemplarily, it is shown for the production substrate 'Heaven42', in combination with the proof substrate 'EFI 3170', that a very precise and illumination independent correlation can be achieved ($\Delta E_{00} = 0.89$ in the case of measurement condition M1). While typical fogra51/fogra52 certified proof substrates perform better compared to previously available substrates in the context of colorimetric agreement, especially extremely brightened production substrates (such as 'Heaven42') cannot be simulated adequately. Actually, if the production substrate 'Heaven42' is simulated using the fogra52 certified proof substrate 'TRUST commercial (Semi-glossy)', a $\Delta E_{00} = 3.61$ ($\Delta b^* = 4.21$) is measured. This match is achieved for D50 being 115% (cf. chapter 1.3). As stated in the chapter 1.3, ISO 3664:2009 allows an UV amount of 60% up to 130% compared to D50 being 100%. This still wide tolerance leads to a $\Delta E_{00} = 3.15$ ($\Delta b^* = 3.98$) if the measurement device shows an UV amount of 60%. If a corresponding light

booth shows an deviating UV amount of 130%, a $\Delta E_{00} = 4.55$ ($\Delta b^* = 7.31$) is observed. In contrast, this study approach leads to a $\Delta E_{00} = 0.53$ ($\Delta b^* = 0.46$) if the measurement device has 60% UV amount and a $\Delta E_{00} = 1.07$ ($\Delta b^* = 0.92$) if the light booth shows an deviating UV amount of 130%.

This scenario points out the limitations of fogra51 & fogra52 and the benefits of the presented approach, if the proof substrate and the production substrate show a varying amount of FBA.

Still broad tolerances of ISO 3664:2009 become irrelevant if both, the proof as well as the production substrate, possess the same FBA amount. This is nearly perfectly fulfilled with this study method. Therefore, the approach of this study offers even the possibility to view a proof and a production substrate under any illumination, without the risk of obtaining FBA induced colorimetric differences.

However, only one single FBA type has been examined, as well as only one single carrier type. Other FBA types and carriers and their combinations are expected to even further extend the FBA emission intensity. Other typical ingredients, i.e. biocides, corrosion inhibitors, thickening agents or detergents, and their interaction with FBAs are included in a recently started research project. Furthermore, no results concerning the light fastness of the used FBA (and other possible FBAs) have been presented. Generally, it is stated that the light fastness of the used FBA is very limited. Anyhow, no detailed research is available in this context. All named aspects will be investigated and discussed in future studies.

Future research will also focus on the performance of the approach in combination with ink printed on it and therefore on the overall performance in proof processes. It is expected to achieve a much better match between printed proof- and production prints, again completely illumination independent.

5. Conclusion

As pointed out in chapter 1.3 State of the scientific knowledge, the effects of FBAs cannot be compensated effectively for every possible color management scenario, until now.

Therefore, the authors of this study propose a method to compensate FBA induced colorimetric differences in proof processes by printing defined amounts of liquid FBAs using inkjet printing. Thereby, the intensity of the fluorescence is directly controlled by changing

the area coverage of the FBA printed on a unbrightened or slightly brightened proof substrate. As shown in chapter 3.2.2 Influence of FBA area coverage in combination with FBA concentration, an undesired greening effect can be observed, already for 5% FBA concentrations, depending on the used substrate. Furthermore, in chapter 3.2.2 it is pointed out, that the emission intensity strongly varies depending on the used substrate. Both effects are believed to be related to varying amounts of OH groups of the substrates.

Therefore, in chapter 3.3 Fluorescence emission of ink compositions with carrier, a fixed FBA concentration of 5% in combination with the substrate ‘EFI 3170’ has been used as a base for analyzing the impact of polyethylene glycol as a carrier on the emission intensity for several FBA area coverages. The results in this chapter clearly show that the addition of 5% polyethylene glycol to a 5% FBA mixture not only prevents greening effects but also helps to significantly increase the FBAs emission intensity, and therefore, efficiency.

In chapter 3.4 White point simulation of production substrates, an actual white point simulation is presented and exemplarily done for the highly brightened production substrate ‘Heaven42’ and the proof substrate ‘EFI 3170’. It is successfully shown that a two-step spectral fit can be used to achieve a very good correla-

tion between the production substrate ‘Heaven42’ and the proof substrate ‘EFI 3170’ of $\Delta E_{00} = 0.89$.

Summed up, it is shown that applying an FBA with variable area coverage can be used to create typical FBA emissions and intensities using any desired slightly brightened or unbrightened substrate to simulate any production substrate as long as the overall reflectance of the proof substrate is equal or higher compared to the reflection of the production substrate.

Overall, it can be stated that the presented approach leads to a significantly improved white point simulation for any proof substrate, by taking the actual FBA emission of any given brightened production substrate into account, which makes proofing processes illumination independent.

References

- Ai, H., 2015. *Introduction to bioanalytical chemistry*. [online] Available at: <<http://research.chem.ucr.edu/groups/ai/lecture/lecture11.pdf>> (Accessed 22 November 2015).
- Bieber, W., Brockes, A., Hunke, B., Krüsemann, J., Loewe, D., Müller, F. and Mummenhoff, P., 1989. *Blankophor: Optische Aufheller für die Papierindustrie*. Leverkusen: Bayer, Geschäftsbereich Farben.
- Blechschmidt, J., ed., 2013. *Taschenbuch der Papiertechnik: Mit 94 Tabellen*, 2nd ed. München: Fachbuchverlag Leipzig im Carl-Hanser-Verlag.
- Blum, T., Linhart, F. and Frenzel, S., BASF AG, 2002. *Verfahren zur Herstellung von beschichtetem Papier mit hoher Weiße*. EP 1 419 298 B1.
- Blum, T., Linhart, F., Kaub, H.-P., Champ, S., Wendker, M., Meck, D. and Geiger, S., BASF Se, 2002. *Verfahren zur Erhöhung der Weiße von Papieren mit kationischen Polyelektrolyten*. EP 1 438 197 B1.
- Brandt, N., 2008. *UV-Stabilität optisch aufgebellter Offsetdruckpapiere: PTS-Forschungsbericht IK-MF 090073*. Heidenau: Papiertechnische Stiftung, PTS.
- Dattner, M., 2010. *Spektrales Farbvorhersagemodell: für den Rasterdruck auf Basis der wellenlängenabhängigen Flächendeckung*. PhD Thesis. Bergische Universität Wuppertal. [online] Available at: <<http://elpub.bib.uni-wuppertal.de/servlets/DerivateServlet/Derivate-2184/de1001.pdf>> (Accessed 22 February 2016).
- Dattner, M., Bohn, D. and Urban, P., 2011. The impact of optical brightener on the color perception of halftones. In N. Enlund and M. Lovreček, eds. *Advances in Printing and Media Technology: Proceedings of the 38th International Research Conference of IARIGAI*. Budapest-Debrecen, September 2011. Darmstadt: International Association of Research Organizations for the Information, Media and Graphic Arts Industries.
- Erhard, K., Alber, W. and Götze, T., 2003. *Optimierung des Einsatzes optischer Aufheller bei der Erzeugung graphischer Papiere: PTS-Forschungsbericht*. Heidenau: Papiertechnische Stiftung, PTS.
- Felix Schöller Group, 2016. *Trust*. [online] Available at: <http://www.felix-schoeller.com/de_de/business-unit/foto-digitaldruckpapiere/produkte/je-produktserie/trust.html> (Accessed 21 February 2016).
- Fiebrandt, B.-O., 2007. *Optische Aufheller in Proof- und Druckpapieren*. Berlin: Bundesverband Druck und Medien e.V. (bvdm).
- fogra, 2014. *Evaluating FOGRA51beta*. (online) Available at: <<http://www.fogra.org/index.php?menuid=1&reporeid=357&getlang=en>> (Accessed 21 February 2016).
- Holik, H., ed., 2006. *Handbook of Paper and Board*. Weinheim: Wiley-VCH.
- International Organization for Standardization, 2009a. *ISO 3664:2009 Graphic technology and photography – Viewing conditions*. Geneva: International Organization for Standardization, ISO.
- International Organization for Standardization, 2009b. *ISO 13655:2009 Graphic technology – Spectral measurement and colorimetric computation for graphic arts images*. Geneva: International Organization for Standardization, ISO.

- International Organization for Standardization, 2013. *ISO 12647-2:2013 Graphic technology – Process control for the production of half-tone colour separations, proof and production prints – Part 2: Offset lithographic processes*. Geneva: International Organization for Standardization, ISO.
- Kraushaar, A., 2012. *Normlight according to ISO 3664:2009: About a quick and a gradual change toward ISO 3664:2009 conforming cabinets: Extra 28*. Munich: Fogra Graphic Technology Research Association e.V.
- Kraushaar, A., 2013. *Die wichtigsten Änderungen der ISO 12647-2: Revision der Offsetdruck-Norm: Fogra Extra 30*. München: Fogra Graphic Technology Research Association e.V.
- Kraushaar, A. and Geßner, F., 2006. *Farbmanagement für Drucke auf aufgebellten Papieren: Forschungsbericht Nr. 32.144*. München: Fogra Graphic Technology Research Association e.V.
- Löffler, E.M. and Green, P., 2008. Estimating the spectral reflectance of fluorescent offset papers for varying illuminants. In: N. Enlund and M. Lovreček, eds., *Advances in Printing and Media Technology: Proceedings of the 35th International Research Conference of IARIGAI*. Valencia, September 2008. Darmstadt: International Association of Research Organizations for the Information, Media and Graphic Arts Industries.
- Nelson, K.L., 2007. *Enhanced Performance and Functionality of Titanium Dioxide Papermaking Pigments with Controlled Morphology and Surface Coating*. PhD Thesis. Georgia Institute of Technology, School of Chemical and Biomolecular Engineering.
- Pertler, H. and Bertholdt, U., 2007. *Farbvergleich und Farbmessung an fluoreszierenden Proben der Druckindustrie: FOGRA, Forschungsbericht Nr. 60.053*. München: Fogra Graphic Technology Research Association e.V.
- Zwinkels, J., 2008. Surface fluorescence: the only standardized method of measuring luminescence. In: U. Resh-Genger, ed. 2008. *Standardization and Quality Assurance in Fluorescence Measurements I: Technoques*. Berlin, Heidelberg: Springer-Verlag.

JPMTR 087 | 1511
DOI 10.14622/JPMTR-1511
UDC 655.1 (774.8)

Case study
Received: 2015-12-14
Accepted: 2016-09-09

Does the use of black ink still comprise the “darkest” issue of CMYK printing?

Yuri Kuznetsov and Maria Ermoshina

St. Petersburg State University of Industrial Technology and Design,
North-West Institute of Printing,
NWIP, Jumbula Lane 13, Saint Petersburg, 191180, Russia
E-mail: yurivk@mail.ru

Abstract

Black ink can be used for multicolor printing to different extent within each of such multiple purposes, as: replacement of the achromatic component of three chromatic inks combination; reproduction of the image achromatic colors; expanding the color gamut; providing print security features ... The relationships and effects within these functions are discussed in the paper on the background of prepress facilities evolution starting from the times of photoengraving and analogue scanners of 60's up to the precise digital color control of today. The results of comparative colorimetric analysis of the sets comprising cyan, magenta and yellow (CMY), and cyan, magenta, yellow and black (CMYK) revealing the black in particular effect of expanding the print gamut by providing the darker chromatic colors which aren't available for any combination of the other three process ones are also presented.

Keywords: color gamut, achromatic component, chromatic color, UCR, GCR, UCA

1. Introduction

Looking back in the latest history of graphic technology developments one can find that thirty to forty years ago there were a number of scientifically approved recommendations on direction and degree of tone and color values correction for print quality improvement. However, even at the times of electronic prepress, there was a lack of means for proper control of desired color setting variations. For example: in the 70's of the last century there was published in advertising specification the drum scanner's ability of replacing the CMY achromatic component by the black ink as “up to 75 %” (against the 65 % of the competing model). The clear knowledge of what had to be done with an image data in some other relations was, as well, short of means to realize the task.

The digital image processing of today allows for practically unlimited print parameter variation in any direction with the discretion of just 25 square micrometers of an ink coverage in surface plane. However, quite a contrary situation of adequate resources but lacking in knowledge of what should be done is often met and the need arises of additional research or training which could substantiate the recommendations and procedures for effective use of such precise, recently appeared control facilities (Kuznetsov, 2013). There is variety of purposes and reasons for black ink use in CMYK printing. It can be in different degree applied for reproduction of

achromatic colors as well as the achromatic component of chromatic ones. Its use can also differentiate from the large area, stationary image area to sharp edges and fine details, as well as from the highlights to midtones and darker areas. So, there is the theoretically infinite continuum of CMY to CMYK transformations which can result in the same or improved colorimetric print values.

The beginning of K-ink use within the CMY triad stems from the times of photoengraving and camera prepress. The facilities of black control according to certain rendering intent and, especially, in isolation from its other effects on resulting color were rather restricted. However, the mostly heuristically found, scanty collection of black ink settings is until now used in wide practice. One of the reasons is in some isolation of numerous participants (publishers/advertisers, prepress operators, quality managers, printers...) from each other. Lack of facilities or time for finding the optimal adjustments which would match the job/process specifics encourages them to follow the narrow path of guaranteed standard parameters (Euroscale, SWOP...) or of a settings stipulated by the available ICC profile.

The other reason of non-optimal black ink use is in vague interpretation of its settings and their relation-

ship essence in “black boxes” of prepress software applications or commenting manuals. When appealing to their “help” option the user is sometimes sent to get an advice from a printer. In this relation E. Enoksson (2004) notes, for example, that only about a quarter of the Swedish print houses have people ever heard of the UCR (Under Color Removal) and GCR (Gray Component Replacement) functions of Photoshop.

Not much “help” the user can get from academic sources as well. Problems start here from providing the proper definitions for these functions because of similar sense of their abbreviations meanings. For example both UCR and GCR indicate in fact the “removal an achromatic component of chromatic inks (CMY) by replacing them with the black (K) one”. Meanwhile the “Complete Color Glossary” defines the UCR procedure as related just to the dark neutral colors (Southworth, McIlroy and Southworth, 1992). In “Handbook of Print Media” one can find the attempt to distinguish UCR, GCR, and UCA (Under Color Addition) functions by

2. Relationships of black and balanced CMY in achromatic component of chromatic inks combination

2.1 Volume of achromatic component replacement

This parameter is often used to be formally illustrated by the diagram of the kind presented in Figure 1, where positions 1b and 1c show the examples of partial (50 %) and complete (100 %) volumes of achromatic share replacement.

This variation is historically related to UCR function, which is first of all used for the darker image areas because of total ink limitation. In fact, it can be varied from 0 % up to 100 % independently of the given image area brightness, i.e. in the highlights, middle tones or shadows.

Volume and range of $(CMY)_{min}$ replacement is, except of the ink limit, stipulated by the number of other technological, economic, operating and image quality considerations including:

- ink consumption costs;
- fidelity and stability of the gray balance within a run;
- color disbalance due to rosettes geometry variation, as well as moiré and rosettes visibility (Daels and Delabastita, 1994);
- gamut mapping intents;
- use of inks which colors are complementary to that of CMY ones in Hi-Fi printing, etc.

Nature of these reasons is well known or described in referred literature while the last one is cleared up by the Figure 1d. It shows that the 100 % removal of one of CMY inks is compulsory over all tonal range to make

the examples of varying just the volume of CMY achromatic part replaced by the black ink (Kipphan, 2001), though this volume can be varied within each of these procedures as well. At last, the “Digital Color Imaging Handbook” stands out GCR as a “generalization” of UCR and K addition (Balasubramanian, 2003, p. 358). There were also attempts to modify UCR under the names of such procedures as PCR (Programmed Color Removal), ICR (Integrated Color Removal), etc., and the new names were as well proposed (Enoksson, 2004).

The number of other explanations of fourth ink application, suffering from mixing the purposes and methods based on the vast variety of CMYK combinations, is continuing. So, it is not out of place to separately discuss the following black ink functions:

- replacement of the achromatic component of three chromatic inks combination;
- reproduction of the image achromatic colors;
- use of this ink for print security purposes;
- expanding the print color gamut.

worthwhile the use of an additional ink of opposite, complementary color (red or orange one in this example) to expand the print color gamut. This makes it also clear that the screen of complementary color can safely use the angle of its corresponding process color. The latter should be completely withdrawn in particular image area to get higher chroma.

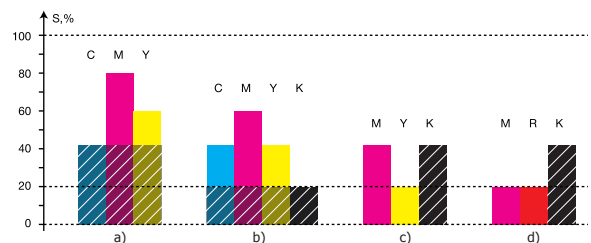


Figure 1: Methods for providing formally the same chromatic color: without black ink (a); at 50 % and 100 % $(CMY)_{min}$ (hatched) replacement by black (b, c); with further removal of equal M and Y on behalf of an orange ink (marked R on the diagram) in HiFi printing

2.2 Varying the replacement volume within the tonal range

The volume variation of such replacement within the tonal range can be illustrated by a diagram in Figure 2, where the straight line 1 corresponds to printing of the whole gray scale of color image exclusively by CMY inks. For simplicity the balanced CMY inks amount changes along lines of this graph in equal proportion ($C = M = Y$), thereby related to the use of “ideal inks”.

With taking the line 1 for a reference, the other curves of Figure 2 demonstrate the possible variants of achromatic CMY and K-ink volumes relationship along the tone range. Thus, curve 2 indicates at its upper point the $(CMY)_{min}$ withdrawal of 40 % where initial $C = M = Y = 100 %$ is replaced by combination of $C = M = Y = 60 %$ and $K = 40 %$ at 220 % of ink total. Following the course of this curve to lighter areas, the use of black ink is gradually reduced to 0 % at middle tone. Starting from $C = M = Y = 50 %$ and until the white point, the achromatic component is again reproduced only by CMY.

Curve 3 illustrates the constant replacement value of 40 % along the whole gray scale. Here, for example, middle tone is presented by $C = M = Y = 30 %$ and $K = 20 %$ with the latter comprising 40 % of achromatic value defined at this point by $C = M = Y = 50 %$ of the reference line 1.

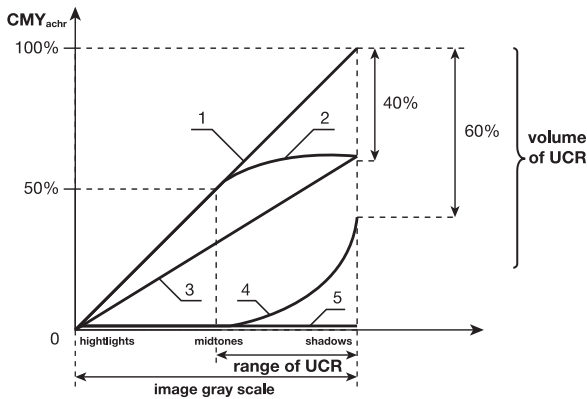


Figure 2: Variation of balanced CMY and K values along the image gray scale, shown with a line/curve: 1 – balanced CMY only, without K; 2 – gradual reduction of CMY replacement by K from 40 % in shadows to 0 % in middle tones; 3 – with 40 % constant volume of replacement along the whole scale; 4 – with gradual growth of CMY replacement by K from 60 % in shadows up to 100 % in middle tones; 5 – without CMY along the whole scale

Gradual replacement increase from 60 % in the darkest areas up to 100 % in middle tones is shown by curve 4. It also indicates the reproduction of lighter part of the gray scale exclusively by black ink.

At last, the curve 5 coincides with horizontal axis of the diagram and relates to complete replacement volume of 100 % along the whole scale. It corresponds to the so called “binary chromatic + black” strategy where CMY inks can’t be altogether found in any chromatic area of a print.

As a result, Figure 2 describes two different dimensions of $(CMY)_{min}$ withdrawal, the first of them relating to the volume of K ink use while the other one indicating the location of its certain volume within the tone range.

It is however common to separate this whole continuum just on two strategies: UCR and GCR, relating the first of them to concave curves of the kind of curve 2, and the latter to convex ones like curve 4. The freedom of choice and manipulating these curves faces in wide practice the difficulty due to their impact on the printing system color profile. Coming from one curve to the other inevitably changes color of the same print area due to variations in halftone dots overlap, their total perimeter, etc., resulting especially in the shift of an ink trap and both physical and optical dot gain.

The amount of primaries in Nuberg model (Nuberg, 1932) for resulting print color estimation through the weighted sum of ink coverage combinations also changes. Nuberg’s model is based on the physical imitation of resulting print color on the rotated Maxwell disk with its sectors dimensions taken in the given proportion of primaries. It is mostly mentioned in the literature with reference to the five years later published Neugebauer (1937) paper as generalization of somewhat earlier b/w model for two primaries (Murray, 1936; Scheberstov, 1936). For example, the primary color of three inks overlap used in this sum for CMY model isn’t included in CMYK model when the strategy of achromatic component replacement corresponds to the case 5 in diagram of Figure 2. At the same time, the colors of CK, MK, YK, CMK, CYK and MYK overlaps become, as it will be shown further, rather significant in such sum.

The black ink effect on the resulting print color should also depend on the “dot-on-dot” or “dot-off-dot” strategy choice of inks placement (Rhodes and Hains, 1993). As Figure 3 shows, their research has evidently indicated the simple form of the 3D color body surface not reaching to the plane for rotated dots in CIELCH space for the first case and the composite one exceeding the plane for rotated dots for the other which should strongly influence the print color gamut.

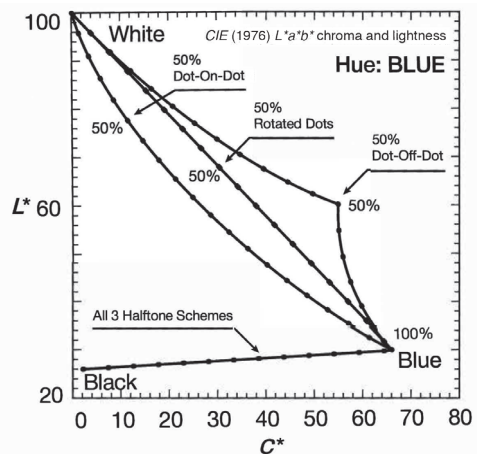


Figure 3: The comparison of the three variants of C and M halftone dots placement in blue (CM) plane of CMY gamut; adapted from Rhodes and Hains (1993)

3. Print security function

The black ink spectral reflectance in the near infrared region is quite different from that of the chromatic inks and, as well, from their neutral combination, as it is shown in Figure 4 for the pigmented black ink and dye based chromatic ones (Bugnon, Brichon and Hersh, 2007). That makes it possible to discern the differently colored neutral print areas under corresponding near infrared illumination and thereby provides the facility of non-costly K-ink use for print security purposes (Žiljak, Žiljak Vujić and Pap, 2008).

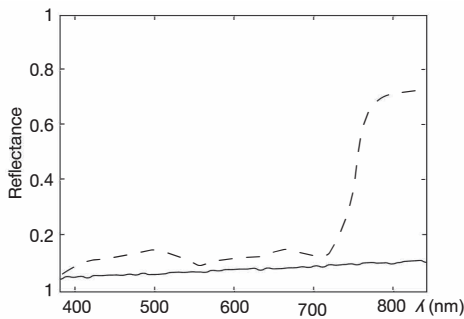


Figure 4: Reflectance spectra of dye based CMY neutral (---) and pigmented black ink (—) of sublimation printer are quite different in the near infrared band (adapted from Bugnon, Brichon and Hersh, 2007)

As we show in Figure 5 for exemplary scan line, it is possible to modulate, for example, the $K = (CMY)_{min}$ component by the auxiliary image with share of K

which exceeds the modulating signal value being retrieved after modulation to the balanced CMY to keep the basic image color non-changed.

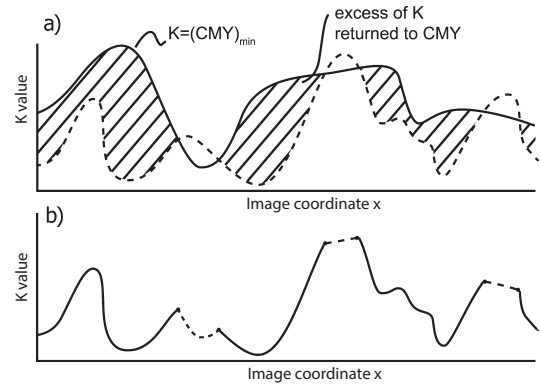


Figure 5: Modulation of $K = (CMY)_{min}$ signal by the security image data (a); resulting dual function signal for the black ink (b)

The resulting black ink signal at the lower part of Figure 5 gets dual function. It both replaces the certain amount of CMY achromatic value and, in spite of being partially distorted, presents the auxiliary image.

This way implemented security image wouldn't formally affect the basic image, stays to be concealed from viewing under any daylight but can be captured in the strong near infrared illumination.

4. Achromatic colors reproduction

Providing the maximum of reproducible gray levels was outlined by R. Hunt (1997) and stipulates the priority of black ink use in color print. The whole achromatic component can be considered as the basic one for image formation while the CMY inks as auxiliary ones, i.e. responsible just for the image chromaticity. Moreover, due to well known degradation of color vision sensitivity with decreasing of detail angular, spatial dimension, the small details and high contrast sharp transitions can also be reproduced with greater share of black or even, as it is done in color TV broadcast, completely achromatic.

The combining of K with accurately balanced CMY is in particular useful for b/w image when it is simultaneously printed on the same sheet with multicolor ones. Our research based on UCR offset atlas (Avatkova, 1987) has shown, for example, that at 290 % ink limit the addition of $C = M = Y = 62\%$ to K solid expands the gray scale optical density range for about 0.3. The effect is especially apparent at visual comparison of such print with its version using just the black ink and confirms the priority of the latter in achromatic colors formation in CMYK printing. Various ways of combining K ink and balanced CMY are formally possible.

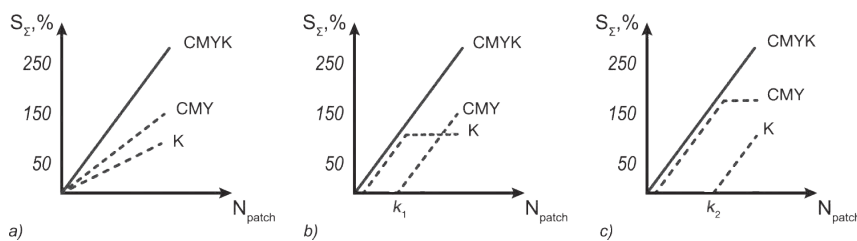


Figure 6: Exemplary variants of the combined use of K and balanced CMY for gray scale optimization at total ink limit $S_{\Sigma} = 250\%$; with constant replacement of CMY with K across the whole scale (a); with GCR settings (b); with UCR settings (c)

Their amounts can be uniformly distributed along the gray scale or each of them alternatively concentrated in its highlights or shadows divided by k_1 and k_2 wedge patch numbers, as indicated in Figure 6 under the assumption of 250 % total ink limit (Kuznetsov, 2002).

It has to be noted that the above considerations to certain extent artificially separate the formation of print

5. Expanding the print color gamut

The combined use of K and CMY inks discussed above expands the gamut in close vicinity to L^* axis of CIELCH space where colors can still be considered achromatic with taking into account their permissible ΔE^*_{ab} , for example, of 5 units from neutral as illustrated in Figure 7.

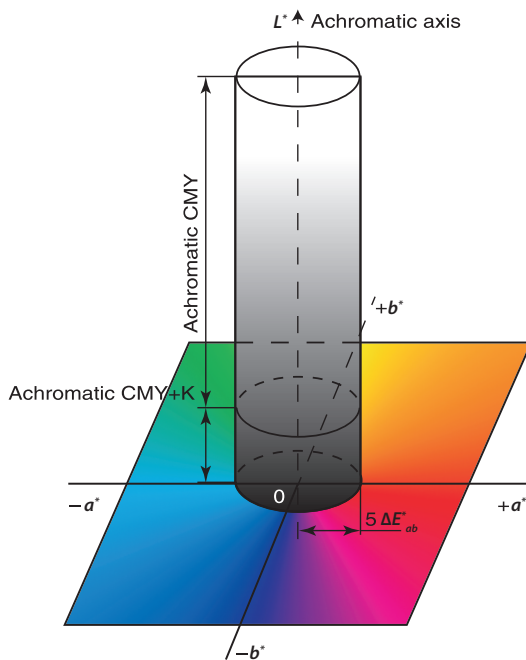


Figure 7: Black ink adds new neutrals to CMY color space in close vicinity of the lower part of its achromatic axis

6. Measurements and results

Our research comprised the comparative analysis of CIE $L^*a^*b^*$ and CIE L^*C^*h data taken by GretagMacbeth Eye-One Pro spectrophotometer calibrated for 2° Standard Observer, D50 illuminant, 0/45° measurement geometry and paper white point from UCR offset atlas (Avatkova, 1987). This atlas was printed in Experimental Print House of All Union Research Print Media Institute in Moscow according the soviet offset standards and comprises the data base of about 1500 color patches produced for different combinations of CMYK tone values. The main pur-

pose of this atlas was to fix the print colors matching at herein above discussed variants of CMY achromatic component replacing by the black ink. It also helped us to reveal the effect of CMY neutrally balanced addition to K solid for expanding the gray scale range.

However, this atlas lacks combinations of CMY near solids and their binary overlaps with different amounts of K. The ink solids (100 % values) are formally prohibited in halftone printing. The upper tone values of C, M, Y or K are mostly limited in practice by the

At the same time, it is practically used to add some K amount to C, M or Y solids to get new, darker chromatic colors. In the analogy to Figure 7, such procedure is formally illustrated in Figure 8 by adding K to one of the lower planes of CMY color body. However, the gamut expanding due to chromatic colors which exclusively appear with applying the fourth, black ink wasn't separately considered in the literature.

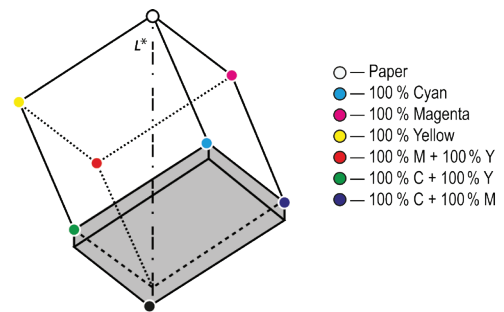


Figure 8: Formal example of color gamut expanding by K adding to CMY solids and their overprints

Moreover, one can find the contrary statement of color gamut reduction with black ink introduction (Balasubramanian, 2003, p. 366). At the same time, the issues of print gamut expanding by the use of intensive inks, addition of complimentary RGB colors to CMY process colors within the so called Hi-Fi Color concept, etc., were widely discussed in last decades.

pose of this atlas was to fix the print colors matching at herein above discussed variants of CMY achromatic component replacing by the black ink. It also helped us to reveal the effect of CMY neutrally balanced addition to K solid for expanding the gray scale range.

However, this atlas lacks combinations of CMY near solids and their binary overlaps with different amounts of K. The ink solids (100 % values) are formally prohibited in halftone printing. The upper tone values of C, M, Y or K are mostly limited in practice by the

still controllable ones of 95 % or 97 % (International Organization for Standardization, 2013; Kouznetsov and Alexandrov, 1997). So, the separate printing trial was provided on HP Premium Plus Photo Paper Matt substrate at drop-on-demand printer Canon PF8300S controlled by FlexiSIGN Pro v8.6 RIP to investigate the effect of K addition to such solids as compared with providing darker chromatic colors in CMY print version by simple adding of complementary process colors or their combinations.

The test objects were produced in Adobe Photoshop especially for this purpose for the variety of three and four inks amounts. They comprised the indexed versions of step wedges for C, M, Y and CM, MY, CY, CMY tone value (%) overprints with the stepwise K addition. Each wedge contained 11 patches for demonstration in meridian sections and on C^*b^* plane of $CIE L^*C^*b^*$ color space. The IT8-7.3 target for CMY and CMYK color gamut computation in MathLab was also used.

Examples of these data are given at $CIE L^*C^*b^*$ color space vertical slices for magenta and blue hues represented in Figure 9. The upper line of the diagram in Figure 9a shows the L^* reduction with continuous addition of the M tone value to the substrate from 5 % to practically used near solids of 95 %, while the upper line of the one in Figure 9b with the similar growth of CM.

It may seem that the further lightness reducing of thus achieved colors can be provided by adding them the complementary process ones. In the first case such color is green produced by the balanced sum of cyan and yellow, while for the blue tint it is yellow. However, the lower lines of both diagrams demonstrate much purer colors generation by adding just the black ink. As compared to said complementary color addition, it increases the target color saturation by 30 chroma units for magenta at $L^* = 30$ level (Figure 9a) and about 40 units for blue at $L^* = 23$ (Figure 9b).

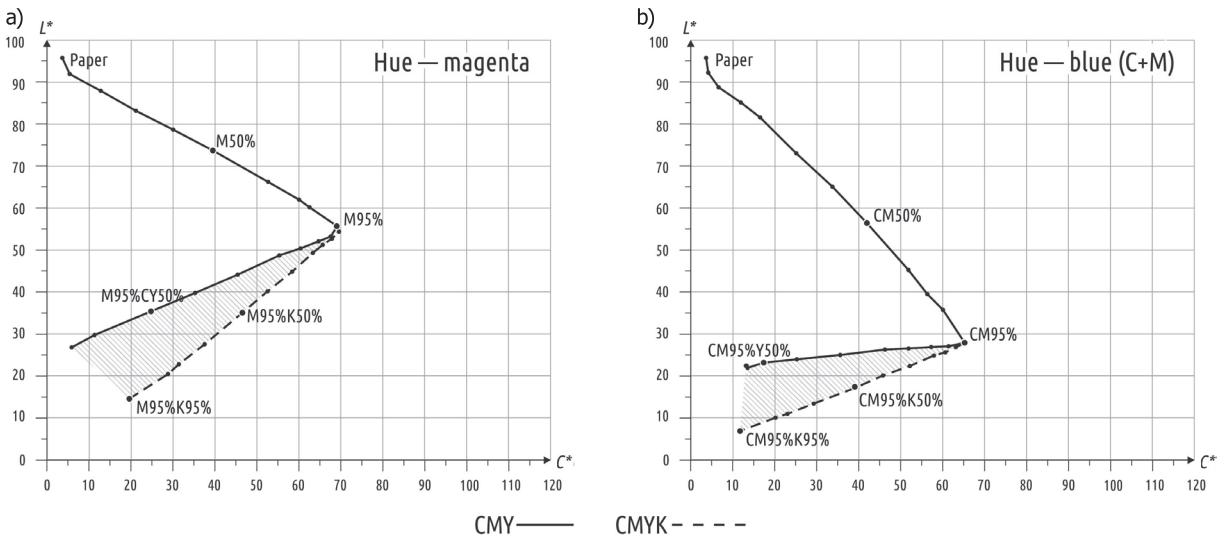


Figure 9: Coordinates of CMY and CMYK dark chromatic colors on meridian sections of $CIE L^*C^*b^*$ space for magenta (a) and blue (b) hues

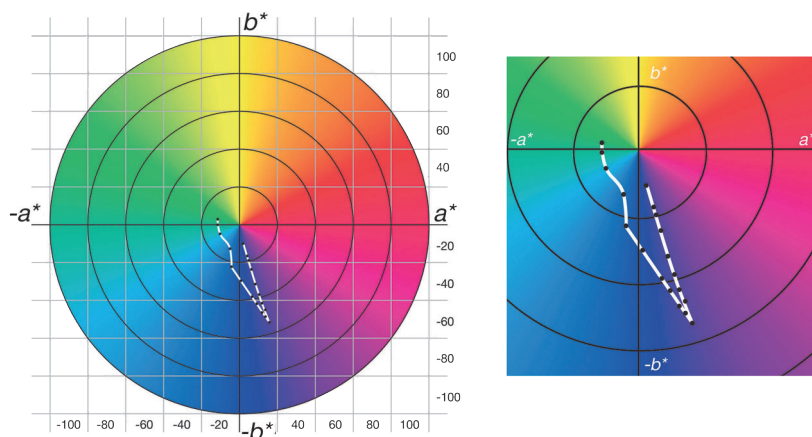


Figure 10: Lower lines of Figure 9b in projection on a^*b^* plane

Such difference is physically explained by that the black ink more or less uniformly reduces reflectance without distortion of source (magenta or blue) spectrum profile. To the contrary, the ink of opposite color not only darkens the source one by suppressing reflectance at its inherent in band of spectrum but also changes its hue as the left curve in Figure 10 shows. However, as the right line of the same figure confirms, the just K addi-

tion to 95 % C + 95 % M overprint keeps its blue hue constant.

The hatched areas of the both Figure 9 diagrams, as well as Figure 11, demonstrate the expanding of lower part of color gamut due to the use of the fourth, K color. According our three dimensional calculations it comprises about 10 %.

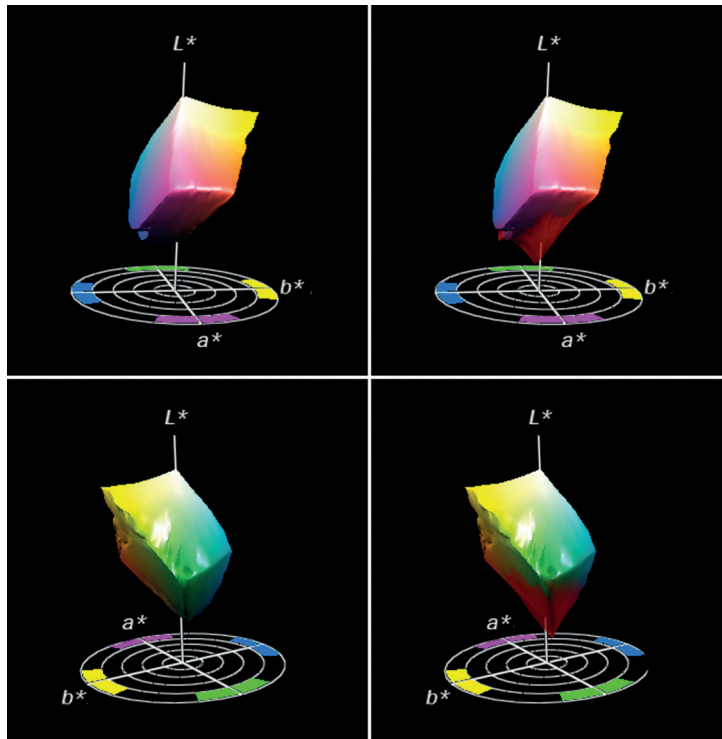


Figure 11: Different views of CMY (left) and CMYK (right) color gamut of the tested ink jet printer

7. Conclusions

It is meaningful to consider the black ink use in CMYK process in relation of its three basic functions:

- replacement of achromatic share of CMY combinations;
- combining black with the certain amount of balanced CMY in reproduction of achromatic colors;
- creating the new chromatic colors unavailable for CMY.

Within the whole continuum of its variants, the first of these functions is in full characterized by two dimensions:

- volume of K as the share of a reference $(\text{CMY})_{\min}$;
- location of replacing K volume within the tone value range of a print.

Within this function the facility also exists of non-costly color print protecting by modulating $K = (\text{CMY})_{\min}$ by the signal of an auxiliary image discernible in near

infrared light. Contrary to the first one, the other two of these functions are completely additional and have no alternatives.

New chromatic colors provided by the black ink use expand the CMY gamut for about 10 %. So, the move from CMY to CMYK which took place in the 30's of the last century can be concerned as the first step to Hi-Fi Color technologies aimed nowadays on a similar effect, reached once again by increasing the number of process inks.

The proper discerning of K use in CMYK printing appears to be beneficial in creating or operating the updated prepress software of foreseen future.

The results of above research and discussion can help to effectively explore the effect of multiple black ink functions in color halftone printing.

References

- Avatkova, N., 1987. Atlas of chromatic colors minimization in offset printing. In: *Experimental print shop of VNII poligrafii*. Moscow. (in Russian: Аваткова Н. А., 1987. Атлас МЦК. Минимизация цветных красок в офсетной печати. Шкала цветового охвата. Москва. ВНИИ комплексных проблем полиграфии.)
- Balasubramanian, R., 2003. Device characterization. In: G. Sharma, ed. 2003. *Digital Color Imaging Handbook*. Boca Raton: CRC Press. Ch. 5.
- Bugnon, T., Brichon, M. and Hersh, R., 2007. Model based deduction of CMYK surface coverage from visible and infrared spectral measurements of halftone prints. In: R. Eschbach and G.G. Marcu, eds. *Proc. SPIE Vol. 6493, 649310, Color Imaging XII: Processing, Hardcopy, and Applications*. San Jose, CA, 29 January 2007. Bellingham, WA: SPIE.
- Daels, K. and Delabastita, P., 1994. Tone dependent phase modulation in conventional halftoning. In: R. Eschbach, ed. 1994. *Recent Progress in Digital Halftoning*. Springfield, VA: IS&T. pp. 46–49.
- Enoksson, E., 2004. Image reproduction practices. In: *2004 TAGA Proceedings: 56th annual technical conference of the Technical Association of the Graphic Arts*. San Antonio, 18–21 April 2004. Sewickley: TAGA. pp. 318–331.
- Hunt, R., 1997. Why is black-and-white so important in color? In: K. Braun and R. Eschbach, eds. 1997. *Recent Progress in Color Science*. Springfield, VA: IS&T. pp. 123–126.
- International Organization for Standardization, 2013. *ISO 12647-2:2013 Graphic technology – Process control for the production of half-tone colour separations, proof and production prints – Part 2: Offset lithographic processes*. Geneva: ISO.
- Kipphan, H., ed., 2001. *Handbook of Print Media: Technologies and Production Methods*. Berlin: Springer. pp. 519, 578–579.
- Kouznetsov, J.V. and Alexandrov, D.M., 1997. Screening technique modification and its effect on halftone print quality. In: *NIP 13: Proceedings of International Conference on Digital Printing Technologies*. Seattle, WA, 2–7 November 1997. Springfield, VA: IS&T. pp. 650–654.
- Kuznetsov, Y.V., 2002. *Image data processing technology*. Moscow: SPb Institute of Printing. (in Russian: Кузнецов Ю. В., 2002. Технология обработки изобразительной информации. Москва – Санкт-Петербург. Петербургский институт печати.)
- Kuznetsov, Y.V., 2013. Providing the balance of an “old” and “new” knowledge in education content: examples from graphic technology teaching. *Advances in Education Research*, 30, pp. 59–65.
- Murray, A., 1936. Monochrome reproduction in photoengraving. *Journal of the Franklin Institute*, 221(6), pp. 721–744.
- Neugebauer, H.E.J., 1937. Die theoretischen Grundlagen des Mehrfarbendruckes. *Zeitschrift für wissenschaftliche Photographie, Photophysik und Photochemie*, 36(4), pp. 73–89.
- Nuberg, N.D., 1932. *Handbook of color*. Moscow: Light industry Gosizdat. pp. 86–87. (in Russian: Нюберг, Н.Д., 1932. Курс цветоведения. Москва: Госиздат легкой промышленности.)
- Rhodes, W.L. and Hains, C.M., 1993. The influence of halftone orientation on color gamut and registration sensitivity. In: *Proceedings of IS&T's 46th Annual Conference*. Cambridge, MA, 9–14 May 1993. Springfield, VA: IS&T. pp. 117–119.
- Scheberstov, V.I., 1936. Quantitative relationships of positive and negative characteristics, necessary for normal reproduction of the original in halftoning process. In: *Proceedings of the Research Institute OGIZ* 3(46). (in Russian: Шеберстов, В.И., 1936. Количественные соотношения характеристик позитива и негатива, необходимые для нормального воспроизведения оригинала в автолithном процессе. Труды НИИ ОГИЗа, 3(46).)
- Southworth, M., McIlroy, T. and Southworth, D., 1992. *The Color Resource Complete Color Glossary: From Desktop to Color Electronic Prepress*. Livonia, NY: Color Resource.
- Žiljak, I., Žiljak Vujić, J. and Pap, K., 2008. Colour control with dual separation for daylight and daylight/infrared light. In: N. Enlund and M. Lovreček, eds. *Advances in Printing and Media Technology: Proceedings of the 35th International Research Conference of Iarigai*. Valencia, September 2008. Darmstadt: International Association of Research Organizations for the Information, Media and Graphic Arts Industries. pp. 273–278.

Professional communication

JPMTR 1510
 DOI 10.14622/JPMTR-1510
 UDC (655.1) 762 | 62-1/9

Professional communication
 Received: 2015-12-10
 Accepted: 2016-05-16

Evaluation of in-line viscosity measurement sensors in gravure printing

Henrik Knauber, Peter Schöffler, Thomas Sprinzing, Armin Weichmann

Hochschule der Medien,
 Institut für Angewandte Forschung (IAF),
 Nobelstr. 10, 70569 Stuttgart, Germany

E-mails: hk037@hdm-stuttgart.de
 ps092@HdM-Stuttgart.de
 sprinzing@hdm-stuttgart.de
 weichmann@hdm-stuttgart.de

Abstract

For the stabilisation of printing quality, gravure printing machines are normally equipped with viscosity measurement systems. Recently two newly developed viscosity measuring systems, a microelectromechanical tuning fork sensor and an acoustic wave sensor, were introduced to the market. Those systems compete with the traditional rotary viscometer and the dropping body measurement. A system comparison of the different systems were implemented and performed at a Rotomec MW 60 rotogravure press. The aim was to find a system for in-line viscosity measuring of printing inks, which is as accurately as possible and does need minimal cleaning effort. Four experiments were conducted to evaluate the different viscosity measuring instruments: accuracy of the solvent concentration measurement, equipment capability, temperature behaviour in ink and influencing factors of viscosity measurement in the printing process. The results show that the acoustic wave sensor and the rotary viscometer are suitable for the viscosity measurement in gravure printing.

Keywords: viscosity sensors, tuning fork sensor, acoustic wave sensor, rotary viscosimeter

1. Introduction and background

For the stabilisation of printing quality, gravure printing machines are normally equipped with viscosity measurement systems. Recently, two newly developed sensor systems were introduced to the market, a microelectromechanical tuning fork sensor and an acoustic wave sensor. Those systems compete with the traditional rotary viscometer and the dropping body measurement. With regard to the technical equipment of the machine, a system comparison of the different measurement systems were implemented at a Rotomec MW 60 rotogravure press.

For the examination of the different sensors, four tests have been designed, investigating their accuracy, behaviour during the printing process, temperature behaviour in ink, and the behaviour in reaction to external disturbing factors. Based on these tests, recommendations were derived.

Most commonly used viscosity parameters are the kinematic viscosity ν and the dynamic viscosity η (Equation 1). Dynamic viscosity η is measured in $\text{Pa} \cdot \text{s} = \text{kg} \cdot \text{m}^{-1} \cdot \text{s}^{-1}$, whereas kinematic viscosity ν is measured in $\text{m}^2 \cdot \text{s}^{-1}$. The conversion is via the the density ρ .

$$\eta = \frac{\nu}{\rho} \quad [1]$$

In gravure printing, efflux cups are most common and with these, viscosity is measured in (efflux cup) seconds. Calibration curves between (efflux cup) seconds and the kinematic viscosity ν are defined, e.g. according to DIN 53211 (1978).

Acoustic wave sensors measure the product of dynamic viscosity and the density of the measurement sample, i.e. the kinematic viscosity, as the measurement of an acoustic wave sensor is based on the acoustic impedance (Equation 2).

$$Z = (\omega \cdot \rho \cdot \eta)^{\frac{1}{2}} \quad [2]$$

where ω represents the angular frequency $\omega = 2 \cdot \pi \cdot f$.

To measure the viscosity, the resonator, an electrostrictive quartz crystal plate, is put in contact with the fluid. The resonator is driven by the electrode at the bottom surface (Figure 1) and moves sinusoidally perpendicular to the sensor surface with the frequency ω and the amplitude U . The frequency is defined by the construction of the sensor, whereas the amplitude depends on the strength of the applied electrical signal. A certain layer of the fluid is hydrodynamically coupled with the sensor surface; its thickness depends on the viscosity.

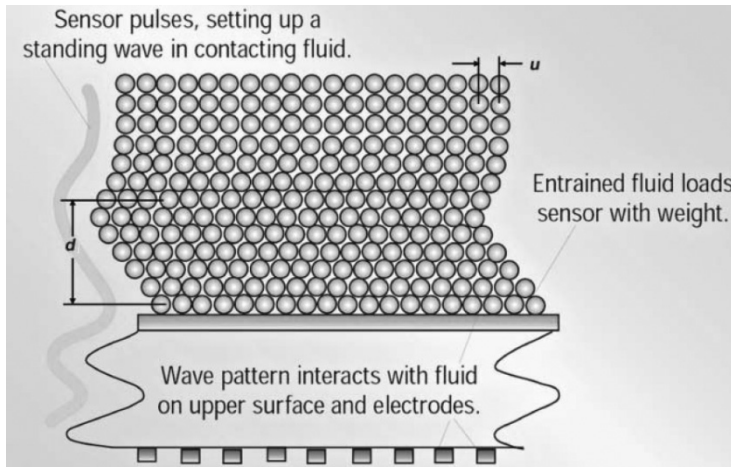


Figure 1: Cross section of acoustic wave sensor (Durdag, 2007)

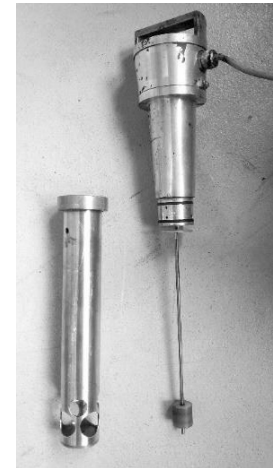


Figure 2: Rotary viscometer with cylindrical test block

The penetration depth d of the wave into the fluid is dependent on the frequency, the viscosity and the density of the fluid (Equation 3):

$$d = \left(\frac{2 \cdot \eta}{\omega \cdot \rho} \right)^{1/2} \quad [3]$$

The acoustic viscosity is measured through the power consumption of the quartz resonator that emits ultrasonic waves into the measurement fluid to a certain depth d .

The measured number (referred by the vendor as “acoustic viscosity”) is the product of the density and the dynamic viscosity (Equation 4) and has the unit $\text{g} \cdot \text{cm}^{-3} \cdot \text{mPa} \cdot \text{s}$ (Durdag, 2007; 2008).

$$\eta_A = \frac{Z^2}{\omega} = \eta \cdot \rho \quad [4]$$

The microelectromechanical tuning fork sensor delivers density, viscosity and temperature, thus it measures kinematic and dynamic viscosity simultaneously. The sensor can be seen as a tuning fork with a flat profile at its end, which is electrically stimulated to an elliptical oscillation within a fluid with its resonant frequency. The surrounding medium impacts the resonant frequency of the tuning fork. As the fork profile is different in the two oscillation directions, the detuning in this two directions provides two distinct values, therefore enabling the calculation of both, dynamic viscosity and density.

A rotary viscometer served as a reference instrument, which was placed directly into the ink tank. As the name suggests, the sensor has a cylindrical measuring body which rotates around its axis (Figure 2).

With increasing viscosity of the measured fluid, the torque resistance at the measuring body increases. As the torque of the motor is held constant, the rotational speed decreases. The reduced rotational frequency is captured by the evaluation unit and transformed to dynamic viscosity.

2. Materials and methods

2.1 Inks and solvents

Rotogravure printing inks are organic-solvent- or water-based inks of low viscosity, with a dynamic viscosity η ranging from 10 mPa · s to 200 mPa · s. To achieve the correct viscosity, the inks are mixed with solvent, which affects the pigment concentration and optical density of the colour.

As solvent evaporates out of the ink during printing, the viscosity increases. Additionally, the behaviour of the ink changes in several respects, including colour strength (pigment concentration), fluid behaviour during cell filling and doctoring, and the behaviour within the printing nip and drying section. For this paper, conventional process colour inks with toluene (publication rotogravure printing) and ethanol / ethyl acetate (packaging gravure printing) in different concentration levels were used. Additionally, a white gravure ink was mixed with varying concentrations of ethyl acetate.

2.2 Experiments

Four experiments were conducted to evaluate the different viscosity measuring instruments. The following inks from Siegwirk Druckfarben AG were mixed (Table 1):

Table 1: Inks used in the experiments (for column L% see section 2.4)

Ink	Solvent portion L% (%)	Kinematic viscosity (Frikmar 3 mm cup) (s)	Temperature T (°C)
Black series NC 133 Solvent: Ethanol Extender: 150 %	51.0	24.5	23.0
	42.9	26.8	22.7
	39.9	27.9	22.5
	36.4	29.0	22.1
	34.1	30.0	22.4
	34.9	30.0	21.9
	30.7	31.9	21.9
	28.9	33.4	21.6
Cyan series NC 133 Solvent: Ethanol Extender: 150 %	60.0	23.1	21.2
	45.8	26.7	21.5
	34.0	31.7	21.6
Black Solvent: Toluol Extender 200 %	44.8	22.8	22.6
	36.5	26.4	22.6
	25.0	32.3	22.7
White – PU-Binder Solvent: Ethyl acetate	33.3	23.1	21.4
	24.8	26.6	21.5
	16.6	32.1	21.6

2.2.1 Experiment 1: Accuracy of the solvent concentration measurement

Reproducibility of the viscosity measurements was tested with different inks representing the whole process range of solvent concentrations. The data obtained from this experiment were used to map the individual measurements to L% (solvent content of the ink).

2.2.2 Experiment 2: Equipment capability study

The equipment capability study is a method to evaluate the accuracy and reliability of different measurement systems. This study allows researchers to analyse and determine the best measurement system for respective areas of application. The commonly used method resulted from decades of experience within the automotive industry. Three analytical procedures, as shown in Table 2, are foreseen:

Table 2: Equipment capability study

Procedure	Purpose	Parameter
Procedure 1	Systematic error and repeatability	C_g, C_{gk}, t -Test, confidence intervals
Procedure 2	Repeatability, reproducibility (with operator influence)	$\%R\hat{e}R, ndc$
Procedure 3	Repeatability, reproducibility (without operator influence)	$\%R\hat{e}R, ndc$

Procedure 1 is normally used by the manufacturer of the measurement system to prove the suitability and capability. Procedures 2 and 3 are deployed by the user to confirm suitability on-site.

Procedure 1

The two most important quality parameters for the measurement equipment are the C_g and C_{gk} values. Procedure 1 uses these values to determine the parameters within its application. With this procedure, measurement series are made at a calibration standard and out of these series (at least 25 values) the arithmetic average and standard deviation are calculated. After that, in combination with the specified characteristic tolerances, the C_g and C_{gk} values, can be calculated (Polák, Drlička and Žitňanský, 2014). A measurement system is defined capable if the C_g and C_{gk} values are greater than 1.3.

Procedure 2

Procedure 2 is also known as $\%R\hat{e}R$ or as the GR&R-Study (Gage Repeatability & Reproducibility). After defining the amount of test objects n and number of testers k , whereby the test objects should cover the process range, the number of repeats (r) are determined, where $n \cdot r \cdot k > 30$ (Dietrich and Schulze, 1998; 2007). An analysis of variation (ANOVA) is made and values obtained are repeatability EV , reproducibility AV and part deviation PV . The EV value is a measure of the influence of the measurement equipment, whereas the AV value is a measure of the user’s influence.

The $R\hat{e}R$ value is calculated by Equation 5:

$$R\hat{e}R = \sqrt{EV^2 + AV^2} \tag{5}$$

For a particular case, the single values ($EV, AV, PV, R\hat{e}R$) are set into relation with the benchmark RF , which can be seen as the tolerance T of the process or the total deviation TV out of the process deviation. If the process deviation is unknown, TV can be derived from Equation 6:

$$TV = \sqrt{EV^2 + AV^2 + PV^2} \tag{6}$$

if only the measurement system is under investigation, PV is not to be considered and therefore:

$$TV = \sqrt{EV^2 + AV^2} = R\hat{e}R \tag{7}$$

The relative values $\%EV, \%AV, \%PV, \%R\hat{e}R$ result by dividing EV, AV, PV , and $R\hat{e}R$ by TV .

The evaluation of the measurement results can be made according to the Ford guideline EU 1880 (1997):

- $\%R\hat{e}R \leq 20 \%$ measurement system is capable,
- $\%R\hat{e}R \leq 30 \%$ measurement system is partly capable,
- $\%R\hat{e}R \geq 30 \%$ measurement system is not capable.

Procedure 3

In this survey, procedure 3 is used. Procedure 3 is a derivation of procedure 2, where the influence of the user is omitted. This is possible if the user has no influence on the results, like in automated measurements or in-line systems. In this case, $n \cdot r > 20$ applies. If there are no different test objects, the amount of repeats has to be increased. As already described, the ANOVA is used for the evaluation of the system, where the reproducibility AV equals zero. The $R\hat{e}R$ value corresponds in that case to the repeatability EV .

2.2.3 Experiment 3: Temperature behaviour in ink

The change in viscosity was measured as a function of temperature. The aim was to examine the behaviour of the different measuring instruments when handling ink which varies in temperature, e.g. cold ink at start up or ink heated up during running the printing process.

2.2.4 Experiment 4: Influencing factors of the viscosity measurement in the printing process

Typical parameters influencing the measurement process – printing speed, flow rate of ink within the inking system, and micro foaming extent – were varied on press. The aim of the experiment was to determine the viscosity measuring instrument with the best resilience within the process environment.

2.3 Experimental setup

The viscosity measuring instruments were installed in the ink circulation of a Rotomec MW60 gravure printing press, which is driven by a double acting pneumatic pump. Figure 3 illustrates the individual components of the general experimental setup.

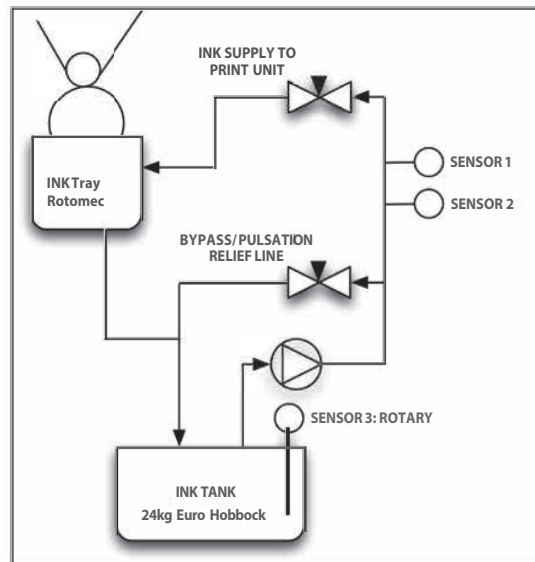


Figure 3: Experimental setup;
Sensor 1: Tuning fork; Sensor 2: Acoustic wave; Sensor 3: Rotary viscometer

To gather the values for each test point, the ink was poured into the tank, the tank was closed and the pump activated. Then the measurement was conducted for 5 min and the values of each sensor collected. After deactivating the pump, the tank was opened, the ink removed and the tank together with the other parts of the ink circulation was cleaned.

2.4 Reference system: Solvent concentration

The meaning of the values of the different viscosity measuring instruments differ according to the different measuring principles (see section 1) and not all deliver dynamic viscosity. Therefore, the correlation between the different systems was based on a reference system solvent concentration: $L\%$ (%), the quotient of the amount of solvent additionally poured into the basic ink, delivered by the ink manufacturer, to the amount of the basic ink itself. As the viscosity is indirectly proportional to this number, the transformation (Equation 8) was used to match the values of the devices to $L\%$, with characteristic constants a and b for each device and ink type.

$$y = \frac{a}{x} + b \quad [8]$$

where x is solvent concentration $L\%$ in %. and y is value of viscosity from given measurement device.

3. Results and discussion

3.1 Experiment 1: Accuracy of the solvent concentration measurement

All measurement values were converted through Equation 8 to the solvent content and given as $L\%$. Figure 4 shows these $L\%$ values of the devices compared to the actual solvent concentration $L\%$.

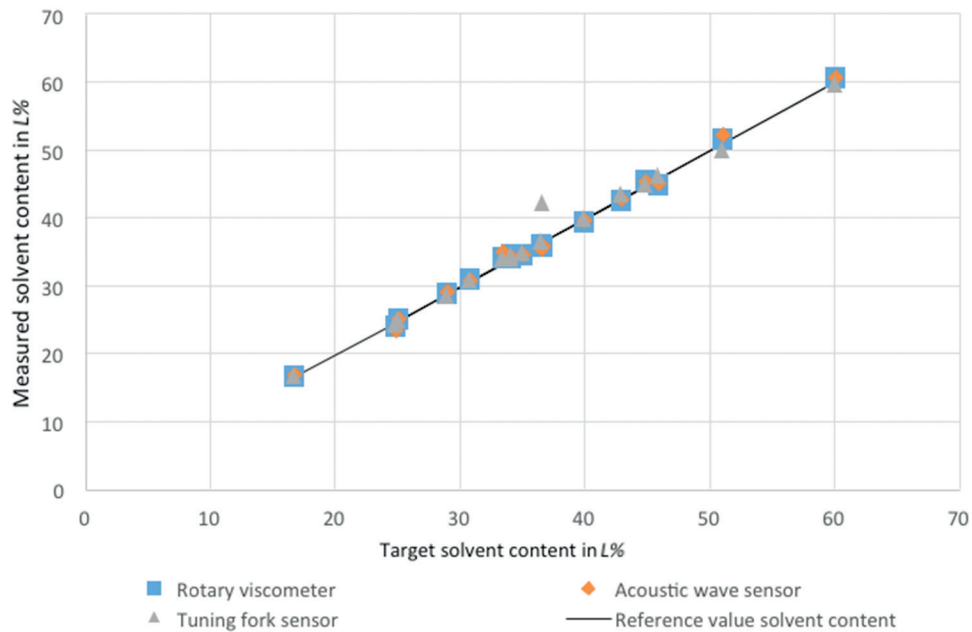


Figure 4: Target-actual comparison of the three sensors for the different dilutions

All instruments can reproduce the different dilutions levels with good accuracy with the exception of one outlier, presumably a faulty measurement. The acoustic wave sensor has the lowest standard deviation of $\pm 0.07 L\%$ of all dilutions, the tuning fork sensor the highest with $\pm 0.09 L\%$. The rotary viscometer with values of $\pm 0.08 L\%$ lies between the results for other sensors.

3.2 Experiment 2: Equipment capability study

The testing fluid for the evaluation was Black NC 133 from Siegwirk Druckfarben AG with 150 % of extender and ethanol as solvent with a solvent content of 36.44 $L\%$. The tolerances were defined to ± 1 s (3 mm DIN cup), which is a common value in order to avoid variations in print. For a solvent content of 36.44 %, flow time of 1 s (3 mm DIN cup) corresponds to a solvent content of 2 %. This leads to a tolerance of 4 $L\%$. Table 3 shows the results of the measurements.

Table 3: Results for the equipment capability study procedure 1 (C_g , T_{min/C_g}) and procedure 3 (%EV and %R \hat{c} R)

Ink	Rotary viscometer in $L\%$	Acoustic wave sensor in $L\%$	Tuning fork sensor in $L\%$
Basic size in $L\%$	36.44	36.44	36.44
Tolerance in $L\%$	4.00	4.00	4.00
Mean in $L\%$	36.11	35.54	36.01
Standard deviation in $L\%$	0.13	0.05	0.70
C_g	1.61	4.00	0.29
T_{min/C_g} in $L\%$	3.309	1.32	18.59
%EV	17.5	5.76	71.61
%R \hat{c} R	17.5	5.76	71.61

The equipment capability study showed that the rotary viscometer and the acoustic wave sensor are capable with a C_g of 1.61 and 4.00, respectively. The tuning fork sensor is with C_g of 0.29 far below the critical value of 1.33 and therefore it is not capable. For the tuning fork sensor, a tolerance of 18.59 L% can be achieved at the best. That means that variations of ± 4.5 s flow time (3 mm DIN cup) are possible. A reason for the poor results of the tuning fork sensor could be the experimental setup, where the cross section of the tube the sensor was integrated in was too low and the measurements were affected by the pulsation of the pump.

The results of procedure 3 confirm the results of procedure 1 and show that the acoustic wave sensor has a very good repeatability ($\%EV = 5.76$). The rotary viscometer with $\%EV$ of 17.5 is also below the limit of 20 % and therefore is capable.

3.3 Experiment 3: Temperature behaviour in ink

The black ink was stored in a closed tank for 24 h at 7 °C. During the measuring operation, the ink container was heated from 12 °C to 36 °C. The measured values of the three sensors are shown in Figure 5.

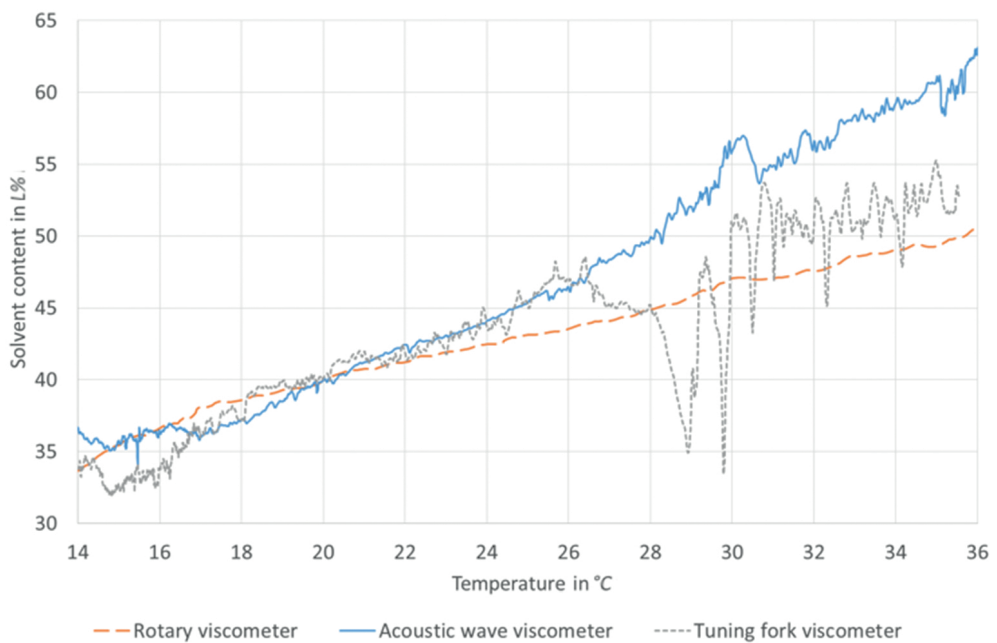


Figure 5: Temperature behaviour in ink (higher L% corresponds to lower viscosity); normalised at 20 °C

The viscosity change due to increasing the ink temperature is accurately reproduced by the sensors. Again, the tuning fork sensor shows big variations. Additionally, the slope of the increase is significantly higher for the acoustic wave sensor. This can be explained by density changes, which occur in parallel to the lowering of the viscosity. As this sensor measures “acoustic impedance” acc. to Equation 2, the density decrease affects the measurement with an additional linear factor. As a result, each sensor has to be calibrated separately to compensate for temperature changes.

3.4 Experiment 4: Influencing factors of the viscosity measurement in the printing process

Firstly, the effect of printing speed was investigated. The diving of the cylinder with the empty cells into the ink brings many small air bubbles into the ink and creates micro foaming. The higher the speed, the bigger this effect is. The following tables (Table 4, Table 5 and Table 6) show the sequence of the test procedures. Viscosity measurements during test procedures, by using different viscometers, are presented in Figure 6.

Additionally, the pumping creates foaming too. This effect was investigated in a second measurement series by varying the pressure to the pneumatic pump, therefore modifying the ink flow and additionally the temporal pressure profile within the tubes. The higher the flow rate, the more foam is created. Moreover, as the tuning fork sensor and the acoustic wave sensor are located within the pumping tube line, the flow through or along the sensor was expected to affect the measurement.

Table 4: Process description: Printing speed

Influence factor	Time	Process description
1	11:32	Rotary viscometer not surrounded with ink – values excluded
2	11:44	Added ink
3	12:10	Printing speed: 180 m · min ⁻¹
4	12:15	Rotary viscometer not surrounded with ink – values excluded
5	12:30	Added ink
6	12:35	Reduced printing speed: 60 m · min ⁻¹
7	12:54	Increased printing speed: 240 m · min ⁻¹
8	12:57	Reduced printing speed: 60 m · min ⁻¹

Table 5: Process description: Pump pressure

Influence factor	Time	Process description
9	13:05	Bypass: off
10	13:08	Air throttling: open
11	13:11	Pump pressure: 3.5 bar / Bypass: closed / Air throttling: open
12	13:14	Pump pressure: 3.5 bar / Bypass: closed / Air throttling: open / Ink throttling: slightly open
13	13:18	Pump pressure: 3.5 bar / Bypass: closed / Air throttling: open / Ink throttling: half open
14	13:21	Pump pressure: 3.5 bar / Bypass: closed / Air throttling: open / Ink throttling: fully open
15	13:23	Pump pressure: 2.2 bar / Bypass: closed / Air throttling: open / Ink throttling: fully open
16	13:26	Pump pressure: 2.2 bar / Bypass: open / Air throttling: open / Ink throttling: fully open
17	13:29	Standard-setting as 13:05 clock

Often a stirring rod is used to ensure a stable dispersion of the ink, especially with special effect pigments (metallic, iriodine) or with white pigments. This again results in increased foaming. In addition, the rotary sensor could be affected by the ink flow generated in the tank. Therefore, a third measuring series was set up with a stirring rod.

Table 6: Process description: Micro foam

Influence factor	Time	Process description
18	14:18	Printing speed: 300 m · min ⁻¹ (without substrate)
19	14:24	Activation of stirrer
20	14:39	Aspiration of foam from the ink surface
21	14:42	Without ink tray
22	14:46	Aspiration of foam from the ink surface

Results: rotary viscometer

The addition of solvent at 11:53 is correctly reproduced by the rotary viscometer. The graph shows the ongoing test procedure in a relative smooth curve.

Between 12:35 and 13:00 the printing speed was changed and between 13:05 and 13:30 parameters of the pump stroke varied. To the end of the experiment, the influence of micro foam was checked. The curve slightly descends, as the solvent evaporates slowly. The rotary viscometer can be described as highly resistant to the tested influencing factors.

Results: Acoustic wave sensor

The addition of solvent at 11:53 is correctly reproduced by the acoustic wave sensor. Nevertheless, the values decrease after reaching a local maximum more than expected, exaggerating the effect of the solvent evaporation.

Results: Tuning fork sensor

The tuning fork sensor is susceptible to pump strokes and micro foam and produces a lot of incorrect measurement values. During the variation of the pump settings, measurement errors resulted when the ink throttle was opened. The reason may be that the diameter of the tube, where the sensor unit sits in, has a diameter which is too small, therefore causing high flow speeds and high pressure peaks, which disturb the measurement. Consequently, a change in the ink flow has a negative effect on the value acquisition by the tuning fork system.

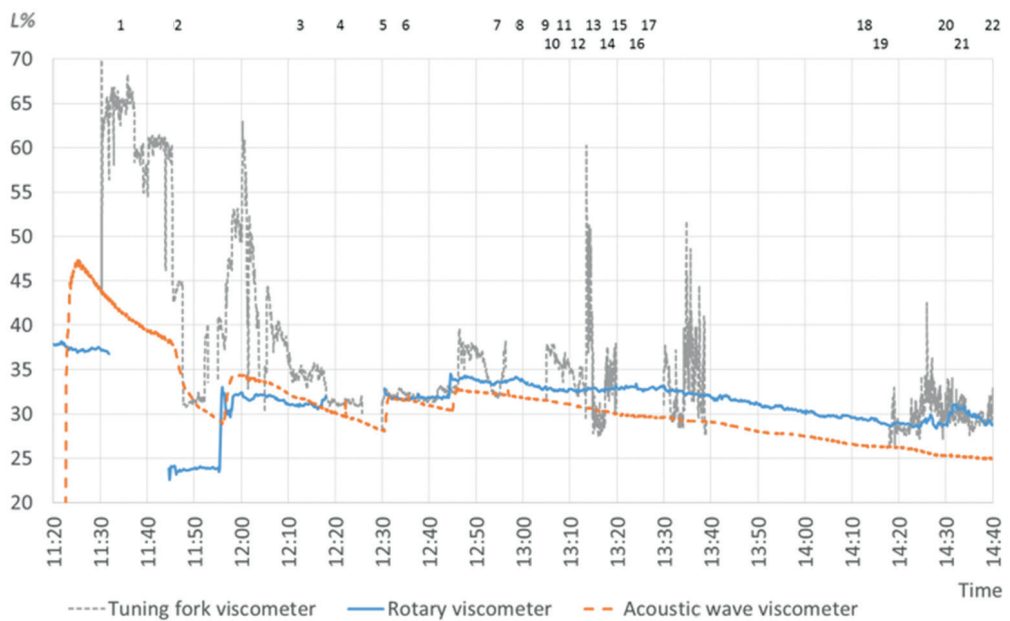


Figure 6: Measurements of viscometers through measurement series; normalised at 12:30

4. Discussion

The evaluation of the three investigated measuring sensors showed that the tuning fork sensor is least tolerant to the pump strokes and to the microfoaming. Pneumatic pumps create a pulsing ink flow, therefore strongly varying fluid velocities and pressures. The measurement is performed through the elliptical oscillations of a rod positioned within the tube for the ink transport from bucket to ink pan, perpendicular to the vector of ink flow. Varying pressures might impact on the rod during pulse cycles, therefore generating erroneous values. A special shunt with homogenized and slow ink flow might solve this problem, however adding to the effort on installation and cleaning. Additionally, it can be assumed that micro bubbles, which come in proximity of the oscillating rod, change the behaviour of the fluid significantly, as they change the mean density and, as relatively big “particles” within the fluid, the mean mobility of the fluid. As this is the number to be measured, these micro bubbles influence every measurement system. Nevertheless, the tuning fork principle seems to be most sensitive to this and seems to be more applicable for unperturbed fluids.

The acoustic wave sensor amplifies the decrease of viscosity due to solvent evaporation as well as by temperature increase. As this sensor measures the “acoustic viscosity”, which is the product of dynamic viscosity and density, and both parameters increase with lower solvent content or higher temperature, it could be assumed that the overall signal is more sensitive compared to measuring dynamic viscosity alone. In any case, the density and its change have to be taken into account when calibrating and transforming the measured values from this measuring principle to one which measures the dynamic viscosity. Unfortunately, we did not measure the density with a separate measuring

device, so we cannot confirm this assumption yet. (The tuning fork sensor delivers values for the density too, but the quality of these values was uncertain to the same extent as the values for the dynamic viscosity itself.)

The rotary viscometer performed as expected over the entire experimental period. If it is ensured that the sensor is always completely surrounded with ink, print speed and pump strokes do not influence the measurement and micro foam does only to a small extent.

5. Conclusion

The tests showed that basically all considered sensors are capable of gathering viscosity. The different levels of dilution are captured accurately by all measurement systems. However, the acoustic wave sensor delivers the smallest measurement variations over all levels of dilution. This result is verified in the equipment capability study, where the acoustic wave sensor proved to be the most capable of the three sensors. The tuning fork sensor could not prove its capability in the test set up used.

As the sensors use different measuring principles, they respond differently to temperature variations of the ink, i.e. the coupled viscosity and density changes, and have to be calibrated to correctly response on the process variability.

The tuning fork sensor reacts very sensibly to pump strokes of the pneumatic pump and to micro foam and therefore it is not suitable for an in-line viscosity measurement system without substantial change of the setup used. The acoustic wave sensor is much more insensitive to these effects. Nevertheless, before applying this sensor it has to be investigated if the measuring principle (product of dynamic viscosity and density) sufficiently explains the measured stronger decline compared to the rotary viscometer when solvent evaporates out of the ink.

The rotary viscometer is capable and represents the current state of the art in the printing industry. However, it was the aim to find a system, which is accurate, minimize cleaning effort and can be installed on the press with minimal handling issues. In this context, the acoustic wave sensor is to be preferred.

References

- Dietrich, E. and Schulze, A., 1998. *Statistische Verfahren zur Qualifikation von Messmitteln, Maschinen und Prozessen*. 3rd ed. München, Wien: Hanser.
- Dietrich, E. and Schulze, A., 2007. *Prüfprozesseignung: Prüfmittelfähigkeit und Messunsicherheit im aktuellen Normenumfeld*. 3rd ed. München, Wien: Hanser.
- DIN Deutsches Institut für Normung e.V., 1987. *DIN 53211: 1987, Paints, varnishes and similar coating materials: Determination of flow time using the DIN flow cup*. Berlin: DIN.
- Durdag, K., 2008. Schnelle Messungen der Viskosität. *Elektro AUTOMATION*, 61(9), pp. 84–87.
- Durdag, K., 2007: Messung der Ölviskosität. *Elektronik Industrie*, 38(11), pp. 72–74.
- Ford EU 1880, 1997. *Guideline for the Capability of Measurement Systems and Gages*.
- Polák, P., Drlička, R. and Žitňanský, J., 2014. Capability assessment of measuring equipment using statistic method. *Management Systems in Production Engineering*, 4(6), pp. 184–186.

Topicalities

Edited by Markéta Držková

Contents

News & more	253
Bookshelf	255
Events	261

News & more

Updates on ISO standards for graphic technology

A year after the summary of ISO standards under the responsibility of ISO technical committee TC 130 Graphic technology provided in 4(2015)3 there is a right time for new updates. The list of confirmed or reconfirmed documents, that remain in current version without any change, is again quite long and contains the technical specification 10128:2009 since September 2015, the standards 15930-7:2010, 15930-8:2010 and 16612-2:2010 since December 2015, the standards 12218:1997, 12645:1998, 16612-1:2005 and 28178:2009 since February 2016, the standards 2846-2:2007, 12640-3:2007, 12643-5:2010 and 15076-1:2010 since March 2016, and since September 2016 also the standard 12640-4:2011.

Among the standards recently decided to be revised is ISO 12636:1998 Graphic technology – Blankets for offset printing, with ISO/DIS 12636 registered in September 2016. Further, it is ISO 2846-1:2006 Graphic technology – Colour and transparency of printing ink sets for four-colour printing – Part 1: Sheet-fed and heat-set web offset lithographic printing, Edition 2 (this standard was last reviewed and confirmed in 2015); DIS ballot for ISO/DIS 2846-1 has been initiated in September 2016. Finally, ISO 17972-4:2015 Graphic technology – Colour data exchange format (CxF/X) – Part 4: Spot colour characterisation data (CxF/X-4) published last year is under revision as well, with ISO/CD 17972-4 approved for registration as DIS in April 2016.

This year in June, two parts of ISO 2846 Graphic technology – Colour and transparency of printing ink sets for four-colour-printing were withdrawn, namely Part 3: Publication gravure printing (published in 2002), and Part 5: Flexographic printing (from 2005). To delete the normative reference on the latter one, a brief amendment on ISO 12647-6:2012 was necessary. The technical report ISO/TR 16044:2004 Graphic technology – Database architecture model and control parameter coding for process control and workflow (Database AMPAC) was withdrawn in August 2016. Recently published ISO standards, mostly the new ones, are introduced in the following text.

ISO 5776:2016 Graphic technology – Symbols for text proof correction

This version published in April 2016 cancels and replaces the first edition from 1983. The standard now allows the text proof-correction symbols to be used in any orthography, including logographic languages. In addition, new symbols have been added, e.g. to change a capital letter to lower case, move characters in respect to the baseline or change the font style.

ISO 12632:2015 Graphic technology – Ink, paper and labels – Requirements on hot alkali penetration and resistance

The new ISO standard for wet glued printed labels, including those on metallized papers, is available since December 2015 and specifies proven test methods for measuring the penetrability and removal times of labels, as well as the resistance of printed labels against hot alkaline solution, which is usually used for the removal of the labels from the bottles and containers during the cleaning process. Tested parameters are important for the stability of the process and for minimizing waste treatment costs.

The Paperbase database in a new version

paperbase INTERNATIONAL The Paperbase, which is produced by Innventia and CTP (Centre Technique du Papier), contains over 260 000 references to technical, scientific and market-focused literature sources, updated every week from 1975 onwards. The abstracted information is relevant for the entire production chain, covering a wide range of subjects – including e.g. wood, non-wood plant fibres, pulps, finished paper and board, nonwovens, composites, cellulose derivatives, etc., as well as all kinds of technology and processes involved in their use, treatment, production or testing, along with related market information and statistics. More than 300 periodicals are on the list and by far are not limited to the major languages. All database entries are in English. Companies can opt for customised accounts, which enables to preserve the confidentiality of the research. Paperbase is also provided via STN as a part of PiraBase.

The new version of the Paperbase database provides direct links to articles on the Internet and the option for federated search, so that results from both international journals and research reports from Innventia are presented in a single search.

Patent on auto-ink restrictions

 ONYX® Onyx Graphics received in June 2016 the U.S. patent 9,373,063 B2 – Establishing ink usage of process channels.

The invention relates to appropriate systems and methods, including ink separation settings in a printing system that includes multiple inks (at least a light ink and a dark ink of the same hue) in at least one of the process channels. The method comprises the characterisation of a system and determining ink separation curves. The intent is to create more efficient colour profiles and achieve better ink utilization.

Measurement of the very small particles in a pulp suspension

The particles that have a diameter approximately one hundred times smaller than the fibre diameter are called crill. These fibrillary particles can be connected to the fibre (bound crill) or entirely separated (free crill).

A patent on the method of measuring the content of fibrillary particles in a pulp containing also fibres of larger dimensions was granted in 1985. The so called crill method comprises illuminating the pulp with light at two wavelengths and separately detecting the corresponding light intensities originating from the pulp. The first wavelength is selected so as to agree with the mean diameter of the crill; the second wavelength is longer than the first one but shorter than the mean diameter of the fibres. The content of the fibrillary particles is then determined from the difference between the absorbance values at the first and second wavelengths, derived from the detected intensities of the light transmitted through the pulp at these wavelengths – the more particles, the higher absorbance values. Therefore, the crill method is not limited by the optical resolution as other methods used for fibre properties measurement, which are usually based on image analysis.



The ABB recently extended the capability of the research-grade analyser L&W Fiber Tester Plus so that it can now provide the crill measurement, in addition to fibre length, fibre width, shape factor, fines content, and fibril index measurements, thus enabling to understand pulp composition in full.

More specifically, the L&W Crill add-on characterises the pulp suspension using one UV and one IR radiation source. It helps to monitor and automatically control refining and dewatering processes, because the contents of very small particles in a pulp suspension, presented as a quota of UV/IR detected intensities (L&W crill quota), increases with the pulp refining, when the fibrils of the fibre walls are exposed to a certain degree. It was shown that the crill quota is directly proportional to refining energy.

ISO 12641-1:2016

Graphic technology – Prepress digital data exchange – Colour targets for input scanner calibration

Part 1: Colour targets for input scanner calibration

Taking into consideration the technical advancements, ISO 12641:1997 is cancelled and replaced by the first edition of ISO 12641-1 from May 2016, which defines the layout and colorimetric values of targets for positive colour transparency film and for colour photographic paper. The targets are based on the colour gamut that is within the capability of common modern materials so that any colour input scanner could be calibrated with any film or paper dye set used to create the target, with different tolerances defined for differing applications. The targets are designed both for visual comparison and as a numerical data targets for electronic systems.

ISO 16763:2016

Graphic technology – Post-press – Requirements for bound products

This new standard available since March 2016 specifies technical requirements and tolerances for the outcomes of industrial post-press operations; requirements applicable to individual major processes and binding quality control are defined in order to enhance production efficiency and accuracy.

ISO 17972-2:2016

Graphic technology – Colour data exchange format (CxF/X)

Part 2: Scanner target data (CxF/X-2)

The second part of ISO 17972, covering the use of CxF when exchanging data from ISO 12641, was published in May 2016. More details on the base document (Part 1) and Part 4: Spot colour characterisation data (CxF/X-4) are available in the News & more section of 4(2015)3. Part 3: Output target data (CxF/X-3) is approved for registration as final draft since this April.

ISO 18620:2016

Graphic technology – Prepress data exchange – Tone adjustment curves exchange

The aim of this new standard available since April 2016 is to provide an alternative to many different proprietary formats in use; a simple and extensible format suitable to exchange data of the so called transfer functions (or plate curves) between applications is specified.

ISO 19445:2016

Graphic technology – Metadata for graphic arts workflow – XMP metadata for image and document proofing

The new standard published in May 2016 defines a set of metadata to communicate the approval status, proof preparation and viewing parameters.

ISO/TS 15311-1:2016

Graphic technology – Requirements for printed matter for commercial and industrial production

Part 1: Measurement methods and reporting schema

In May 2016, the first part of a new technical specification has been published, identifying print metrics, measurement methods and reporting requirements that can be used in communication within a colour reproduction workflow to unambiguously define print quality requirements. Only clearly specified current metrics, correlating well with human perception, are included. Part 2: Commercial production printing is under preparation.

Bookshelf

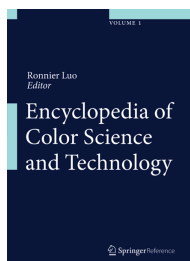
Encyclopedia of Color Science and Technology

The volume is edited by Ronnier Luo, an expert in the field of colour science and technology, who is active in a number of related institutes and committees. The main goal was to provide a multidisciplinary, single source reference of colour science, enabling to understand and apply the concepts of colour to all scientific and technological sectors, as the colour “spans physics, chemistry, computing, psychology, and perception, and contributes fundamentally to art, design, and media”.

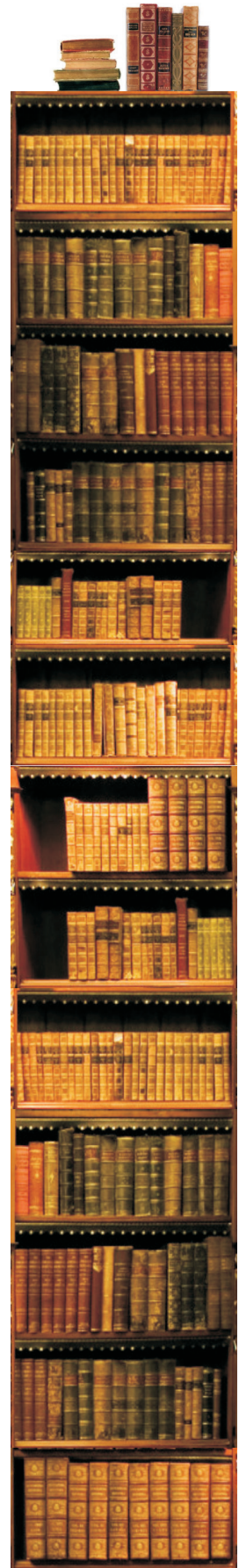
Over 250 entries of the Encyclopedia of Color Science and Technology are contributed by 164 authors and cover the history, development and recent technological advances related to colour, and also speculate its future. Many topics discuss the phenomena, physiology and various concepts of vision, as well as related language and cognition terms. The entries in this area include e.g. photoreceptors, parafovea, opponent theory of colour vision, binocular colour matching, colour categorical perception, tetrachromatic vision, environmental influences on colour vision, environmentally based impairments, inherited colour vision deficiencies, colour vision testing, pseudoisochromatic plates, comparative colour categories, motion and colour cognition, vantage theory of colour, approaches to colour category learning or ancient colour terminology. Other core sections deal with materials, lighting, physics, metrology, and CIE standards. Respective entries include, among others, different types of dyes, pigments and coatings, as well as lamps, and explain relevant physical principles, instruments, observers, colour matching functions, standard illuminants, colour spaces, colour difference equations, and colour appearance models. Further, computations applicable in colour engineering and science are presented, and also the information on colour in respect to computer graphics and art and design. In addition, many entries are dedicated to the people who significantly advanced the field.

Printing as such is referenced to the entry on textile coloration. There one can find only basic definition of printing as a process where colorants are added to selected regions of the medium, and a sentence on continuous printing processes. However, when searching for ‘printing’ within the whole reference work, the results link to numerous related entries, dealing with various colorants, such as ink-jet dyes, theoretical models, like Clapper-Yule model for halftone prints on diffusing substrates, and many more. Similarly, there are several mentions of e.g. inks, or colour management, but they don’t have their own entries. At the same time, the provided list of entries contains some confusing items; to give an example, the entry named ‘History, Use and Performance’ is in fact only a cross-link to the ‘CIELAB’ entry.

Therefore, at least in case of the printing industry, the online edition turns out to be a better option than the printed volume. This is supported also by the fact that the Encyclopedia of Color Science and Technology is designed as a living reference work, which means that the authors should update their contributions accordingly and also it is planned to include new content as it becomes relevant and available.



Encyclopedia of Color Science and Technology
 Editor: M. Ronnier Luo
 Publisher: Springer
 1st ed., May 2016
 ISBN: 978-1-4419-8070-0
 1284 pages, 831 images
 Hardcover
 Available also as an eBook



3D Printing: Legal, Philosophical and Economic Dimensions

*Editors: Bibi van den Berg,
Simone van der Hof, Eleni Kosta*

Publisher: T.M.C. Asser Press
1st ed., January 2016
ISBN: 978-9462650954
212 pages, Hardcover
Also as an eBook



With the rapid development and growing application possibilities of 3D printing, the importance of discussion of its nontechnical aspects increases as well. This volume collects academic and expert contributions related to social, ethical, regulatory and legal questions – on intellectual property rights when creating original products, product copies or replacement parts, societal consequences of the various 3D-printable products, the extent of regulation needed, the business impacts of printing-on-demand, the role of product designers, and more.

Socio-Legal Aspects of the 3D Printing Revolution

Author: Angela Daly

Publisher: Palgrave
Macmillan
1st ed., April 2016
ISBN: 978-1137515551
122 pages, Hardcover
Also as an eBook



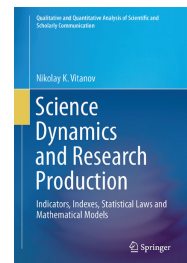
This is another contribution to the above-mentioned topic, published a few months later and drawing from almost two hundred secondary sources as well as from relevant cases and legislation. Namely, the international, European, UK, US and Australian legislation is considered. The author examines the position of 3D printing in various areas of law, including intellectual property rights, product liability, gun laws in connection to printing dangerous objects, data privacy and fundamental or constitutional rights, e.g. with respect to the implications of 3D scanning. As 3D printing is considered to be the 'disruptive technology' similarly to the Internet some years ago, the comparison between the two technologies from a legal perspective is made.

Science Dynamics and Research Production: Indicators, Indexes, Statistical Laws and Mathematical Models

As in short summarizes the title, this book deals with two selected areas of the 'science of science' – indicators and indexes for assessment of research production and statistical laws and mathematical models connected to science dynamics and research production. The subject matter is presented at the introductory level, from the point of view of applied mathematics.

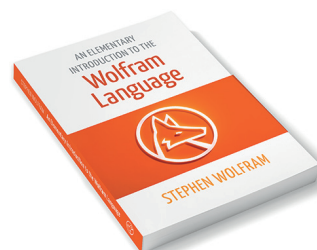
The interest in this topic increases significantly due to the increasing costs connected with scientific work. Therefore, a number of models, indicators and indexes have been developed. Many of these tools and concepts are explained in a compact form, supported by more than a thousand references, and discussed with respect to the outcomes of their implementation. In the first part, the author briefly introduces mathematical models describing the importance of science for economic growth and systems for the evaluation of research organizations of different size. The second part brings an overview of selected indicators and indexes, along with many examples for their calculation to illustrate their strengths and weaknesses. Finally, in the third part, the focus is on the models of research production connected to the units of information and to units of importance of this information. There are discussed non-Gaussian statistical power laws, statistical distributions, deterministic models of science dynamics, models based on the reproduction–transport equation and on a master equation, etc.

Science Dynamics and Research Production:
Indicators, Indexes, Statistical Laws and Mathematical Models
Author: Nikolay K. Vitanov
Publisher: Springer
1st ed., August 2016
ISBN: 978-3-319-41629-8
278 pages, 5 images
Hardcover
Available also as an eBook



An Elementary Introduction to the Wolfram Language

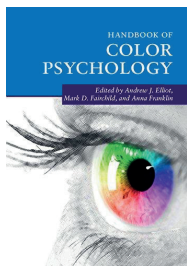
To anyone who is interested in modern computational thinking and practical application of the latest Wolfram technology, Stephen Wolfram explains what is the Wolfram Language and how it works with functions, lists, arrays, tables, graphics, text, real-world data, etc. Options for formatting, visualisation, manipulation and other treatments are illustrated as well. In spite of the focus on computer language, no prior knowledge of programming is required. The book is supported by numerous examples and has gained a lot of positive ratings from both the beginners and experienced Wolfram Language users; for the latter, the new and special programming features are presented. The content of the book is freely available for online reading at Wolfram website, where can be downloaded also the Notebook edition, i.e. the collection of computational documents for use in Wolfram System.



An Elementary Introduction
to the Wolfram Language
Author: Stephen Wolfram
Publisher: Wolfram Media
1st ed., December 2015
ISBN: 978-1944183000
324 pages
Softcover
Available also as an eBook

Handbook of Color Psychology

Unlike the most of colour science disciplines, colour psychology literature lacked the comprehensive review of the state-of-the art of the knowledge in the field. This handbook with more than 50 contributors fills that gap, bringing the overviews of emerging theory and research on the relations between colour vision and psychology on over 750 pages, accompanied by numerous tables and figures. The intention was to give a complete picture and to promote the interaction among researchers. After an introduction, two parts summarize basics of colour science and colour vision development, differences and deficiencies. Remaining six parts start with the categorization of colour, its development and comparison across cultures and languages, and then explore colour symbolism and association – e.g. colour in ritual, folklore, mimicry, and warnings, as well as colour emotion, harmony and metaphoric associations. Next, ecological aspects of colour preference and also biological, cultural, and developmental influences on colour preferences are discussed. Colour effects on psychological and biological functioning and, vice versa, psychological effects on colour perception, are then reviewed. Finally, colour appearance phenomena, visual illusions and synesthetic colour experiences are presented.



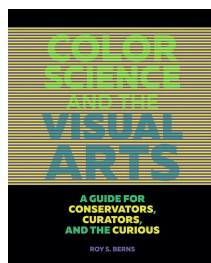
Handbook of Color Psychology
 Editors: *Andrew J. Elliot, Mark D. Fairchild, Anna Franklin*
 Publisher: Cambridge University Press
 1st ed., March 2016
 ISBN: 978-1107043237
 762 pages, 167 images
 Hardcover
 Available also as an eBook

Color Science and the Visual Arts: A Guide for Conservators, Curators, and the Curious

Roy S. Berns has written a reference guide for the entire visual arts community – students and professionals dealing with conservation, art collections and art history, as well as artists themselves. Drawing from his expertise in colour science, the author explains complex concepts of colour technology and offers solutions to the various issues occurring when art is displayed, conserved, imaged, or reproduced, which are related to the way the colour is produced, perceived, described or measured.

The book is organised into seven chapters, with topics including spectral measurements, metamerism, colour inconstancy, artwork display, painting materials, colour reproduction, and more. The colour science fundamentals as well as its applications are provided in an engaging manner, benefiting from 250 well chosen and elaborated images exemplifying the content and making it easier to understand. An annotated bibliography provides suggestions for further reading and more in-depth study of particular topics.

Color Science and the Visual Arts:
 A Guide for Conservators, Curators, and the Curious
 Author: *Roy S. Berns*
 Publisher: Getty Conservation Institute
 1st ed., July 2016
 ISBN: 978-1-60606-481-8
 208 pages, 250 images
 Softcover



Digital Design Theory: Readings from the Field

Editor: *Helen Armstrong*



Publisher: Princeton
 Architectural Press
 1st ed., June 2016
 ISBN: 978-1616893088
 152 pages, Softcover
 Also as an eBook

The carefully selected texts written by thirty influential designers and programmers in the past almost six decades are presented in chronological order and put light on the impact of digital technologies on graphic design, which naturally must be different than traditional static print design due to growing requirements on the interactivity and responsibility. The essays, covering e.g. programmatic design, digital aesthetics, and the move to experience-based design, are organized into three sections and framed by a discussion on their relevance for digital designers and accompanied by glossary.

Digital Creativity: Something from Nothing

Author: *Gregory Sporton*



Publisher: Palgrave
 Macmillan
 1st ed., June 2015
 ISBN: 978-1137486400
 182 pages, Hardcover
 Also as an eBook

This is another recent contribution focused on the work of creative designers in the digital age, presenting the relevant facts and explaining a lot of related terms, doing so from a critical point of view.

Gregory Sporton examines how the way of creative work and its outcomes are influenced or even determined by digital technology, which very quickly became ubiquitous in our present-day lives. The author is aware of the problems ahead if technology comes to dominate creative practice, either by defining it or by imitating it, pointing out that “what is missing is a wider debate about what we want from technology in our lives”. If creativity should retain a human form and scale, computing must be seen as a craft practice.

3D Printed Science Projects: Ideas for Your Classroom, Science Fair or Home

Authors: Joan Horvath, Rich Cameron

Publisher: Apress
1st ed., May 2016
ISBN: 978-1484213247
203 pages, 113 images
Softcover
Also as an eBook

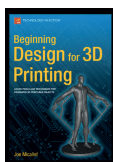


The proven author team describes how to create 3D printable models that can help children and students of any age understand a number of principles and phenomena. The topics are designed to be customized by the reader to create a wide range of didactic projects. Individual chapters advise how to create the surfaces to demonstrate 3D math functions, produce the models of light and other waves interaction and diffraction, the models for gravity explanation, investigation of aerofoils, and demonstration of simple machines, and finally the models of plants and their ecosystems, atoms and molecules, and trusses. In appendices, a brief introduction to 3D printing is provided for those who start from scratch, as well as the aggregate list of all the numerous links appearing in the text.

Beginning Design for 3D Printing

Author: Joe Micallef

Publisher: Apress
1st ed., October 2015
ISBN: 978-1484209479
375 pages
Softcover
Also as an eBook



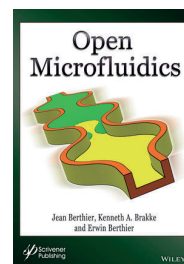
In accordance with the title of this book, the author introduces 3D printing and the corresponding design process, the available software, and the essential design techniques for solid modelling, organic modelling and customisation, going from basic through intermediate to advanced techniques, and similarly from basic geometry – boxes, spheres, and cylinders – to more complex shapes of many kinds. In addition, 3D-scanning techniques and advices on how to outsource the 3D printing are included. The emphasis is put on the proper workflow to ensure the printability of prepared models.

Open Microfluidics

The book builds on 'The Physics of Microdroplets' volume published four years ago and reflects the growing cross-disciplinary interest in microflows with open boundaries, i.e. with liquid–air interfaces. Open microfluidics is becoming fundamental in scientific domains such as biotechnology, biology, energy and space. There are several reasons for this. The fabrication of open systems is very simple, they are compatible with the new techniques of 3D printing, and also they can be easily converted into fully or partly closed systems. Further, fluids in these systems are moved solely by capillary forces, without the need for external energy. Moreover, in bio applications it is important that the liquid is accessible, which enables to add reagents or, on the contrary, to retrieve the fluid, while the reduced weight is advantageous in space exploration.

In order to offer the widest possible view, the theoretical aspects are complemented by numerical approaches and experimental examples. The authors go through the theory of spontaneous capillary flow, describe the formation of capillary filaments and discuss spontaneous capillary flow in open U-channels and in channels with constrictions and enlargements, suspended capillary flow, and spontaneous capillary flow between horizontal rails. Two chapters then deal with paper-based and fibre-based microfluidics, with inkjet printing briefly mentioned as a possible fabrication technique, followed by concluding remarks. Supplementary material including the interactive application for the phase diagrams is available online.

Open Microfluidics
Authors: Jean Berthier, Kenneth A. Brakke, Erwin Berthier
Publisher: Wiley-Scrivener
1st ed., August 2016
ISBN: 978-1-118-72080-6
336 pages
Hardcover
Available also as an eBook



Additive Manufacturing: Innovations, Advances, and Applications

The book reviews individual existing and emerging techniques in additive manufacturing, including the chapters on 'Printed and hybrid electronics enabled by digital additive manufacturing technologies' and 'Reactive inkjet printing of nylon materials for additive manufacturing applications'. The content is written to satisfy the needs of wide audience, ranging from students to researchers and engineers, and covers specific processes for metallic, powder-based, ceramic and polymeric materials, then the use of additive manufacturing in several biomedical applications and, finally, additive manufacturing of rare earth permanent magnets. In each case, the present applications as well as future prospects are discussed.

Additive Manufacturing:
Innovations, Advances, and Applications
Editors: Tirumalai S. Srivatsan, Tirumalai S. Sudarshan
Publisher: CRC Press
1st ed., September 2015
ISBN: 978-1498714778
444 pages, 385 images
Hardcover
Available also as an eBook



Bookshelf

Academic dissertations

Individual Colorimetric Observers for Personalized Color Imaging

Presented thesis deals with an observer metamerism caused by large variations in color matching functions among people. It is identified as an issue in color-critical applications where colors are compared on different displays, recently becoming more serious due to spectrally narrow primaries of wide-gamut displays. This dissertation provides a possible solution by personalized color imaging, introducing individual colorimetric observers. At first, current knowledge on observer variability is summarized, along with the resulting observer metamerism, its experimental evidence, and possible solutions. As the first step in developing a personalized color imaging workflow, the color matching data from 151 color-normal observers were obtained at four different locations, allowing to determine observer functions. In the design of a color matching experiment, light sources were selected by simulating color matches to highlight inter-observer variability. The device utilized two sets of four LEDs and was named with a term 'nomaloscope', as opposed to an anomaloscope to test color vision anomalies and deficiencies. Based on the collected data, two types of individual colorimetric observer functions were then derived and validated. The color vision model for individual observers is an extension of the CIE 2006 physiological observer, in this thesis incorporating eight physiological parameters to model individuals in addition to their age and field size: the lens density, optical density of macular pigment, and optical density as well as peak-wavelength (λ_{\max}) shift of L-, M-, and S-cone photopigments. The second type of observer functions, categorical observers, is seen as a more convenient approach towards the personalized color imaging. The number of categorical observers required depends on application. For observer characterization, two workflows were tested: one using the nomaloscope and the other using proposed spectral pseudoisochromatic images. The personalized color imaging was evaluated in a color image matching study on an LCD monitor and a laser projector and in a perceived color difference variability study on a SHARP Quattron four-primary display. Finally, the personalized color imaging was implemented using an iccMAX profile.

Doctoral thesis – Summary

Author:
Yuta Asano

Speciality field:
Color Science

Supervisor:
Mark D. Fairchild

Defended:
*2 August 2015 at Rochester Institute of Technology / Munsell Color Science Laboratory
Rochester, New York, United States*

Contact:
yuta@motorola.com

Spectrally Based Material Color Equivalency: Modeling and Manipulation

This dissertation comprises finding and using a transformation of tristimulus values to realize a color equivalency representation, i.e. color coordinate system that minimizes changes due to differences in observer or lighting conditions or both. While the initial focus was to develop mechanisms to manipulate spectral reflectances in a spectral reproduction system driven by a spectrally based color management system, it was recognized that at first a means of dealing with differences in observer and lighting conditions must be developed. Overall, an alternative approach to colorimetry is explored. After the introductory part of the text, two chapters explain Wpt and WLab. Wpt (pronounced 'Waypoint') is a material color equivalency coordinate space, which preserves the perceptive concepts of lightness, chroma and hue, as well as the white point, and provides a direct linear relationship between sensor based perceptive aspects of color and spectral reflectance. It utilizes the so called similarity of color defined by a select set of material colors. Based on the spectral representations of observer, illumination, and object, the sensor values are normalized relative to these

Doctoral thesis – Summary

Author:
Maxim W. Derhak

Speciality field:
Color Science

Supervisor:
Roy S. Berns

Defended:
*4 August 2015 at Rochester Institute of Technology / Munsell Color Science Laboratory
Rochester, New York, United States*

Contact:
max.derhak@onyxgfx.com

material colors. WLab (Waypoint Lab) is a more perceptually uniform representation resulting from an invertible non-linear transformation of Wpt. Euclidean WLab distances ΔE_w were found to not be statistically different from ΔE_{94}^* and ΔE_{00}^* color differences under Illuminant C and performing better at predicting color difference experiments under Illuminant A. The ΔE_w differences represent material color differences, remaining fairly constant for changes in observing conditions. Further, the applicability of Wpt and WLab spaces to color difference metrics using variability of object and/or observing conditions has been investigated. Presented Wpt shift manifolds are based on sets of Wpt coordinates for variations in reflectance, illumination, or observers. WLab distances of corresponding points within or between these manifolds are utilized to define metrics for color inconsistency, metamerism, observer or illuminant rendering, and differences in observing conditions. The 'Direct Wpt' chapter presents two methods for estimating a Wpt normalization matrix when spectral data of the illuminant are not available, with prospective benefits for camera color correction and computer vision. Finally, two chapters describe different approaches to manipulating color matching functions and spectral reflectance, along with practical applications of the presented methods, including the iccMAX color management workflow.

Doctoral thesis – Summary

Author:

Jelle Wiebe Boumans

Speciality field:

Corporate Communication

Supervisors:

*Rens Vliegenthart
Hajo Georg Boomgaarden*

Defended:

*25 May 2016 at University of
Amsterdam / Amsterdam School
of Communication Research
Amsterdam, Netherlands*

Contact:

j.w.boumans@uva.nl

Outsourcing the News? An Empirical Assessment of the Role of Sources and News Agencies in the Contemporary News Landscape

The dissertation focuses on the situation of newspapers and journalism in the Dutch context, showing the developments very similar to global trends – decreasing newspaper circulation rates, advertising revenues and readership levels, with increasing competition from other media. Among others, this leads to the decrease in journalistic workforce, which is in conflict with the substantial increase in editorial content. This is connected with the so called churnalism – recycling subsidized material in the form of public relations press releases and news agency copy, expectably reflected in the growth of public relations industry. In order to provide robust insight, this work brings an extensive empirical assessment on the news agencies' reliance on source content, as well as the impact of the agency copy on the news media in the Netherlands. Large-scale collections of texts were created, with two of the three datasets spanning a period of a decade, including a variety of sources and newspaper types. To explore the relationship between subsidized content and print and online news, this dissertation employs novel automated content analyses. Two measures are introduced that allow for a very specific assessment of the degree of overlap between texts: the intermedia agenda-building ratio indicates what percentage of news articles is initiated by the news agency; the churnalism index indicates to what extent a news article consists of replicated agency material. The results suggest that non-governmental organizations (NGOs) are generally more successful in accessing the media than corporations, i.e. the themes that NGOs promote are more reflected in the media. Very interesting is the comparison between print newspapers and online news. It has been shown that neither Dutch print newspapers nor news agencies are 'churnalism factories' and no increased presence of agency copy or press releases in the print news was found in the longitudinal datasets over the past ten years. In contrast, the agency is to a great extent steering both the news agenda as well as the literal content of the online news. The agency is responsible for the majority (66 %) of the online agenda; moreover, many of the online articles are more or less verbatim agency copy. This dominance of a single news provider supports the suspicion of the possible lack of diversity of viewpoints in online news. Finally, the applicability of the proposed approach of automated text comparison was expanded to the field of framing research.

Events

TAPPI Advanced Coating Symposium



Stockholm, Sweden
4–6 October 2016

This forum, where paper manufacturers, product developers, researchers, academics, and other experts meet to present and discuss the research in paper coating, surface properties, converting, and interactions in printing operations for over twenty years already, is held in Europe at the Innventia headquarters in 2016.

The program opens the keynote 'Challenges with shift towards the use of renewable materials in coated paper products' by Anna Jonhed. The morning session on printing and products then explores influences of substrate composition and various properties on mottle, and more generally on print quality, with one lecture dealing with thermal paper coating structure. The afternoon is reserved for the barrier coatings session, namely the performance of dispersion barrier coatings, including those based on polyvinyl alcohol, and convertibility of materials with the new generation water-based barrier coatings, followed by the poster session. On Wednesday, the invited talk on 'A cellulose based society' introduces the nanocellulose session, discussing, among others, its versatility and coatability. In the modelling/structures session, both theoretical and experimental methods for the study of bending and tensile properties or cracking are covered. The last symposium day starts with the invited lecture on 'Foam coating' and continues with two sessions on functional materials and active packaging, presenting the research on antimicrobial coatings employing modified cellulose nanocrystals, printed microfluidic platform, effect of calendaring and coating formulations on conductivity in paper-based electrodes, active packaging by paper coating, holographic paper and print, and laser processing of graphene oxide on coated paper substrates.

3rd Annual InkJet Conference 2016

TheIJC.com Düsseldorf, Germany
5–6 October 2016

The purpose of TheIJC is to provide a platform for researchers to present their findings, having potential for future commercial applications, to representatives of technology companies in packaging, textiles, ceramics, 3D printing, glass, graphics, newsprint, and printed electronics industries; the event expands quickly, with almost 400 attendees in 2015. The 3rd edition again offers two conference tracks each day. The lectures cover advances in UV-LED curing systems, industrial inkjet printing of variable data, printing of special materials, like resists or nanopigment dispersions, printing on wide range of substrates, including textile, design of single pass industrial inkjet printers or the significance of the holistic approach to the ink-substrate-process interaction in the development process – and much more.

Six free inkjet workshops are organised on October 4th for conference delegates on first come, first serve basis. The topics go from 'Introduction to inkjet' through 'Masterclass in waveform tuning', 'Colour and print' and 'Functional fluids' to 'Speciality effects in textiles' and 'Inkjet in packaging'.

Autumn Packaging Events by EasyFairs



All four shows complementing each other – Empack dedicated to packaging technology, Label & Print focused on packaging printing, labelling, marking and conversion, Packaging Innovations for branded and inspirational packaging, and self-explaining Luxury Packaging, are co-located in Stockholm, Sweden on 5–6 October 2016. The seminar program of the event offers panel discussions, as well as talks on branding, examples of novel packaging, the requirements connected with sustainability and bioeconomy, chances to improve food security and credibility through the packaging text, and also the lectures on 'The future of design' by a renowned designer Karim Rashid, the author of numerous award-winning designs, are scheduled for both days.

Later, on 23–24 November 2016, Packaging Innovations are organised in Amsterdam, Netherlands, as well as in Madrid, Spain, where will be combined with Empack.

Security Printers 2016

Seville, Spain
5–7 October 2016



International Security Printers conference and exhibition organized by Intergraf since 1976 is open solely to security printers, their suppliers, banknote issuing authorities, government authorities, law enforcement organisations and postal authorities. The program features e.g. the opportunities and challenges in banknotes and IDs, their procurement, security print quality, and also virtual currencies and darknet marketplaces.

WAN-IFRA Events



Besides the Vienna event briefly introduced below, WAN-IFRA autumn schedule consists of the course on 'Generating new advertising revenue' taking place in Bangalore, India (25–26 October 2016), two Digital Media conferences – at first the Asia edition in Singapore (8–10 November 2016) and a week later the LATAM in Buenos Aires, Argentina (17–18 November 2016), and finally the 'Infographics & data visualisation' workshop in New Delhi, India (6–7 December 2016).

World Publishing Expo 2016

Vienna, Austria
10–12 October 2016

Visitors of the annual exhibition for the news publishing industry can attend the



Print World Conference and the Digital Media World Conference sessions during all three days; each informational session will be followed by a guided tour dedicated to the same topic. For 2016, the International Newspaper Color Quality Club and the Digital Media World Awards will be celebrated together during Media Tech Nite on the evening of 11th October.

Wolfram Technology Conference 2016

Champaign, Illinois, USA
18–21 October 2016



Regardless of familiarity with Wolfram technologies, anyone interested in developing with these technologies and their deployment e.g. in data science and visualization, connected devices, mobile and cloud deployment, engineering, signal and image processing or educational technology can attend this four-day event to explore presented cutting-edge applications, as well as take part in workshops and interact with the creators of Wolfram technologies.

Fall Conference 2016

Louisville, Kentucky, USA
10–12 October 2016



Not surprisingly, this year the Fall Conference of FTA (Flexographic Technical Association) starts with a session reserved for highlights from drupa 2016 with flexography and complementary technologies in focus, reporting on the most innovative solutions within the overall package printing production workflow presented in Düsseldorf earlier this year. The second session of the first day offers a chance to learn about the technologies that won the 2016 FTA Technical Innovation Award, including their benefits for customers, in a roundtable discussion.

The opening sessions of remaining two days deal with the training, helping to develop productive and skilled employees. The program of the second day continues with a session advising how to use FTA's First to plan and execute a successful and productive workflow ensuring high-quality results. The 5th edition of First, the set of specifications, guidelines and tutorials, is currently available in version 5.1. Later in the day, a session on production and quality control and a session discussing the specific requirements of both paper and foil substrates are scheduled. On the last conference day, the program is concluded by a debate among experts representing leading anilox roll manufacturers, exploring current options that are available on the market and their features. As usually, an integral part of the event is the exhibition.

4th CIDAG International Conference of Design and Graphic Arts

Barcelona, Spain
26–28 October 2016



This event is organised each even-numbered year since 2010 for the experts active in areas associated with the graphic production and design within the industry as well as universities and research institutes. The three official languages of the conference are Portuguese, English and Spanish; the oral presentations should be supported by visual presentation in English or bilingual. The scope ranges from the use and development of advanced technologies for the production of new materials, equipment, software and IT tools to innovations in design processes and communication.

In 2016, the three-day conference program involves two discussion panels, namely 'The standards of ISO/TC 130 Graphic Technology committee in the new paradigm of international graphic communication' and 'The role of academic research in the new era of professional graphic communication'. Plenary lectures will be given by seven invited speakers, with the announced topics discussing the connection of designer and history, illustrators as graphic novelists, relevant international standards, brand design and security printing, and the selection of materials in the design process. Oral communications are grouped in sessions focused on design and communication, print production and multimedia, and innovation in education, which are mostly scheduled in two simultaneous tracks.

ICGIP 2016 8th International Conference on Graphic and Image Processing

Tokyo, Japan
27–29 October 2016



2016 8th International Conference on Graphic and Image Processing
Tokyo, Japan October 29-31, 2016

Already well-established ICGIP event aims at the global audience comprising the scientists, scholars, engineers and students, providing an opportunity to present ongoing research activities and foster research relations between the universities and the industry. The scientific program is concentrated in the second conference day, with keynotes in the morning and oral or poster presentations in the afternoon.

The list of the 8th ICGIP edition keynotes has five entries. Shigeo Takahashi will present recent results on schematisation techniques for enhancing the quality of scientific and information visualisation images through either emphasising or suppressing their intrinsic important features, while still preserving our mental maps of the associated original images; the examples include line-based image abstraction, schematic map design, and perceptual image enhancement. The topic of Tuan D. Pham's talk is 'Texture Analysis in Biomedical Imaging using Geostatistics and Nonlinear Dynamics', allowing for statistical characterization of random-like signal changes in a spatial domain. The keynote of Patrick Wang deals with fundamental aspects of similarity, semantics, ambiguity, intelligent pattern recognition and applications, especially with respect to 3D biometric technology and importance of security. Vít Voženílek will share his knowledge in visualization and processing of images in extreme resolution, showing the application of the image processing methods widely used in Earth remote sensing for processing and visualisation of images in nanoresolution, which nowadays play an essential role in physics, medicine, and chemistry. The suitability and applicability of these methods were proved by three case studies demonstrating different image visualisation and image analysis approaches for different scales at the nanoresolution level. Finally, Hiroshi Fujita will present a keynote on the 'State-of-the-art of computer-aided diagnosis (CAD) for medical images', which has become one of the major research subjects in medical imaging and diagnostic radiology.

WCPC Annual Technical Conference 2016



Swansea, UK
7–8 November 2016

The two-day event filled mainly with the presentations of the latest WCPC (Welsh Centre for Printing and Coating) research this year starts with the keynote speech by Ray Gibbs, focused on graphene and other nanomaterials and their short term commercial applications for the printing market.

The schedule again reflects a wide scope of WCPC research topics, including issues connected with the printing of functional layers and nanomaterials deposition for various printed electronics elements and devices, the study of related processes on both laboratory and production scale along with the development of appropriate theoretical models and measurement techniques, the formulation and characterisation of tailored functional inks – that all when developing existing technology as well as designing novel applications, such as a printed wearable heater for use in elite sport.

SEMICON Europa

SEMICON EUROPA Grenoble, France
25–27 October 2016

Gathering thousands of exhibitors and attendees, with an audience from many segments of the European microelectronics industries, including semiconductors, light emitting diodes, microelectromechanical systems, printed, organic, and flexible electronics, and adjacent markets, the claim to be the largest microelectronics event in Europe is justified. In 2016, the program combines 20th Fab Management Forum, Advanced Packaging Conference, Imaging Conference, Power Electronics Conference, and 2016FLEX Europe Conference, two Technology Arenas with more than 60 presentations on the latest technologies, products and innovations, and much more.

Paper Recycling Conference Europe

Rotterdam, Netherlands
2–3 November 2016



The 2016 program is opened by an executive roundtable discussing paper and board in Europe, continued by presentations on impacts and perspectives of recovered fibre collection, and two panel sessions focused on correct data interpretation when analysing the trends, and next on the global flow of recovered fibre. The second day is dedicated to the high-tonnage packaging grades and Europe's transportation challenges. The registrants also have access to the co-located Plastics Recycling Conference sessions.

The VIP Event for Print & Publishing

Berlin, Germany
7–8 November 2016



An open educational event organized by axaia, callas and Four Pees offers mainly technical sessions and presentations of products and solutions distributed by Four Pees for users in print, publishing and packaging industries.

Digital Print Europe 2016

Amsterdam, Netherlands
28 November to 1 December 2016

This event organised by IMI Europe includes in 2016 the IMI Europe Digital Printing



Conference as well as the Inkjet Academy, Market Reports Live, and Technology Short Courses program. The 2016 conference with a slogan 'Inkjet Market and Technology Advances' will start on 30 November. The talks announced so far will recap the current growth rates and print market estimates for upcoming years, as well as the current restrictions and barriers to be overcome in individual market sectors. After the opening lecture on digital print opportunities in general and key inkjet technology directional trends as identified at drupa 2016, the inkjet applications in packaging, digital textile printing, including the comparison of pigment and dye printing technologies, and décor printing will be discussed. Further, the challenges of single pass technology and the Si MEMS process will be presented, as well as the development of new business models.

All delegates can get the feel of the products and technology of event sponsors and also will receive a free copy of the latest 'The Numbers' Market Report by IT Strategies.

Color 2016

Phoenix, Arizona
3–6 December 2016

The annual Color Conference held by the Printing Industries of America will this year start on the first Saturday in December with the



pre-conference class providing the introduction to colour management. The schedule for following two days offers the keynotes 'Let the art work' by John McWade, 'Expanded gamut 101: The big picture' by Abhay Sharma and John Seymour, 'Case study – The branding of Union City California' by Steve Decker, 'Bringing your brand values to life through creative work' by Kristy Cameron, and 'Considerate color design' by Brian Lawler. The last keynote 'Haptic brain, haptic brand' will give Daniel Dejan during Tuesday morning wrap up.

CIC24 – 24th Color and Imaging Conference

San Diego, California, USA
7–11 November 2016



The Society for Imaging Science and Technology (IS&T) and more than ten cooperating societies have, as usually, elaborated a colour and imaging program for a full working week. In the first two days, two related events are co-located this year. On Monday, it is the ICC DevCon 2016 described below, scheduled in parallel with a popular short course dedicated to colour, vision, and basic colorimetry (offered since 22nd edition). The short course program continues on Tuesday, with four tracks on colour and vision, appearance and 3D, colour and display, and psychophysics and images, respectively. On this day, anybody interested is also welcome to attend the meetings of CIE (International Commission on Illumination) Division 8, which are open to the public. In case of the topic on common colour appearance, remote participation will be possible as well. As stated in the invitation: "One objective is to determine whether common colour appearance is a shared concept across observers and, if so, whether the degree of colour similarity of a set of colour reproductions can be measured objectively." The establishment of a CIE Technical Committee to study this topic is anticipated.

The remaining three days are more or less framed by the opening keynote of Wolfgang Heidrich on 'Full color computational imaging with diffractive optics' and CIC Awards. In the meantime, technical sessions dealing e.g. with creating, processing, displaying, viewing, perception and assessment of colour images as well as their special features, multispectral imaging, or colour vision, observers and illuminants will take place, including 'Modelling incomplete chromatic adaptation and colour contrast using memory colour', winner of the CIC 24 Best Paper Award. Thursday will start with the keynote speech of Gerald H. Jacobs exploring 'The evolution of primate color vision', with Interactive Paper sessions later in the day and the evening talk on 'The confluence of art and technology: 3D printing at LAIKA's award-winning animation studio' with Brian McLean and Rob Ducey. Colour and imaging workshops are organised on Friday morning. The last keynote is reserved for Luc Vincent and Rom Clement and their topic 'Google Street View: Unique challenges of collecting imagery at global scale'.

ICC DevCon 2016

San Diego, California, USA
7 November 2016



The topic of the 2016 International Color Consortium (ICC) Developers Conference are real-world solutions and applications using iccMAX, the new specification approved by the ICC on 29 July 2016, which significantly extends the possibilities of colour management based on ICC profiles.

In the morning, iccMAX will be introduced from the business perspective and several examples of its utilisation will be presented – colour tuning of a painting by a multispectral lighting system, a spectral workflow for encoding and analysing artwork, modelling colour vision deficiency, correction of display viewing angle, and implementing observer metamerism correction on wide colour gamut display. In the afternoon, Max Derhak will give a hands-on workshop with ReflccMAX, the reference implementation library and tools supporting the creation and use of iccMAX profiles.

Call for papers

The Journal of Print and Media Technology Research is a peer-reviewed periodical, published quarterly by **iarigai**, the International Association of Research Organizations for the Information, Media and Graphic Arts Industries.

JPMTTR is listed in Index Copernicus, PiraBase (by Smithers Pira), Paperbase (by Innventia and Centre Technique du Papier) and NSD – Norwegian Register for Scientific Journals, Series and Publishers.

Authors are invited to prepare and submit complete, previously unpublished and original works, which are not under review in any other journals and/or conferences.

The journal will consider for publication papers on fundamental and applied aspects of at least, but not limited to, the following topics:

- ⊕ Printing technology and related processes
Conventional and special printing; Packaging; Fuel cells, batteries, sensors and other printed functionality; Printing on biomaterials; Textile and fabric printing; Printed decorations; 3-D printing; Material science; Process control
- ⊕ Premedia technology and processes
Color reproduction and color management; Image and reproduction quality; Image carriers (physical and virtual); Workflow and management
- ⊕ Emerging media and future trends
Media industry developments; Developing media communications value systems; Online and mobile media development; Cross-media publishing
- ⊕ Social impact
Environmental issues and sustainability; Consumer perception and media use; Social trends and their impact on media

Submissions for the journal are accepted at any time. If meeting the general criteria and ethic standards of scientific publishing, they will be rapidly forwarded to peer-review by experts of high scientific competence, carefully evaluated, selected and edited. Once accepted and edited, the papers will be printed and published as soon as possible.

There is no entry or publishing fee for authors. Authors of accepted contributions will be asked to sign a copyright transfer agreement.

Authors are asked to strictly follow the guidelines for preparation of a paper (see the abbreviated version on inside back cover of the journal). Complete guidelines can be downloaded from:

<http://www.iarigai.org/publications/>

Papers not complying with the guidelines will be returned to authors for revision.

Submissions and queries should be directed to:

journal@iarigai.org

Vol.6, 2017

Prices and subscriptions

Journal of Print and Media Technology Research
A peer-reviewed quarterly ISSN 2414-6250 (Online)

Starting newly in 2016, the journal is published in digital form.
A print version is available on-demand and at additional price.

Please, find below the prices charged for the Journal, as well as for a single paper. Use the opportunity to benefit from the Subscriber's discount price!

By ordering a publication, or by subscription a password will be provided to you for downloading. The password protection of every issue is active during a period of six months. After this period the publications will be available free of charge.

iarigai members will be given the download password free!

Regular prices

Four issues, digital JPMTR, (password protected)	300 EUR
Single issue, digital JPMTR, (password protected)	100 EUR
Single paper from JPMTR (pdf file)	20 EUR
Four issues, print JPMTR, (on-demand)	400 EUR
Single issue, print JPMTR, (on-demand)	100 EUR

Subscription prices

Annual subscription, four issues, digital JPMTR, (password protected)	240 EUR
Annual subscription, four issues, print JPMTR, (on-demand)	400 EUR

Prices for **iarigai** members

Four issues, digital JPMTR, (password protected)	Free of charge
Single paper from JPMTR (pdf file)	Free of charge
Four issues, print JPMTR, (on-demand)	400 EUR
Single issue, print JPMTR, (on-demand)	100 EUR

Place your order online at:

<http://www.iarigai.org/publications> (open: Order/Subscribe here)

or send an e-mail order to: journal@iarigai.org

Guidelines for authors

Authors are encouraged to submit complete, original and previously unpublished scientific or technical research works, which are not under review in any other journals and/or conferences. Significantly expanded and updated versions of conference presentations may also be considered for publication. In addition, the journal will publish reviews as well as opinions and reflections in a special section.

Submissions for the journal are accepted at any time. Papers will be considered for publishing if meeting the general criteria and ethic standards of the scientific publication. When preparing a manuscript for JPMRT, please strictly comply with the journal guidelines, as well as with the ethic aspects. The Editorial Board retains the right to reject without comment or explanation manuscripts that are not prepared in accordance with these guidelines and/or if the appropriate level required for scientific publishing cannot be attained.

A - General

The text should be cohesive, logically organized, and thus easy to follow by someone with common knowledge in the field. Do not include information that is not relevant to your research question(s) stated in the introduction.

Only contributions submitted in English will be considered for publication. If English is not your native language, please arrange for the text to be reviewed by a technical editor with skills in English and scientific communication. Maintain a consistent style with regard to spelling (either UK or US English, but never both), punctuation, nomenclature, symbols etc. Make sure that you are using proper English scientific terms.

Do not copy substantial parts of your previous publications and do not submit the same manuscript to more than one journal at a time. Clearly distinguish your original results and ideas from those of other authors and from your earlier publications - provide citations whenever relevant. For more details on ethics in scientific publication, please consult:

<http://www.elsevier.com/ethicguidelines>.

If it is necessary to use an illustration, diagram, table, etc. from an earlier publication, it is the author's responsibility to ensure that permission to reproduce such an illustration, diagram etc. is obtained from the copyright holder. If a figure is copied, adapted or redrawn, the original source must be acknowledged.

Submitting the contribution to JPMTR, the author(s) confirm that it has not been published previously, that it is not under consideration for publication elsewhere and - once accepted and published - it will not be published under the same title and in the same form, in English or in any other language. The published paper may, however, be republished as part of an academic thesis to be defended by the author. The publisher retains the right to publish the printed paper online in the electronic form and to distribute and market the Journal (including the respective paper) without any limitations.

B - Structure of the manuscript

Title: Should be concise and unambiguous, and must reflect the contents of the article. Information given in the title does not need to be repeated in the abstract (as they are always published jointly).

List of authors: i.e. all persons who contributed substantially to study planning, experimental work, data collection or interpretation of results and wrote or critically revised the manuscript and approved its final version. Enter full names (first and last), followed by the present address, as well as the e-mail addresses.

Separately enter complete details of the corresponding author - full mailing address, telephone and fax numbers, and e-mail. Editors will communicate only with the corresponding author.

The title of the paper and the list of authors should be entered on a separate cover page (numbered as 0). Neither the title nor the names of authors can be mentioned on the first or any other following page.

Abstract: Should not exceed 500 words. Briefly explain why you conducted the research (background), what question(s) you answer (objectives), how you performed the research (methods), what you found (results: major data attained, relationships), and your interpretation and main consequences of your findings (discussion, conclusions). The abstract must reflect the content of the article, including all the keywords, as for most readers it will be the major source of information about your research. Make sure that all the information given in the abstract also appears in the main body of the article.

Keywords: Include three to seven relevant scientific terms that are not mentioned in the title. Keep the keywords specific. Avoid more general and/or descriptive terms, unless your research has strong interdisciplinary significance.

Abstract and keywords should be entered on a separate page, numbered as page 1. Do not continue with the main body of the text, regardless of the possible empty space left on this page.

D - Submission of the paper and further procedure

Before sending your paper, check once again that it corresponds to the requirements explicated above, with special regard to the ethic issues, structure of the paper as well as formatting. Once completed, send your paper as an attachment to: journal@iarigai.org. You will be acknowledged on the receipt within 48 hours, along with the code under which your submission will be processed. The editors will check the manuscript and inform you whether it has to be updated regarding the structure and formatting. The corrected manuscript is expected within 15 days. At the same time the first (or the corresponding) author will be asked to sign and send the Copyright Transfer Agreement.

Your paper will be forwarded for anonymous evaluation by two experts of international reputation in your specific field. Their comments and remarks will be in due time disclosed to the author(s), with the request for changes, explanations or corrections (if any) as demanded by the referees. After the updated version is approved by the reviewers, the Editorial Board will consider the paper for publishing. However, the Board retains the right to ask for a third independent opinion, or to definitely reject the contribution. Printing and publishing of papers once accepted by the Editorial Board will be carried out at the earliest possible convenience.

Introduction and background: Explain why it was necessary to carry out the research and the specific research question(s) you will answer. Start from more general issues and gradually focus on your research question(s). Describe relevant earlier research in the area and how your work is related to this.

Methods: Describe in detail how the research was carried out (e.g. study area, data collection, criteria, origin of analyzed material, sample size, number of measurements, equipment, data analysis, statistical methods and software used). All factors that could have affected the results need to be considered. Make sure that you comply with the ethical standards, with respect to the environmental protection, other authors and their published works, etc.

Results: Present the new results of your research (previously published data should not be included). All tables and figures must be mentioned in the main body of the article, in the order in which they appear. Do not fabricate or distort any data, and do not exclude any important data; similarly, do not manipulate images to make a false impression on readers.

Discussion: Answer your research questions (stated at the end of the introduction) and compare your new results with the published data, as objectively as possible. Discuss their limitations and highlight your main findings. At the end of Discussion or in a separate section, emphasize your major conclusions, specifically pointing out scientific contribution and the practical significance of your study.

Conclusions: The main conclusions emerging from the study should be briefly presented or listed, with the reference to the aims of the research and/or questions mentioned in the Introduction and elaborated in the Discussion.

Introduction, Methods, Results, Discussion and Conclusions - as the scientific content of the paper - represent the main body of the text. Start numbering of these sections with page 2 and continue without interruption until the end of Conclusions. Number the sections titles consecutively as 1, 2, 3 ..., while subsections should be hierarchically numbered as 2.1, 2.3, 3.4 etc. Use Arabic numerals only.

Note: Some papers might require different structure of the scientific content. In such cases, however, it is necessary to clearly name and mark the appropriate sections.

Acknowledgments: Place any acknowledgments at the end of your manuscript, after conclusions and before the list of literature references.

References: The list of sources referred to in the text should be collected in alphabetical order on a separate page at the end of the paper. Make sure that you have provided sources for all important information extracted from other publications. References should be given only to documents which any reader can reasonably be expected to be able to find in the open literature or on the web. The number of cited works should not be excessive - do not give many similar examples. Responsibility for the accuracy of bibliographic citations lies entirely with the authors.

Please use only the Harvard Referencing System. For more information consult, e.g., the referencing guide at:

<http://libweb.anglia.ac.uk/referencing/harvard.htm>.

List of symbols and/or abbreviations: If non-common symbols or abbreviations are used in the text, you can add a list with explanations. In the running text, each abbreviation should be explained the first time it occurs.

Appendix: If an additional material is required for better understanding of the text, it can be presented in the form of one or more appendices. They should be identified as A, B, ... etc., instead of Arabic numerals.

Above sections are supplementary, though integral parts of the Scientific content of the paper. Each of them should be entered on a separate page. Continue page numbering after Conclusions.

C - Technical requirements for text processing

For technical requirement related to your submission, i.e. page layout, formatting of the text, as well of graphic objects (images, charts, tables etc.) please see detailed instructions at <http://www.iarigai.org/publications/journal>.

3-2016

Journal of Print and Media Technology Research

A peer-reviewed quarterly

The journal is publishing contributions
in the following fields of research:

- ⊕ Printing technology and related processes
- ⊕ Premedia technology and processes
- ⊕ Emerging media and future trends
- ⊕ Social impacts

For details see the Mission statement inside

JPMTR is listed in

Index Copernicus International

PiraBase (by Smithers Pira)

Paperbase (by Innventia and
Centre Technique du Papier)

NSD – Norwegian Register for
Scientific Journals, Series and Publishers

Submissions and inquiries
journal@iarigai.org

Subscriptions
office@iarigai.org

More information at
www.iarigai.org/publications/journal



Publisher

The International Association of Research
Organizations for the Information, Media
and Graphic Arts Industries
Magdalenenstrasse 2
D-64288 Darmstadt
Germany

Printed in Slovenia by Collegium Graphicum, d. o. o. Ljubljana

